UNIVERSIDADE DA BEIRA INTERIOR

Ciências

Proteomic analysis of the human vitreous humor in Retinal Detachment

Leonor Isabel Mesquita Gaspar

Dissertação de Projeto para obtenção do Grau de Mestre em

Biotecnologia

(2º ciclo de estudos)

Orientador: Prof.ª Doutora Cândida Ascensão Teixeira Tomaz

Co-orientador: Mestre Fátima Raquel Milhano dos Santos

Covilhã, outubro de 2015

“Começa por fazer o que é necessário, depois o que é possível e de repente estarás a fazer o impossível”

São Francisco de Assis

Agradecimentos

Em primeiro lugar gostava de deixar o meu profundo agradecimento à Professora Doutora Cândida Tomaz pela sua orientação, apoio, compreensão, e por todos os conhecimentos partilhados ao longo deste ano. Obrigada por ter aceite trabalhar comigo neste projeto.

À minha co-orientadora e amiga Fátima Santos, por todo o apoio, carinho e dedicação incondicional ao longo deste ano. Por todos os conhecimentos que me transmitiu, e por toda a motivação que me deu no decorrer deste trabalho. O meu sincero obrigado, por tudo o fizeste por mim.

Ao Dr. João Paulo Castro Sousa do Centro Hospitalar de Leiria – Pombal, pelas amostras biológicas que disponibilizou ao longo de todo este trabalho, garantindo assim o sucesso deste.

À NOVARTIS-FARMA SA pelo financiamento do projeto intitulado "Human vitreous proteomics of ophthalmologic diseases", em qual o presente trabalho se insere.

À Ana Sílvia Rocha, pelo apoio científico na fase inicial do meu trabalho.

Aos meus pais Nuno e Nanda, por todo o amor e carinho que me dão todos os dias e pela paciência com que me aturam até nos dias mais difíceis. Obrigada por tudo o que sempre fizeram por mim. A vocês devo tudo o que sou hoje.

À minha irmã Hélia por todo o seu amor e amizade incondicional ao longo deste ano e de toda a minha vida. Agradeço igualmente ao meu cunhado Luís e aos meus sobrinhos Henrique e Tomás por todo o carinho e ânimo sempre demonstrado.

A toda a minha família e amigos que sempre me apoiaram ao longo da vida, especialmente ao longo deste ano, e que me fortalecem todos os dias.

Por fim, agradeço à Universidade da Beira Interior e a todos os membros do CICS, em especial ao grupo de Biotechnology and Biomolecular Sciences, por todo o apoio e entreajuda sempre manifestada.

Resumo

Nos últimos anos, tem-se verificado um grande incremento de doenças oculares na população mundial. A incidência destas patologias surge com a progressão da idade, levando a um declínio da função ocular normal e, em alguns casos, podendo levar à cegueira. As patologias oculares são frequentemente desencadeadas por doenças crónicas, tais como diabetes ou hipertensão, ou por alterações no posicionamento da retina, o que ocorre no descolamento de retina (DR). Estudos recentes indicam que o humor vítreo (HV) humano sofre alterações proteómicas, de acordo com o estado fisiológico e patológico da retina. No entanto, existem poucos estudos publicados sobre o proteoma do HV no DR. Assim, este estudo centra-se essencialmente na análise proteómica de amostras de HV em DR, e posterior identificação das proteínas presentes nestas amostras, de que forma estão interligadas e como atuam. Desta forma, pode ter-se acesso ao proteoma do HV em doentes com descolamento de retina, que é o principal objetivo deste trabalho.

Para atingir estes objetivos, diversas estratégias foram combinadas, incluindo a depleção de proteínas abundantes, fracionamento e análise de proteínas por espectrometria de massa (MS), a fim de maximizar o número de proteínas identificadas. A estratégia final otimizada combinou o fracionamento de proteínas por cromatografia líquida (LC) e SDS-PAGE e a identificação das proteínas por MALDI-TOF/TOF. Usando esta metodologia, foram identificadas 236 proteínas com uma confiança de 95%, usando o ProteinPilot, onde 46 proteínas partilham associações biológicas comuns, com um score mínimo de 0.900 de acordo com o STRING10. A maioria dessas 46 proteínas estão envolvidas em processos de regulação e têm funções de ligação. Em simultâneo, analisou-se o mesmo grupo de amostras através de LC e MALDI-TOF/TOF, de forma a compreender a importância da implementação de SDS-PAGE no processo. Verificou-se que através de LC-MALDI, apenas 110 proteínas foram identificadas. Em conclusão, a estratégia desenvolvida (LC-SDS-MALDI) permitiu encontrar proteínas que não tinham sido anteriormente identificadas usando outras estratégias proteómicas.

Palavras-chave

Análise proteómica; Descolamento da retina; Humor vítreo; Identificação de proteínas; MALDI-TOF/TOF.

Resumo Alargado

Nos últimos anos, tem-se verificado um grande incremento de doenças oculares na população mundial. A incidência de patologias oculares surge com a progressão da idade, levando a um declínio da função ocular normal e, em alguns casos, podendo levar à cegueira. Em 2010, a Organização Mundial de Saúde estimou que mais de 285 milhões de pessoas, em todo o mundo, sofriam de deficiência visual, das quais 39 milhões sofriam de cegueira. Na Europa, numa amostra de população de 13,2 milhões de indivíduos, verificou-se que 7% da população sofria de cegueira, 10,4% de perda de visão e 9,9% de deficiência visual, e as previsões indicam que estes números poderão aumentar dentro de 20 anos. Assim, é importante encontrar estratégias que permitam a diminuição destes casos na população em geral.

As patologias oculares são frequentemente desencadeadas por doenças crónicas, tais como diabetes ou hipertensão, e por alterações na posição da retina, o que ocorre no descolamento de retina (DR). Assim, para entender estas patologias, é crucial o estudo da composição do olho humano e do seu funcionamento, bem como o estudo dos diferentes mecanismos e das interações que permitem a manutenção deste órgão. O olho humano é um órgão altamente organizado e complexo, responsável pela perceção da visão. É formado por estruturas que estão sujeitas a alterações proteómicas causadas por diversas condições fisiológicas e patofisiológicas. É composto por 3 fluídos principais, sendo o mais importante o humor vítreo (HV). Este ocupa o segmento posterior do olho, entre a lente e a retina, e é um gel transparente, altamente hidratado, constituído por 98% de água e 2% proteínas e matriz extracelular. A sua estrutura tipo gel é devida à presença de fibras de colagénio e moléculas de ácido hialurónico.

O DR, embora possa suceder em jovens adultos em determinadas circunstâncias, ocorre mais frequentemente em pessoas mais velhas e/ou portadoras de um elevado grau de dioptria. Nestes casos, o HV pode liquefazer, devido ao enfraquecimento da sua adesão à retina, e, possivelmente, devido a alterações no seu proteoma. Quando isto ocorre, sucede uma separação física entre a camada fotorrecetora da retina e o pigmento do epitélio retinal. Consequentemente, a informação visual recebida pelo olho não vai ser transferida para o nervo ótico, resultando numa perda de visão. Existem 3 tipos de descolamento de retina, sendo o mais comum o descolamento regmatógeno da retina (DRR). Estudos recentes indicam que as alterações proteómicas do HV humano refletem o estado fisiológico e patológico da retina. No entanto, existem poucos trabalhos publicados referentes ao proteoma do HV durante o DR.

A principal vantagem da análise proteómica é a deteção e identificação de um conjunto de proteínas presentes numa matriz biológica, num determinado tempo ou em determinadas condições fisiológicas ou patofisiológicas. Isto é um facto bastante interessante, uma vez que as possíveis localizações, modificações, interações e expressão das proteínas podem variar significativamente, quando expostas a diversos estímulos externos. Assim, o maior propósito da proteómica em doenças oculares é essencialmente a identificação das proteínas presentes em

determinadas patologias oculares, como DRR, e de que forma estas estão interligadas e como atuam. Assim, o presente estudo centra-se, essencialmente, no estudo do proteoma do HV em pacientes de DRR, a fim de, futuramente, encontrar alterações proteómicas e assim descobrir potenciais biomarcadores que poderão apoiar o diagnóstico precoce da doença, diminuindo a incidência desta patologia ocular na população atual.

Para atingir estes objetivos, diversas estratégias foram realizadas, incluindo a depleção de proteínas abundantes, fracionamento e análise de proteínas por espectrometria de massa (MS), a fim de maximizar o número de proteínas identificadas. As amostras de HV de diferentes doentes com DRR foram agrupadas de forma a diminuir a variabilidade da amostra, fazendo com que o conjunto das amostras fosse mais representativo do proteoma de DRR.

Em fluídos biológicos como o HV, certas proteínas como a Albumina e a IgG estão presentes em elevada abundância, representando 60 a 80% da sua constituição proteíca. Estas proteínas podem ocultar as proteínas com baixa abundância, que geralmente são mais significantes em situações patológicas, ou seja, as chamadas proteínas de interesse. Para se poder ter acesso a essas proteínas com baixa abundância, foi necessário então proceder à depleção das proteínas abundantes, conseguida através da realização da cromatografia de afinidade, usando uma coluna com a afinidade para a albumina e para a IgG. De seguida, foi efetuado o fracionamento da amostra resultante da depleção que abrange as proteínas de interesse, as proteínas de baixa abundância. Este passo é crucial pois diminui a complexidade da amostra, uma vez que a divide em frações de acordo com o ponto isoelétrico das proteínas. Este processo foi conseguido através da cromatografia de troca-iónica usando uma Q-Sepharose como trocador de aniões.

Após o fracionamento, seguiu-se a separação das proteínas por peso molecular por eletroforese SDS-PAGE. Esta separação reforça a redução da complexidade da amostra, e o seu fracionamento, uma vez que se procede à separação das proteínas numa segunda dimensão.

Seguidamente, a identificação de proteínas efetuou-se por MALDI-TOF/TOF. Este equipamento baseia-se num sistema de ionização, que produz iões carregados a partir da colisão entre o laser e os péptidos, e possui dois analisadores de espectrometria de massa alinhados em série que medem a razão massa/carga (m/z) de cada ião. A informação dos iões percursores e dos iões filhos resultantes dos espectros MS/MS é, então, traduzida em listas de valores m/z que posteriormente são cruzados com a informação de bases de dados de proteínas, identificando assim as proteínas de interesse. Numa primeira abordagem, foram encontradas 236 proteínas com uma confiança de 95%, usando o ProteinPilot, onde 46 proteínas partilham associações biológicas comuns, com um score mínimo de 0.900 de acordo com STRING10. A maioria dessas 46 proteínas está envolvida em processos de regulação e tem funções de ligação. Em relação à análise KEGG, as proteínas identificadas estão envolvidas em mecanismos metabólicos, de regulação e de sinalização como o da hormona tiróide, Fc epsilon RI e HIF-1.

Em conclusão, a estratégia desenvolvida permitiu encontrar proteínas que não foram anteriormente identificadas usando outras estratégias proteómicas como LC-MS.

Abstract

Over the past few years, there has been an intensification in onset of ocular diseases among worldwide population. The incidence of eye pathologies upsurges with advancing age, leading to a decline of normal eye function and even to blindness. Ocular diseases are frequently triggered by chronic disorders, such as diabetes or hypertension, or by alterations in retinal positioning, which occurs in retinal detachment (RD). Recent studies indicates that human vitreous humor (VH) suffers proteome alterations according to the actual physiological and pathological state of the retina. However, there are few published articles regarding RD proteome. Hence, this study is focused in the proteomic analysis of VH samples in RD and posterior identification of the present proteins in these samples, as well as to understand in what way they are connected and how they act. In this way, we can get access to the VH proteome in RD patients, which is our main goal. To achieve these goals, several strategies were combined, including high abundant proteins depletion, protein fractionation and analysis by mass spectrometry (MS), in order to maximize the number of identified proteins. The final optimized strategy combined protein fractionation using liquid chromatography (LC), SDS-PAGE, and protein identification by MALDI-TOF/TOF. Using this methodology, we found 236 proteins with a 95% confidence, using ProteinPilot, where 46 proteins share common biological associations, with a minimum score of 0.900 according to STRING10. The majority of these 46 proteins are involved in regulation processes and share binding functions. Simultaneously, the same VH group sample was analyzed by LC and MALDI-TOF/TOF, in order to understand the importance of the implementation of SDS-PAGE in the process. Thus, we verified that with LC-MALDI only 110 proteins were identified. In conclusion, the developed strategy allowed to find proteins which were not identified using other proteomic strategies.

Keywords

MALDI-TOF/TOF; Protein identification; Proteomic analysis; Retinal detachment; Vitreous humor.

Table of Contents

List of Figures

List of Tables

List of Acronyms

1D-PAGE	One-Dimensional Sodium Dodecyl Sulfate–Polyacrylamide Gel Electrophoresis
2D-DIGE	Two-Dimensional Fluorescence Difference Gel Electrophoresis
2DE	Two-Dimensional Electrophoresis
2D-PAGE	Two-Dimensional Sodium Dodecyl Sulfate–Polyacrylamide Gel Electrophoresis
AC	Affinity Chromatography
AH	Aqueous Humor
AMD	Age-related Macular Degeneration
BRB	Blood-Retinal Barrier
CID	Collision Induced Dissociation
ERM	Epiretinal Membrane
ESI	Electrospray Ionization
ESI-MS	Electrospray Ionization Mass Spectrometry
FDA	Food and Drug Administration
GO	Gene Ontology
HAPs	High Abundant Proteins
HGP	Human Genome Project
HSA	Human Serum Albumin
IEC	Ion-Exchange Chromatography
IEF	Isoelectric Focusing
IgA	Immunoglobin A
IgG	Immunoglobin G
IOP	Intraocular Pressure
IP	Immunoprecipitation
iTRAQ	Isobaric Tag For Relative And Absolute Quantitation
LAPs	Low Abundant Proteins
LC-MS	Liquid Chromatography coupled to Mass Spectrometry
MALDI	Matrix-Assisted Laser Desorption/Ionization
MALDI-MS	Matrix-Assisted Laser Desorption/Ionization Mass Spectrometry
MH	Macular Hole
MS	Mass Spectrometry

PDGF	Platelet-Derived Growth Factor
PDR	Proliferative Diabetic Retinopathy
PEDF	Pigment Epithelium Derived Factor
pI	Isoelectric Point
PPV	Pars-Plana Vitrectomy
PTMs	Post-Translational Modifications
PVR	Proliferative Vitreoretinopathy
RD	Retinal Detachment
RPC	Reversed-Phase Chromatography
RPE	Retinal Pigment Epithelium
RRD	Rhegmatogenous Retinal Detachment
SDS-PAGE	Sodium Dodecyl Sulfate–Polyacrylamide Gel Electrophoresis
TOF	Time-Of-Flight
VH	Vitreous Humor
WHO	World Health Organization

Chapter 1

Introduction

1.1 Ocular Pathologies

Over the past few years, there has been an intensification in onset of ocular diseases among worldwide population, affecting all manner and ages of people [1]. In 2010 the World Health Organization (WHO) estimated that more than 285 million people were visually impaired around the world, from which 39 million were blind. In Europe, in a study with a population of 13.2 million, was verified that 7% of the population was blind, 10.4% had low vision and 9.9% was visually impaired, and forecasts indicate that the prevalence of ocular diseases will increase within 20 years [2,3].

Since the world's population is ageing due to the increased average life expectancy, the consequences of blindness and visual impairment can be devastating, having a considerable impact on daily life activities, creating social and economic difficulties and reducing drastically the quality of life in overall population [4,5]. Fortunately, it is a fact that 80% of all visual impairment can be prevented or cured. For this reason, and to overcome this global issue, it is important to develop new strategies for the management of non-communicable ocular diseases that may decrease the incidence of these pathologies in worldwide population.

The incidence of ocular pathologies upsurges with advancing age, leading to a decline of normal eye function and even to blindness [5]. Ocular diseases are frequently triggered by chronic disorders, such as diabetes or hypertension, and by alterations in retinal positioning, which occurs in retinal detachment (RD).

For the elucidation of ocular pathologies, there is a growing interest in understanding how different factors may interact to produce several disease manifestations. Several factors have been demonstrated to have crucial importance to ocular diseases, including environmental, genetic and lifestyle factors. For instance, poor diet and nutrition are highly correlated with inflammatory and age-related ocular pathologies [5].

Thus, to understand these pathologies, it is first important to understand the human eye composition and functioning and how the biochemical mechanisms and interaction of different factors may be correlated with eye diseases, and their different manifestations.

1.1.1 The human eye

The human eye is a very interesting structure and a highly organized and complex organ, responsible for the perception of sight [5]. It is responsible for about 38 to 40% of the total

sensory input to the brain [6]. For an optimal visual function, it is essential the integrity and transparency of the ocular medium. Distortion of the visual axis of the eye and modification of eye components and structure, due to factors such as inflammatory processes and aging, may harmfully affect vision [5].

The human eye is formed by different structures, and its organization is subjected to changes caused by various diseases. If the cellular constituents and protein composition of these structures differ, the functions of each region of the eye will suffer changes, and may lead to serious complications [7].

As we can observe in Figure 1, the eye is composed by several structures, each one with a different function in processing the light received by the eye. Firstly, the light enters the eye through the cornea, which is the transparent part of the eye that covers the anterior chamber [7,8]. The cornea, along with the lens, provides a transparent layer which focuses the light rays. Then, the light meets the retina, a photosensitive, thin and transparent layer that consists of a number of specialized cells that modulates the visual signs that will be processed by the brain [6,9]. Thus, the retina's function is to perform the phototransduction of the received light, which transforms it into a neural signal that travels through the optic nerve into the brain, giving us the sense of seeing [7,8]. The retina appears to be a very important structure since many researchers begun to characterize retinal proteins in order to track proteomic changes that occurs with ageing and retinal disease [9].

The eyeball is divided into three chambers that combines the anterior chamber, between the cornea and iris, containing the aqueous humor; the posterior chamber between the iris and the lens; and the vitreous chamber extending from the back of the lens to the retina [10]. Inside the vitreous chamber there is a fluid called vitreous humor (VH) which contemplates a great interest for proteomic research, since it can suffer significant alterations at protein level indicating a certain ocular disease state [11].

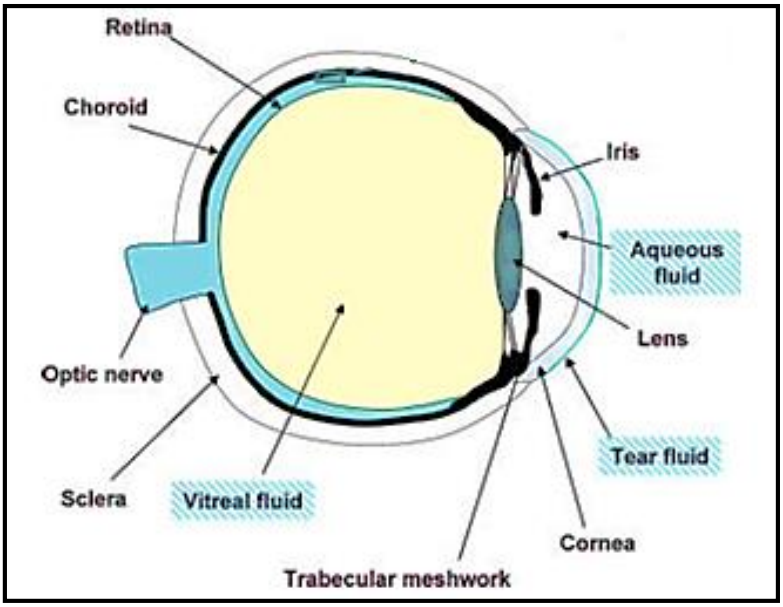

Figure 1 - Illustration of the human eye and of the ocular fluids (adapted from [12]).

1.1.1.1 Eye Fluids

Intraocular fluids include tears, aqueous humor and vitreous humor, and are extremely important because they act as a barrier, mediating the exchanging substances between blood and eye tissues. Thus, they can indicate the health state of blood vessels and eye tissues. Therefore, if abnormal exchanges of substances occurs between ocular fluids and tissues, protein expression levels in this fluids changes, indicating the presence of an ocular alteration [13]. Indeed, it was demonstrated that changes in protein expression levels in eye fluids such as aqueous and vitreous humor are correlated with major eye diseases [14]. For this reason, there has been an increase of the proteomic study of intraocular fluids in various eye disorders, leading to advances in ophthalmology and ocular science.

Tears

Tears are an extracellular fluid which covers the surface epithelial cells, and constitutes the anterior component of the ocular surface [15]. The majority of tears are produced by tear glands situated within the eyelid and conjunctiva, while the lacrimal gland is responsible for reflexive tearing through small pores called lacrimal punctum, as seen in Figure 2 [10].

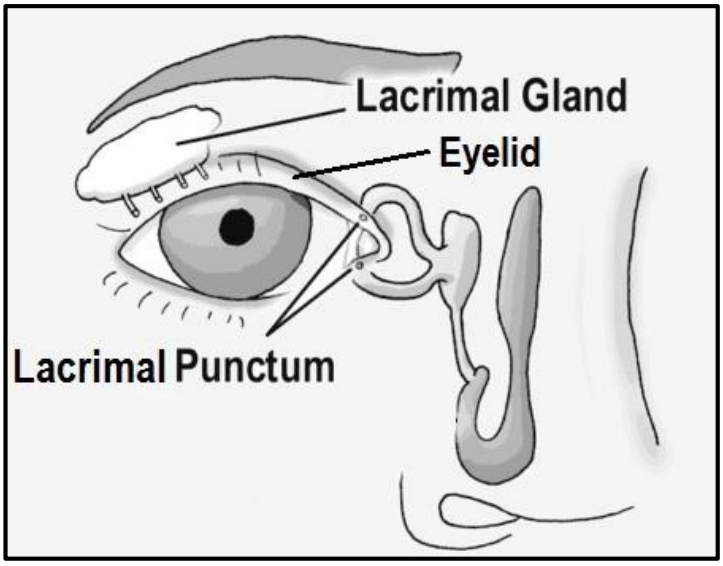

Figure 2 - Illustration of tear production and drainage (adapted from [10]).

The tear film, besides refracting light onto the retina and providing protection, nutrients and lubrication to the eye, is a complex fluid composed by many proteins, lipids, carbohydrates, mucin and other small molecules such as metabolites and electrolytes [16].

Tears can be collected, for various analysis, by non-invading procedures using glass microcapillary tubes or through Schirmer strips [16]. Recent studies have revealed that tear proteins can protect the ocular surface and have a vital role in modulating the wound healing process. For this reason, tear fluids have been receiving a growing attention for determining the effect of functional proteins expression [17].

Aqueous humor

The human aqueous humor (AH) is an important intraocular fluid responsible for the supply of nutrients and removal of metabolic wastes from the eye tissues. AH is a transparent fluid, with a total volume of approximately 250µl [18], which fills the anterior and posterior chambers of the eye (Figure 3). It is produced by the ciliary process and secreted from anterior segment tissues into the posterior chamber through active transport of ions and solutes [19].

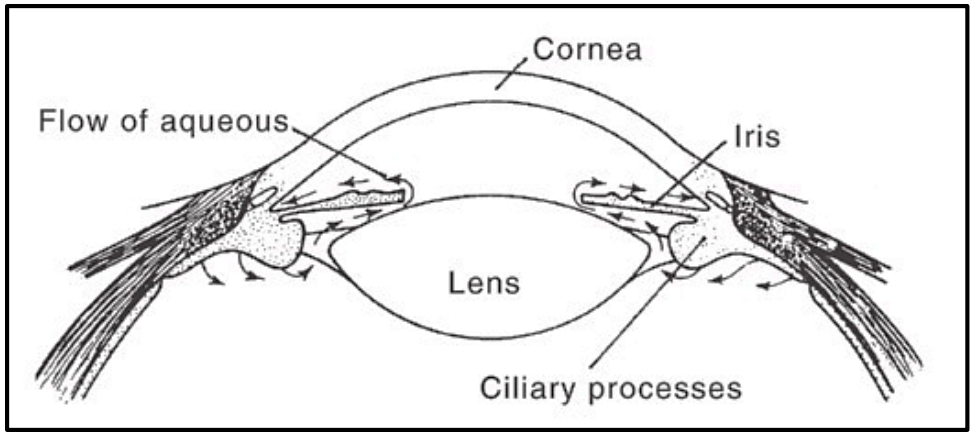

Figure 3 - Illustration of the aqueous humor flow. The arrows indicates the aqueous humor flow (adapted from [20]).

AH is very important for the maintenance of certain eye functions, including refraction, shape, local ocular defense, and intraocular pressure (IOP). When an imbalance occurs between the secretion and outflow rates of the AH, there is a disruption in the flow, causing an increase of intraocular pressure. As a result, this manifestation can lead to progressive optic degeneration, and even to blindness [20].

In 1992, Taylor and colleagues found several immunosuppressive factors in AH, which supports the fact that this fluid has an important role in the regulation of immunological responses [21]. An increasing number of studies have demonstrated that protein alterations in AH may be correlated with pathogenic mechanisms of many eye disorders, which may be helpful in its prognosis [22]. For that reason, the analysis of protein expression in this fluid is vital for the understanding of such pathologies.

Vitreous humor

The human vitreous humor (VH) is a transparent and highly hydrated gel, which occupies the posterior segment of the eye between the lens and the retina [4,23]. It occupies about 80% of the total volume of the eyeball, reaching up to 4.5mL, and it consists in about 98% of water and 2% of proteins and extracellular matrix [24]. VH has a gel-like structure due to a network of collagen fibrils (type II, V, VI, IX and X) and large molecules of hyaluronic acid, as it is shown

in Figure 4. Low molecular weight solutes including inorganic salts, sugars and ascorbic acid are present in this fluid. It also contains soluble proteins that are necessary to sustain normal ocular morphology and functions [11,25].

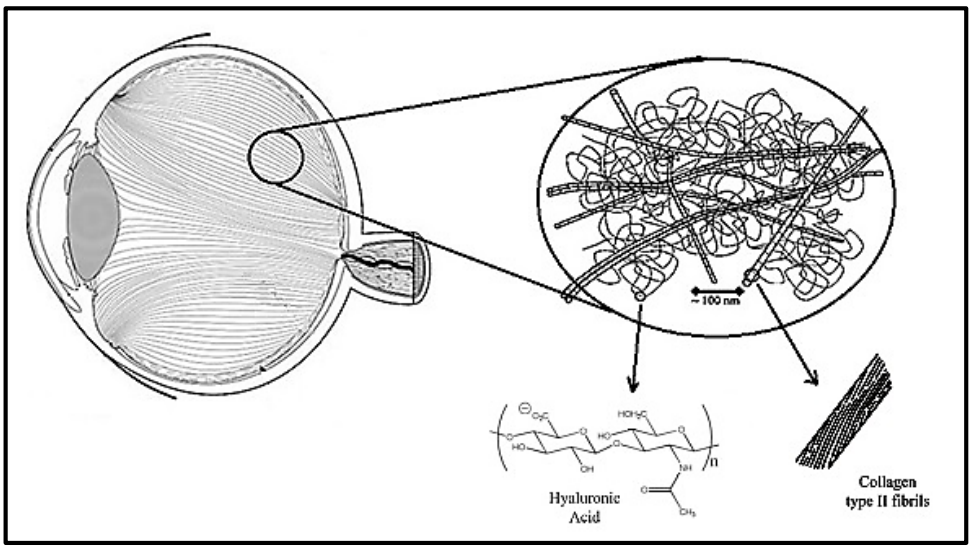

Figure 4 - Illustration of the vitreous humor structure (adapted from [27,28]).

In the normal eye, although VH appears to be a quiescent compartment, various changes in retina can affect it composition, indicating that this fluid may have a fundamental role in the pathogenesis of several ocular disorders [28,29].

The composition of the vitreous is crucial to the human eye health, therefore, alterations in protein expression may be indicative of ocular disease [11]. These alterations are important to be studied, since they can give additional information, contributing for an overall knowledge about pathogenesis mechanisms and processes underlying various eye diseases. This can be achieved through quantitative and qualitative protein analysis of the vitreous humor [30]. To analyze the vitreous humor, it must be surgically removed from the human eye through pars-plana vitrectomy (PPV). This surgery is only performed in severe cases of eye diseases. This allows the removal of hemorrhage blood, inflammatory cells, and other debris that may obscure the visual axis. Also, the surgeon removes any fine strands of vitreous attached to the retina to relieve traction, or to fix a detachment, [10]. The vitreous humor is removed with an instrument called vitrector which operates with a cutting device that safely removes the vitreous and replace it with a saline solution, to ensure that the eye does not lose its primary spherical conformation [31].

The aetiology of several vitreoretinal disorders, including proliferative vitreoretinopathy (PVR), proliferative diabetic retinopathy (PDR), and age-related macular degeneration (AMD), has already been linked to expression changes of several vitreous fluid proteins [11,25]. Plus, although vitreous humor is considered limited through surgical access, it is demonstrated that the research of the protein profile of healthy and diseased vitreous humor is important for the

understanding of ocular diseases and has become promising due to its ability of identifying subtle changes in the expression of lower abundance proteins [25].

1.1.2 Retinal Detachment

Retinal Detachment (RD) can cause blindness, even in young adults under certain circumstances including violent head and facial traumas. However, RD is more frequent with advancing age and in some degenerative conditions, having more incidence in older people, and in people with higher diopter degree. Although there is not, at this point, much well-known information about this ocular pathology, RD is considered to be a retinal accumulation of fluid between the neurosensory retina and the underlying retinal pigment epithelium (RPE) [32]. In these cases, eye fluids as VH can liquefy due to the weakening of vitreoretinal adhesion. When this occurs, the vitreous falls upon itself causing the physical separation between the photoreceptor layer of the retina and the underlying retinal pigment epithelium, leading to the disruption of the transfer of nutrients to photoreceptor cells within retina, inducing chronic disturbances in cellular metabolism [10]. These manifestations may cause vision loss and permanent alterations in color perception [32,33]. So, RD is four to five times more likely to occur in cases where the vitreous humor has been removed through vitrectomy simultaneous with cataract extraction, happening in 4.6% of those cases [24,34].

There are three types of retinal detachment: exudative, tractional and rhegmatogenous as seen in Figure 5 [10,35]. The most common detachment phenomenon is rhegmatogenous retinal detachment (RRD), which is characterized by a full thickness retinal break [32]. At the moment, the treatment of RRD is exclusively surgical, so, if left untreated, it may evolve into a major complication, technically dominated as (PVR) [36].

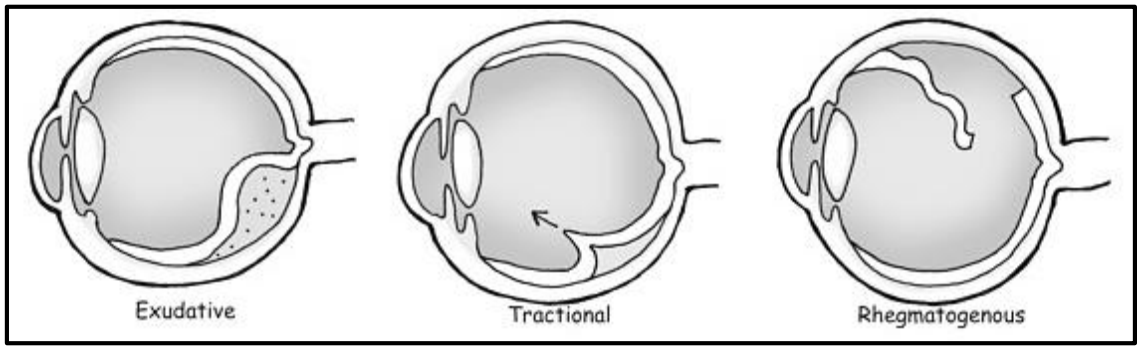

Figure 5 - Types of retinal detachment (adapted from [10]).

In RRD, degenerative changes in VH fluid precedes the detachment and are usually present in both eyes, even though detachment may be present in only one [37].

Proteomic analysis, which has become increasingly common, already provides useful information for understanding these eye pathologies. It has been shown that pathological concentrations of several proteins present in the aqueous and vitreous fluids are closely

associated with major eye diseases, such as RRD [14]. For instance, in normal cases, VH avoids the retinal breakdown and indirectly maintains the adhesion between the retina and the RPE, and consequently prevents retinal detachment. Thus, some studies propose that the physical structure and proteomic composition of VH might be important in the maintenance of retina [38].

So, the analysis of ocular fluids as VH using proteomics methodologies may be relevant for a deeper knowledge of pathologic mechanisms of RRD.

1.2 Proteomic Analysis

Recent studies revealed that the total number of coding genes in humans seems to stand between, at least, 25 000 and 30 000. However, when compared to genome, the complexity of the human proteome can be overpowering [39].

Biological information required for protein expression is codified into DNA, however genomic data do not have the capacity to answer all biological questions. For instance, not all genes are expressed, and genes transcribed into messenger RNA (mRNA) are not always translated into proteins, making difficult to predict the time and rate of proteins expression and turnover. Also, a single gene may codify the information for the synthesis of several different proteins, leading to the existence of a larger number of cellular proteins than genes [40]. Furthermore, many proteins only become functional when associated or complexed with other molecules, like DNA, RNA and organic and inorganic cofactors [41]. Therefore, the analysis of constituents such as genes and transcripts presents as drawbacks its easy degradation, and the incoherence correlation between gene and protein levels.

Also, protein related information including protein interactions and post-translational modifications (PTMs), which affects protein function, activity and structure, cannot be analyzed through genetic analysis [12,42]. PTMs are dynamic and reversible and often occur in mature and biologically active proteins [41], and therefore cannot be predicted through DNA coding. Typical PTMs include phosphorylation, glycosylation, acetylation, methylation and ubiquitylation. The study of these modifications is essential since they can increase the protein diversity and, therefore, cause dramatic changes in protein structure and function [15]. Hence, fundamental information about cellular metabolism and process, including protein turnover, PTMs subcellular localization or protein-protein interactions, are not revealed by genomic expression [40]. So, the study of human proteome is gaining attention, focusing on the evaluation of alterations of protein expression.

Proteomics is a field of great interest since it encompasses the study of proteome, including protein structure, function, interactions, expression levels and stages in an organism, without losing any information [5,25,43]. The term “proteome” was introduced by Marc Wilkins in 1994 and describes “all proteins expressed by a genome, cell or tissue” [44,45]. The research of the human proteome is highly complex due to the physical and chemical diversities of proteins [40]. Proteomic analysis have become increasingly common showing great success, and rapid growth during the past few years, and has contributed significantly to advances in science [46],

becoming an essential tool in biomedical and clinical research [16]. Proteomics has many study applications including, for example, proteome mining, protein modification, proteins complexes, and bioinformatics [45], as described in Table 1.

Table 1 - Proteomic study applications (adapted from [45]).

Study applications	Definition
Proteome mining	- Identification of known and unknown proteins - Association between proteins and study conditions (biomarker discovery)
Protein modification	- Identification of post-translational modifications - Association between protein changes and functions
Protein complexes	- Stable complexes - Transitory interaction
Bioinformatics	- Coordination of information - Development of databases

The principal purpose of the proteomic study is to identify proteins and detect protein expression alterations on a cell, biological tissue or fluid, or organism, at a specific time, under specific conditions. This is very interesting since proteins localization, modifications, interactions and expression can vary significantly when exposed to different environmental, physiological and pathophysiological conditions [40].

Thus, the major focus of proteomics, and of this study, is the expression proteomics, where we attempt to identify all the proteins expressed in VH under a certain ocular disease, in this particular case RRD. Thereby, we would get access to RRD proteome, and consequently revolutionize proteomics in ophthalmology.

1.2.1 Proteomic investigation in ophthalmic disease

To this date, proteomic analysis has been widely applied in the examination of various kinds of biological materials and fluids. [47]. In particular, proteomics has gain a great attention in ophthalmology field, since it allows the detection of protein changes in ocular samples and can be correlated with several ocular diseases processes, leading to the identification of potential markers [12,30]. Protein biomarkers are described as a molecular signature of a certain disease and can provide a view of a specific disease stage. According to Food and Drug Administration (FDA), an ideal biomarker must be highly sensitive, specific, reproducible and predictable [48,49]. In the future, these biomarkers may become a promising strategy to understand and support an earlier diagnosis, prognosis, as well as to improve therapeutic outcomes and successful prevention of ocular diseases [40,48].

To identify pathological changes during eye disease progress, mapping of proteins involved in normal eye functions is crucial. This objective can be achieved through the application of proteomic technologies [11]. At this moment, different methodologies are being experimented, allowing the understanding of proteomic mechanisms involved in human diseases, particularly in ocular diseases.

1.3 Vitreous Humor Proteomics

Comparing to other ocular fluids, such as tears and AH which were presented previously, VH offers a great potential for proteomic analysis owning to its close and direct contact with retina. Because of that close contact, physiological and pathological conditions of the retina may affect the VH proteome and its biochemical properties [50]. Even though tears and aqueous humor may present a more simple collection than VH, the limited sample volume holds a major difficulty in proteomic studies what does not happen with VH [16].

In 2007, Minamoto et al. compared the proteome of vitreous humor and serum samples, in diabetic retinopathy and idiopathic macular hole. Minamoto and his colleagues found that in vitreous samples most of the identified proteins were correspondent to serum proteins but the proteins related to the disease state corresponded to vitreous specific proteins, i.e., were identified in VH samples but not in serum [29].This suggests that VH is a unique fluid, interesting to be studied since subtle alterations occur in its protein profile during ocular diseases. For that reason, VH analysis may help to understand eye pathologies and to found potential biomarkers which may improve its treatment.

1.3.1 Proteomic Approaches

As previously indicated, the main focus of proteomics is expression proteomics, which encompasses the identification of the entire set of proteins expressed in a given complex biological system at a specific time, commonly denominated as proteome [46,51]. The identification of differential proteins is only possible due to the conclusion of the human genome project (HGP). HGP, initiated in 1990 and developed over the last years, is an international project that defends the public access of the human genome sequence into data bases [52]. Since a single gene can codify the information for the synthesis of several different proteins, HGP may simplify the protein identification once its understanding leads to the consequent understanding of proteomics [53]. To achieve the complete proteome, through qualitative and quantitative analysis, it is required that each individual technology involved in a proteomic set-up have an improved functioning [46]. For a complete successful set-up, the basic analytical requirements in proteomic analysis are high sensitivity, resolution and high-throughput [51].

Proteomic analysis is performed combining several techniques, where each technique aims to achieve the adequate preparation and fractionation of target sample in order to accomplish

the final goal, the protein identification. Table 2 summarizes the several technologies that can be used in proteomics analysis for protein preparation, fractionation and identification.

Table 2 - Strategies used in Proteomics (adapted from [47]).

Protein Preparation	Protein Fractionation	Protein Identification

• Collection
• Storage
• Anticoagulants
• Protease inhibitor
• Desalting
	• Chromatography
	  ○ Affinity approaches
	  ○ Ionic-exchange approaches
	• Electrophoresis
	  ○ SDS-PAGE (1DE)
	  ○ 2DE
		• Mass spectrometry
		  ○ MALDI-TOF/TOF
		  ○ ESI-TOF/TOF

In vitreous humor analysis, there are several possible variants in the proteomic process that can be thought out, as shown in figure 6. The grey boxes represent the standard procedure, while the white boxes represent the possible variants [11].

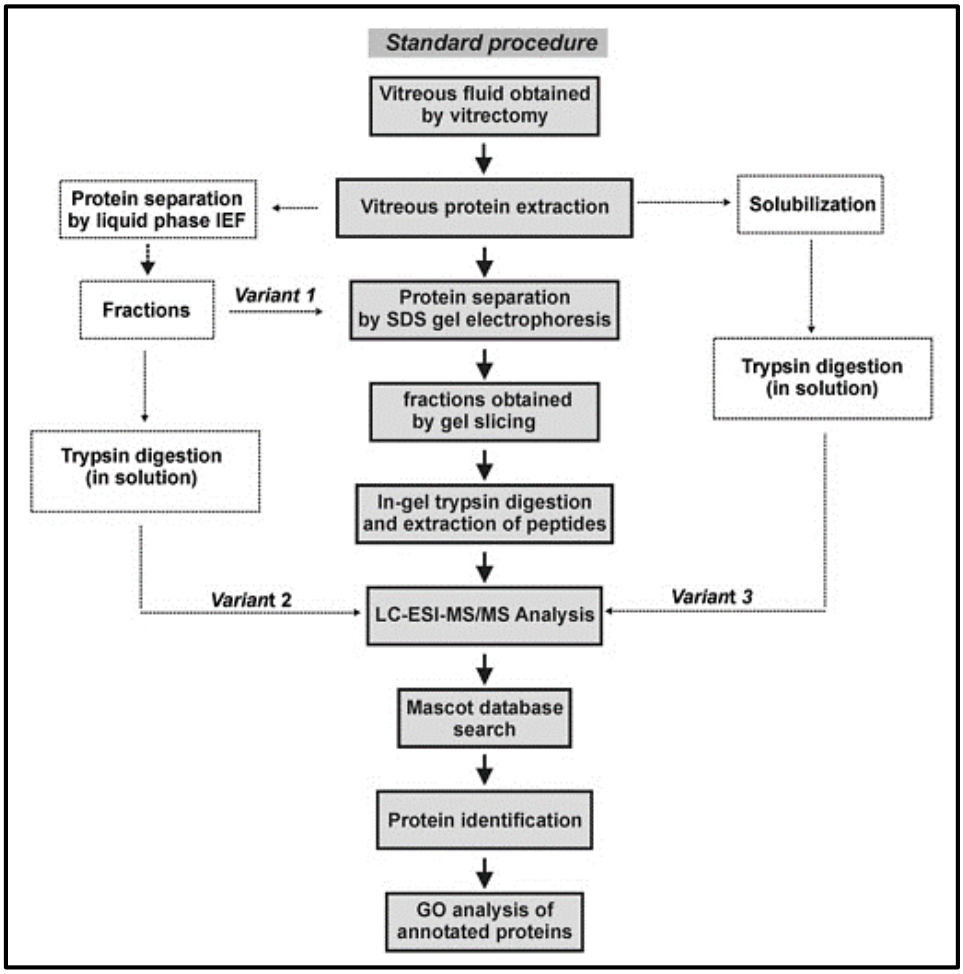

Figure 6 - Proteomic experimental work flow for vitreous samples. IEF: Isoelectric Focusing; GO: Gene Ontology (adapted from [11]).

It is interesting to note that, while instrument developments has received enormous attention in recent years, the separation techniques used for protein analysis have remained fairly conservative, showing once more the importance of these methodologies [54]. One limitation of the vitreous analysis, is the probable occurrence of haemorrhage in some patients, which may overlap the presence of less abundant proteins, yet important, leading to difficulties in identifying proteins [12]. Different approaches were experimented by several researchers in order to achieve the best performances and results. Over the last decade, different studies have shown a range of proteomic methodologies including two-dimensional electrophoresis (2DE), two-dimensional fluorescence difference gel electrophoresis (2D-DIGE), electrospray ionization-mass spectrometry (ESI-MS), matrix-assisted laser desorption/ionization-mass spectrometry (MALDI-MS), and liquid chromatography-mass spectrometry (LC-MS), in order to compare vitreous proteome from patients, with various stages of severe ocular diseases such as PDR and non-diabetic patients, being Macular Hole (MH) disease usually used as control sample [50].

Also, for a better protein identification, VH samples should be pooled, becoming a protein mixture or a peptide mixture. The main advantage in pooling is the overall decrease of the sample variability which is due to differences between individual samples. Thus, that individuality and variability is lost, making the global sample more representative [19].

1.3.1.1 Enrichment of human vitreous humor proteins

Regarding protein constituents, there are highly abundant proteins in VH, including Human Serum Albumin (HSA), Immunoglobin G (IgG), Immunoglobin A (IgA), transferrin, alpha-1-antitrypsin, haptoglobin, and fibrinogen. Albumin and IgG are the two most abundant proteins in VH, representing 60-80% of total protein content in VH, as illustrated in figure 7 [25,55,56]. Frequently, albumin and IgG present in VH are originated from serum and the increasing concentration of this proteins may indicate contamination of the vitreous humor, which may occurs due to blood-retinal barrier (BRB) breakdown or during PPV [57,58].

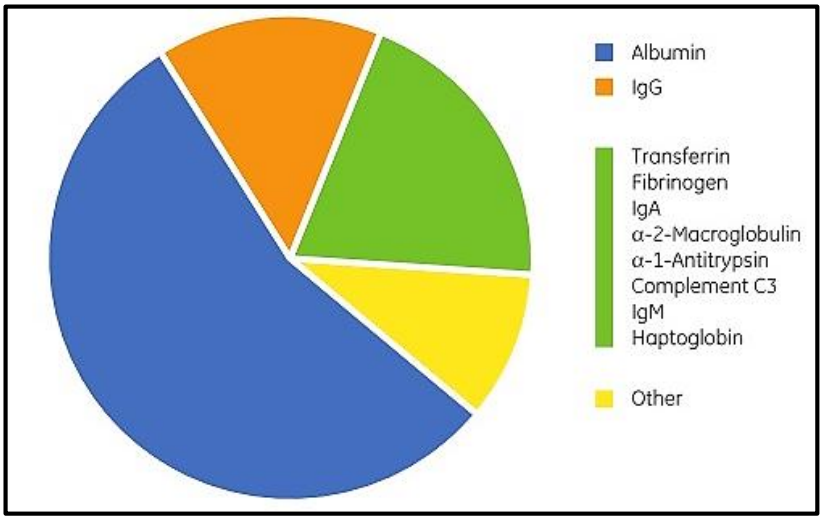

Figure 7 - Relative abundance of different proteins (adapted from [56]).

These proteins can overlap the most significant ones, present in lower concentrations, and therefore, prevent their detection [50]. Since the less abundant proteins are the more relevant proteins, i.e., proteins whose expression changes may be related to eye physiological and pathological events, the lack of their detection can give rise to difficulties in protein identification [59]. This issue can be overcome using a procedure designed as Depletion of High Abundant Proteins (HAPs), where abundant proteins are removed, so that we can get access to the proteins of interest, the low abundant proteins (LAPs). Using this strategy, it is possible to increase the concentration of LAPs, increasing the sensitivity of the method for these specific proteins, and thus improving the efficiency of protein identification [55].

For the depletion of HAPs in vitreous humor samples, several methods such as immunoprecipitation and immunoaffinity chromatography can be applied [60].

Immunoprecipitation (IP) is a technique that uses antibodies attached to a beaded support, usually agarose resin, which specifically binds to an immunoglobin, removing it from the sample under low speed centrifugation. This methodology can be performed using the commercial kit Protein G-Sepharose 4 Fast Flow from GE Healthcare [61,62].

Affinity chromatography (AC) separates proteins through a reversible interaction between the protein and a specific ligand coupled to a matrix under specific mobile phase conditions. These specific interactions demonstrated between ligand and target protein, can be caused by electrostatic or hydrophobic interactions, van der Waals, or hydrogen bonding. After establishing the affinity bonds, elution must be executed, in order to detach the protein of interest from the matrix. The specific nature of the established interactions is a major advantage of affinity chromatography since it results in a high selectivity and high resolution [63].

Immunoaffinity chromatography, is a specialized form of AC and it is based on the highly specific non-covalent interaction between an antigen and its antibody [64]. Hence, the depletion of albumin and IgG can be carried out using a chromatographic column whose ligands are, normally, anti-albumin antibody and recombinant protein G fragment. These ligands interact with HAPs separating them from LAPs, enabling the enrichment of the VH sample. The percentage of removal of these proteins using this methodology is up to around 90% [56,57,65].

The typically used immunoaffinity chromatographic approaches are columns including HiTrap™ Protein G (GE Healthcare), HiTrap™ Albumin and IgG (GE Healthcare), Multiple Affinity Removal column (Agilent Technologies), and also kits such as ProteoExtract™ Albumin/IgG Removal Kit (Merck Darmstadt), POROS® Affinity Depletion Cartridges (Applied Biosystems) and Albumin and IgG Removal Kit (Amersham Biosciences) [55].

Figure 8 illustrates the typical protein behavior in affinity chromatography, where the first peak represents the depleted sample, i.e., all the proteins which did not interact to the column ligands in stationary phase. The second peak, shown in the chromatogram, is Albumin and IgG which did bind to the ligands column.

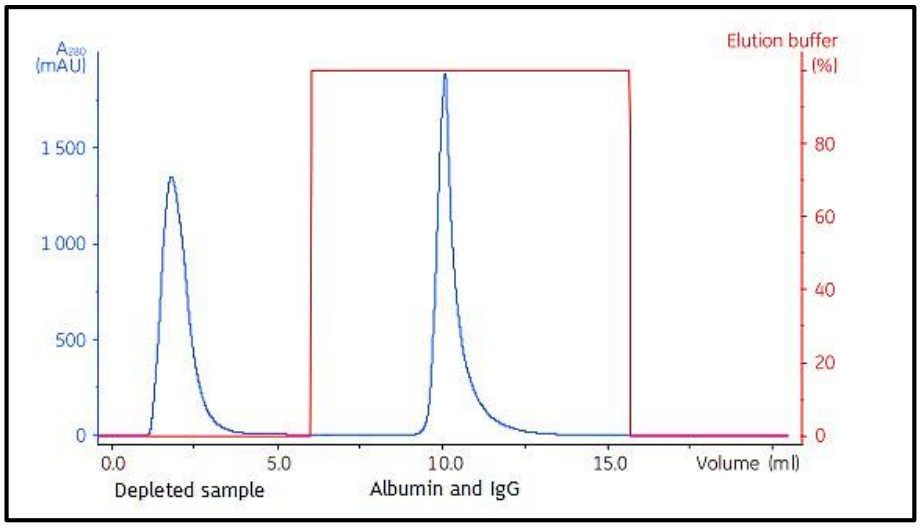

Figure 8 - Typical chromatogram of Albumin and IgG depletion through affinity chromatography (adapted from [66]).

1.3.1.2 Fractionation of human vitreous humor proteins

The biggest concern in identifying proteins from biofluids such as VH, lies in the high protein dynamic range which is due to the diversity of expressed proteins, and to the amount of proteins with different molecular weight, isoelectric point (pI) and hydrophobicity [67]. Therefore, sample must be fractionated before MS analysis in order to decrease sample complexity and to improve further protein identification [46].

The protein fractionation techniques that are usually performed, can be divided into two main categories: gel-based and gel-free [25].

Fractionation of human vitreous humor proteins using gel-free methodologies

Gel-free techniques apply liquid-phase chromatographic methods such as Reversed-Phase Chromatography (RPC), Ion-Exchange Chromatography (IEC), and Isoelectric Focusing (IEF). These methods show as advantages the improvement of sample recovery, reproducibility, throughput and possibility of coupling with MS.

RPC is one of the most used technique for sample fractionation, and separates proteins and peptides with different hydrophobicity based on the reversible interaction between the sample with a hydrophobic stationary phase and a polar hydrophilic mobile phase. The binding is usually very strong, and the elution is performed through the application of an organic solvent, commonly acetonitrile. This technique can be combined with other chromatographic techniques such as IEC with the advantage of increasing the amount and quality of analytical information [68].

IEC is an interesting approach to achieve an efficient separation of complex protein mixtures based on the differences in their net surface charge, by either salt-gradient or pH-gradient elution [69,70].

IEC is used in both protein analysis and protein purification/preparation. It is one of the most common chromatographic techniques due to its high capacity, and relatively low cost. An important advantage of this technique is the capability of adapting the buffer conditions to a certain range of proteins, instead of a single functional group of proteins [71]. The fundamental of IEC is the separation of biomolecules based on its charge [72] that, in case of proteins, it is based on their pKa, depending on their structure and chemical microenvironment. So, proteins can exhibit different degrees of interaction with the charged ligands on chromatography media according to their overall surface charge. This fact seems to be an advantage in protein fractionation, since the relationship between the net surface charge and pH is unique for a specific protein [70]. These protein characteristics depends on its composition in terms of amino acids, whose weak acidic and basic groups are highly influenced by pH changes. In the table 3 are listed some of the amino acids that are charged at physiological pH and its respective charges at this pH.

Table 3 - Amino acids charges at physiological pH (adapted from [71]).

Amino acids charges at physiological pH	
Positive	- Lysine - Arginine - Histidine
Negative	- Aspartic acid - Glutamic acid

So, using this technique, it is possible to influence the protein charge by changing the pH of mobile phase, in order to proceed the protein fractionation. Depending on pH, the protein will be positively charged, at a pH below its pI having the tendency to interact with the negatively charged ligands; or will be negatively charged, at a pH above its pI, binding to a positively charged ligand [70], as showed in figure 9.

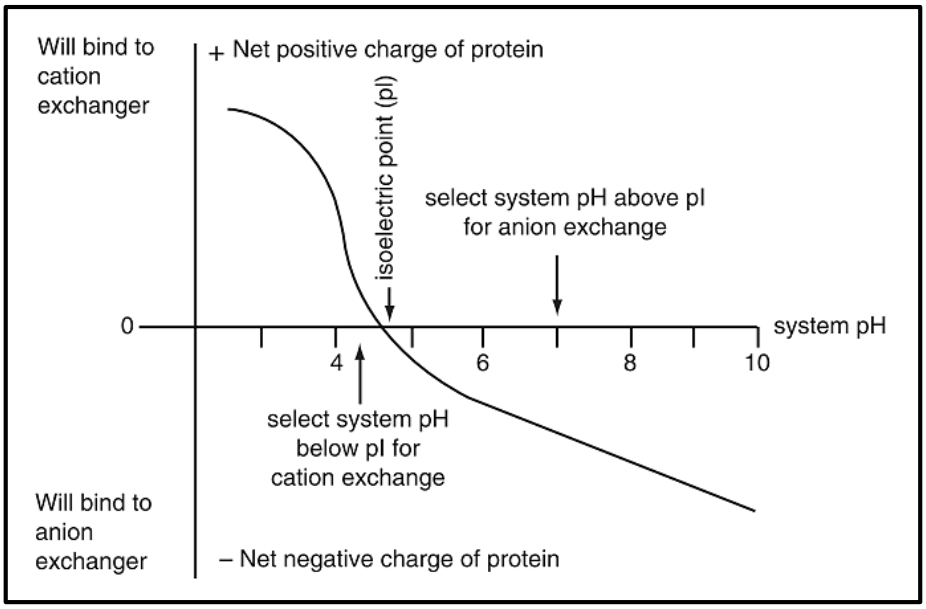

Figure 9 - Representation of the variation of the proteins net charge as function of pH (adapted from [72]).

IEC counts on the interaction between positively or negatively charged molecules loaded in the column and oppositely charged groups coupled on the stationary phase.

Then, depending on the charge of interest proteins, the strategy applied may be anion-exchange chromatography or cation-exchange chromatography. These two strategies differ on the ion-exchange ligands used, which are divided into two major types according its charge: anion and cation exchangers (table 4). Anion exchangers are used in anion-exchange chromatography, retaining anions, whereas cation exchangers are used in cation-exchange chromatography, retaining cations. Ion exchangers are also categorized into strong and weak ion exchangers. A strong ion-exchanger has the ability of maintaining their charge characteristics and ion-exchange capacity over a wide pH range, while weak ion exchangers are more susceptible to pH variations [73].

Therefore, the anion exchanger Quaternary ammonium (Q), commonly called as Q-Sepharose®, constitutes a positively charged ligand. They have the capacity to bind negatively charged proteins and, since proteins have an overall negative charge at a pH above their pI, pH conditions of mobile phase can be manipulated to bind this type of biomolecules. On the other hand, cation exchangers constitutes a negatively charged ligands, having the capacity of binding positively charged proteins. They may be used for binding proteins that are positive at pH value below the pI [71].

Table 4 - Ion exchangers and respectively functional groups (adapted from [70]).

Anion exchangers		Functional group
Quaternary ammonium (Q)	Strong	$-O-CH_2N^+(CH_3)_3$
Diethylaminoethyl (DEAE)	Weak	$-O-CH_2CH_2N^+H(CH_2CH_3)_2$
Diethylaminopropyl (ANX)	Weak	$-O-CH_2CHOHCH_2N^+H(CH_2CH_3)_2$
Cation exchangers		**Functional group**
Sulfopropyl (SP)	Strong	$-O-CH_2CHOHCH_2OCH_2CH_2CH_2SO_3^-$
Methyl sulfonate (S)	Strong	$-O-CH_2CHOHCH_2OCH_2CHOHCH_2SO_3^-$
Carboxymethyl (CM)	Weak	$-O-CH_2COO^-$

A successful IEC must comprise several steps, starting with equilibration step to establish ideal mobile phase conditions for interest biomolecules binding, followed by sample application. The proteins, oppositely charged to ligand, interact with ligand and bind to the column, whereas the uncharged or the similarly charged proteins elute instantaneously, showing the lowest retention time. After establishing the binding of interest biomolecules, its elution from the matrix is needed. Here lies the main difference between the application of IEC for sample purification and for protein fractionation. For sample purification, the elution step, commonly referred as wash step, is required in order to remove possible contaminants, present in the sample, and which interacted with the ligands of the column. On the other hand, in protein fractionation, the elution is required but not as a wash step, as all the proteins are wanted. This step only induces the bonded proteins to elute from the ligands [74].

The elution of biomolecules may be trigged by changing mobile phase conditions, including increasing of ionic strength (Figure 10) or changing of pH. Finally, to stablish the state of equilibrium of the column and to remove any ionic compound bound to matrix, a wash step at high salt concentration must be applied, followed by a re-equilibration step.

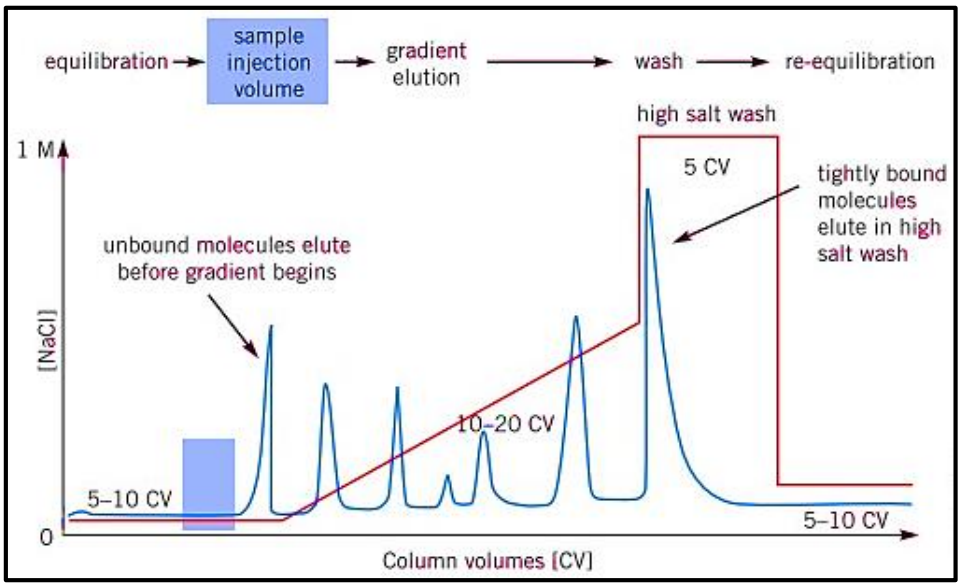

Figure 10 - Typically approach in an ion-exchange chromatography (adapted from [70]).

IEC is very advantageous due to its high resolution and ability to fractionate proteins from complex samples as biological fluids, either by pI or due to distinct charge characteristics of proteins.

Isoelectric Focusing (IEF) can also be applied as a fractionation technique upstream of LC/MS workflows. IEF consists of protein separation according to their pI, and in this case, it can be performed using the MicroRotofor cell. This technique is very advantageous since it is designed for an efficient and reproducible IEF of samples with limited availability, as it is the case of fluids like VH [75].

Fractionation of human vitreous humor proteins using gel based methodologies

Over the past years, researchers have developed and optimized the electrophoresis process for application in proteomics set-ups, where one-dimensional sodium dodecyl sulfate–polyacrylamide gel electrophoresis (1D-PAGE or SDS-PAGE) and two-dimensional sodium dodecyl sulfate–polyacrylamide gel electrophoresis (2D-PAGE) are the two most common techniques.

SDS-PAGE consists of protein separation according its molecular weight through a denaturing polyacrylamide gel matrix. This can be achieved through subjecting proteins to high electric current. Proteins are first denatured by SDS, which confers them a negative charge, allowing their migration from the negative pole to the positive. Also, proteins are denatured by extremely high temperatures, losing their native structure, which allows their migration only by molecular weight and not to differences in its structure.

The applied acrylamide percentage influences the pore size and the gel matrix rigidity, thus affecting the electrophoresis resolution, the dispersion of biomolecules, and magnitude of migration [76]. According to Rath and colleagues (2013), gels with low acrylamide concentration causes an increased mobility of both large and small proteins. However, increasing of acrylamide concentrations prevents the migration of larger proteins, facilitating the migration of smaller proteins, and thus providing better resolution [77].

This technique has been included in proteomics set-up, either as first step for protein fractionation or after pre-fractionation using chromatography or isoelectric focusing. However, due to the high complexity of proteome, before using 1D-PAGE to separate peptides or proteins, sample fractionation must be successfully performed using another methodology in order to reduce its complexity [68]. Hence, combining IEC and 1D-PAGE, the number of bands in 1D-PAGE is increased and, each band can be forwardly digested to proceed to protein identification.

In typical 2D-PAGE procedure, the sample is firstly subjected to an isoelectric focusing (IEF), which consists in the separation of the proteins according to their pI, in a strip gel with a large pH range. After the first step, proteins separated by pI are then separated by molecular weight,

by aligning the strip in the top of acrylamide gel and exposing proteins denatured with SDS to electric current [78].

Over the past few years, 2D-PAGE has been increasingly applied in proteomics studies, since it can display several proteins simultaneously on a single gel, allowing an high resolution separation of the sample proteome and facilitating the detection of protein isoforms and PTMs [79].

Due to the high loading capacity of sample, this technique is capable of detecting and identifying low abundance proteins, making 2D-PAGE a high sensitive approach. However, variations in sample handling before 2D-PAGE can give rise to loss or gain of protein spots [80]. Combining IEC and 1D-PAGE, it is possible to achieve the same degree of separation, albeit with less resolution, but compared with 2D-PAGE, the sample must be firstly fractionated through IEC, contrarily to 2D-PAGE. Also, when comparing several 2D-PAGE gels, only the differential spots are then identified, whereas in 1D-PAGE all the observed bands in the gel are identified.

After performing 1D or 2D-PAGE, the polyacrylamide gels must be stained in order to reveal the separated proteins. It is ideal that the staining does not influence the amino acid composition, hydrophobicity, but allows the bind of proteins to the stain. There are several stains that can be applied in ophthalmology studies, including organic dyes, silver staining, and fluorescent stains. The choice of the ideal stain is crucial for the sensibility and success of the vitreous humor protein identification and so it must be compatible with the downstream procedure [54,81].

Protein gel stains

Organic Dyes

The most common organic dye is Coomassie Brilliant Blue (CBB) R-250 (red-tinted) and its dimethylated derivative G-250 (green-tinted), represented in figure 11.

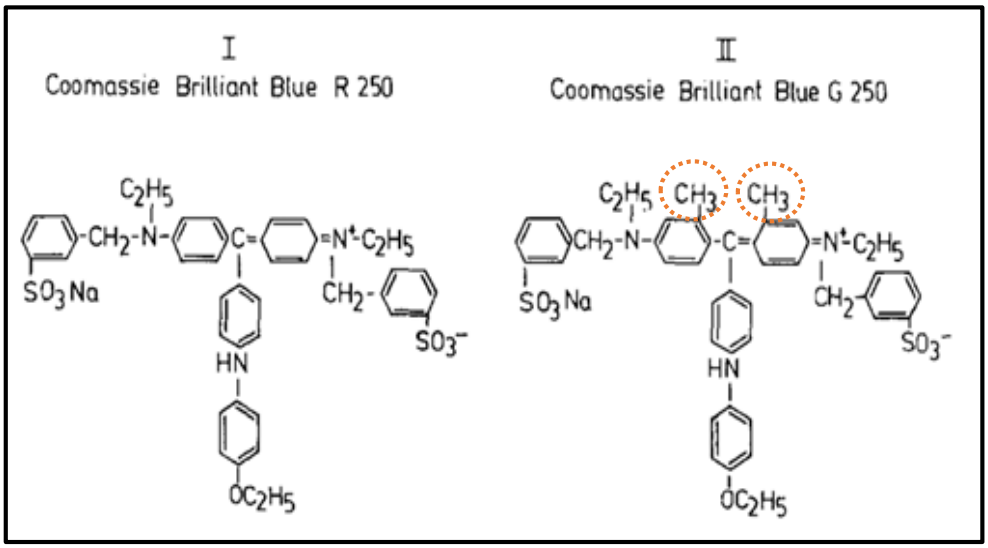

Figure 11 - Organic structure of Coomassie Brilliant Blue R-250 (I) and G-250 (II). The orange circles indicates the presence of the two methyl groups in CBB G-250 (adapted from [82]).

For classical Coomassie Blue staining, R-250 is used, and it is demonstrated that this staining follows the Lambert-Beer law since shows higher color intensity with higher protein concentrations [54]. However, Coomassie Blue staining R-250 has proven not to be as sensible as G-250. G-250 has two additional methyl groups compared to R-250, so this dye has colloidal properties and improved sensitivity, being denominated colloidal coomassie dye. Colloid suspensions are produced due to its relatively low solubility, allowing the dye to exist in micellar form. Since the micelles are too large to penetrate most gel matrices, the colloid suspensions only have affinity with zones of gel containing proteins. This allows a background free staining, with well-defined protein bands/spots. The main advantage of colloidal coomassie blue is its easy performance and direct compatibility with mass spectrometry [54].

Silver Staining

Silver staining methods are proved to be far more sensitive than CBB in polyacrylamide gels, having a detection level of 0.2-2ng. However, this value depends on the binding of silver ions to the amino acid side chains [83,84].

The silver ions have the ability to bind proteins through electrostatic interactions with COO^- groups of Asp and Glu or by attaching with the imidazole, SH, SCH_3 and NH_3 groups of His, Cys, Met and Lys, respectively [54,81]. After binding to these groups, free metallic silver is reduced. The reduction of silver only occurs at the gel surface, where unbound silver ions are in lower concentrations. Hence, is the reduction of silver that allow the visualization of protein bands, as spots [84].

Although this method shows a high sensitivity, it has several disadvantages since it is quite laborious, complex and expensive, and may not always be compatible with subsequent processes [83]. For instance, silver staining is incompatible with mass spectrometry since this staining method oxidizes amino acid side chains and introduces glutaraldehyde cross-links, interfering with sequence determination.

Fluorescent Stains

Fluorescent stains show an equivalent sensitivity to silver staining method (1-2ng), and has a widely compatibility to subsequent MS procedure [85].

There are a group of fluorescent dyes that are becoming very common, called CyDyes, which includes Cy3 and Cy5, represented in figure 12. CyDyes are cyanine dyes carrying N-hydroxysuccinimidyl ester reactive group derivatives (propyl-Cy3 and methyl-Cy5) that binds covalently with ε-amino group of lysine residues in proteins [57,86].

These dyes (Cy3 and Cy5) can be used together in two-dimensional fluorescence difference gel electrophoresis (2D-DIGE), with the purpose of labelling proteins and quantify them, improving the sensitivity and accuracy of their identification [87].

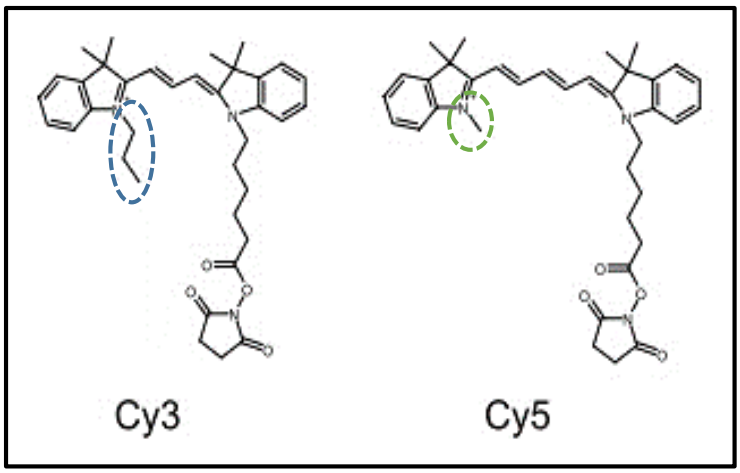

Figure 12 - Illustration of Cy3 and Cy5. The blue circle indicates the presence of the propyl group in Cy3. The green circle indicates the presence of the methyl group in Cy5 (adapted from [86]).

1.3.1.3 Identification of human vitreous humor proteins

After its fractionation, VH samples should be in optimal conditions to perform the proteins identification. Mass Spectrometry (MS) is the most used analytical technique for the identification of proteins. It allows a precise determination of the structure and molecular weight of molecules, including proteins and peptides, through analysis of their mass/charge (m/z) ratio [88,89]. This is possible due to an ionization source that focuses the charged and neutral molecules present in a sample, under vacuum, and generates charged ions into the gas phase [89]. After all the molecules are ionized, a separation occurs according to their mass/charge ration, giving result to a mass spectrum, as seen in figure 13. The two most common ionization techniques are Electrospray ionization (ESI) and matrix-assisted laser desorption/ionization (MALDI).

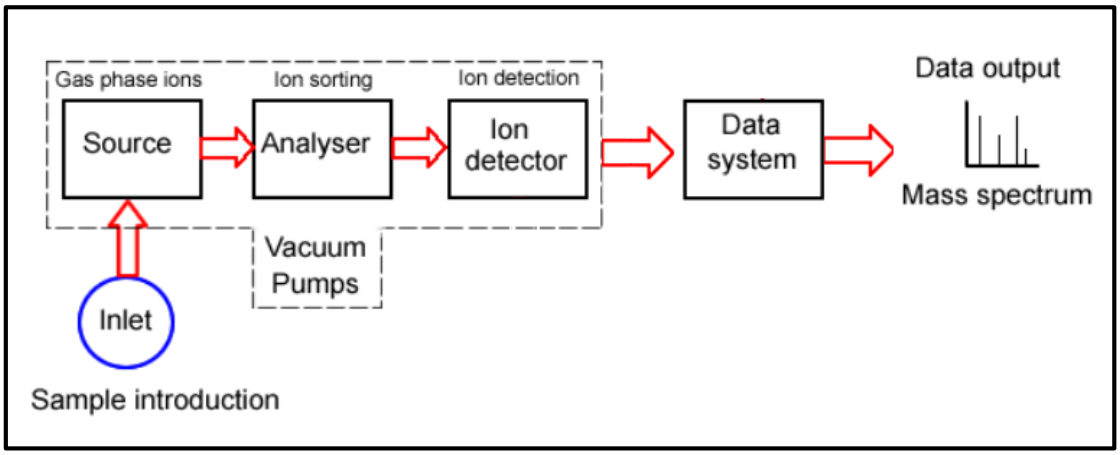

Figure 13 - Simplified diagram of a typical mass spectrometer (adapted from [90]).

Electrospray ionization

In ESI the protein dissolved in an acidic solution is pulverized through a metal needle, under an intense electric field, causing its ionization [91].

In order to perform ESI, the solvent must be dissolved, and the way to do so is through an inert gas stream, which flows in the opposite direction from the pulverization. Lastly, the protein in the ionized and gaseous state is then drawn to inside the mass spectrometer, where is analyzed [91].

Matrix-assisted laser desorption/ionization (MALDI)

Contrarily to ESI, MALDI performance is less affected by buffer components, detergents and contaminants, and allows mass determination of intact protein and also peptide, with sufficient accuracy for sequence validation. Thus, MALDI currently represents an effective alternative to ESI [92].

The principal desorption mass analyzer that allows the analysis of biomolecules is called matrix-assisted laser desorption/ionization (MALDI), which is combined with time-of-flight mass spectrometer (TOF), that separates and detect ions according to their m/z ratio.

MALDI has an ionization system that generates ions through the collision between the laser and a chosen matrix [89]. For protein sequencing and posterior identification, MALDI ionization system is combined with TOF (MALDI-TOF) or with two mass spectrometry analyzers in tandem (MALDI-TOF/TOF) [91]. For measure m/z ratio, TOF analyzer uses a high-voltage electric field which accelerates ions into the chamber and therefore measures the time they take until they reach the detector. As all ions have the same charge, their velocity will depend on their mass. As figure 14 shows, a laser is fired in the analyte-matrix mixture, providing the ionization of the analyte. After ionization, a high voltage is applied, allowing the acceleration and flight of the ions, from the source, into the TOF analyzer, until reaching the detector. The path of ions into TOF analyzer is crucial to differentiate ions since smaller molecules will travel faster and longer distances than larger molecules. So, small ions present lower TOF and large ions larger TOF because they take more time to achieve the detector. Each TOF correspond to m/z ratio, defined by the calibration of MALDI-TOF-TOF, information that is used to provide a peptide mass mapping, which will be analyzed in order to identify the corresponding protein [93].

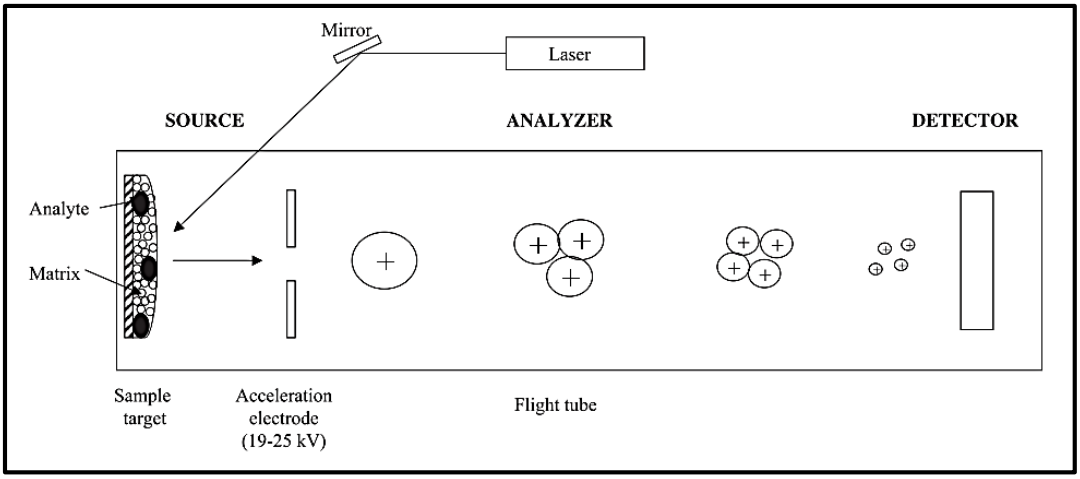

Figure 14 - Fundamental of the MALDI-TOF-TOF (adapted from [93]).

In MALDI occurs a soft ionization, since it does not decompose or fragments the analyzed biomolecules. Hence, to facilitate the ionization process, it is used a matrix which is generally a small organic molecule. Hence, in this technique, the protein mixture is firstly dissolved in an acid matrix, and then, through the energy induced by a laser, the sample is desorbed into the gas phase. Thus, the matrix absorbs photon energy from the laser beam and transfers it into excitation energy of the sample [91], protonating the sample into ions (+1 charge).

The choice of the acid matrix is crucial for the good performance of the experiment, and depends on the analyte and its properties [94]. The matrix mixture allows a better resolution [92] and is responsible for the transfer of protons to the molecules, making them positively ionized [91]. The ideal matrix should form micro-crystals with the sample, and should have a low sublimation temperature. The most common acid matrix applied in proteomics approaches are α-Cyano-4-hydroxycinnamic acid (CHCA), sinapic acid (SA) and 2,5-Dihydroxybenzoic acid (DHB), characterized in table 5.

Table 5 - The most common matrix used for the sample preparation for MALDI-TOF/TOF. (✓) Soluble; (×) Insoluble (adapted from [94]).

Matrix	Analyte	Solubility	Characteristics
CHCA	Low mass proteins and peptides	- Organic solvents (✓) - Water (×)	- Forms small homogeneous crystals - High internal energy in the analyte **High resolution for low mass proteins**
SA	High mass proteins	- Organic solvents (✓) - Water (×)	- Forms small homogeneous crystals - Low internal energy in the analyte **High resolution for high mass proteins**
DHB	Peptides, glycoproteins and glucans	- Organic solvents (✓) - Water (✓)	- Forms big crystal needles **Lower resolution**

When the matrix is applied along with analyzed molecules, the solvent evaporates leaving the sample in crystalized state in the plate spot, ready to be analyzed through MALDI-TOF. Then, the sample is examined under vacuum and subjected to a UV laser. Matrix molecules absorbs the laser energy, and leaves the sample surface, carrying ionized molecules of the sample into the gas phase.

Afterwards, TOF mass spectrometer accelerates the ions, under a high-voltage electric field, where they reach the detector with different velocities, enabling the calculation of mass/charge ratio of each ion detected. The resulted m/z information is, then, translated in a mass spectrum. Peptides within a specific mass range are selected and are submitted to fragmentation through Collision Induced Dissociation (CID). In this stage, the peptide is exposed to a chemically inert gas which separates the peptide into two fragments, where one is ionized and the other becomes uncharged. After fragmentation, m/z values of the resulted ions are calculated according their TOF. As a final point, MS/MS data is compared to database information using bioinformatic methods, in order to identify the peptide and posteriorly, the protein [95]. In this way, MALDI-TOF/TOF allows versatile molecular analysis with broad-ranging applications, showing several advantages. MALDI is a soft ionization, i.e. does not fragmentizes or decomposes the molecules, which allows the analysis of thermosensitive samples. Permits the analysis of a sample mixture, generating well-defined peaks, and as the samples are in the solid state, they can be stored for a long period of time [96].

Bioinformatic analysis of proteomics data

There are several possible ways to perform peptide identification, for instance, MS/MS spectra can be carried out through database dependent or independent searching.

In database independent searching, the peptide identification is performed by *de novo* sequencing without using any protein database. This type of identification can be useful when researching un-sequenced organisms, novel peptides and peptides with PTMs.

On the other hand, there are several database dependent search programs that allow protein database search. In this type of strategy, experimental MS/MS spectra is compared against theoretical mass values from a protein database [97]. The calculated theoretical peptide mass values are obtained after submitting them to the used cleavage rules. Then, using the proper algorithm, the peptide with the highest matching score is selected and identified according to the match protein sequence.

In ProteinPilot software, MS/MS information is analyzed with two database search programs, Paragon™ and Mascot™ which work independently from each other [98]. ProteinPilot Software is a revolutionary protein database search tool, since it combines these two algorithms.

Paragon™ is a probability approach that allows the rapid and simultaneous searching of a large number of biological and other modifications, genetic variants and unexpected cleavages. After peptide identification, Paragon Algorithm performs a statistical analysis regarding the ProtScores for each protein, where peptides with higher confidence have the ability to contribute more to ProtScores. The Total ProtScore is based on the sum of all peptides that are

related to a certain protein, whereas the Unused ProtScore represents the measure of protein confidence of the unique peptides used to a protein identification, i.e., peptides that only correspond to a unique protein [99]. For 95% confidence, the required Unused/Total ProtScore must be 1.3/1.3, representing the cutoff for protein identification.

Although the number of identified proteins has been increasing with the number of published articles, there is still a long way to evolve, in order to acquire the best and significant results.

1.3.2 Identified proteins in retinal pathologies

Before proteomic techniques were commonly performed, the used strategies were based essentially in biochemical or immunological techniques, such as enzymology, immunoblotting and ELISA. However, with the evolution and improvement of proteomic strategies, several studies were carried out with the view to characterize the VH proteome and explore biochemical and physiological networks of related proteins in a certain ocular disease context [100]. In table 6, it can be observed the list of the most prominent proteins which expression is altered in VH in a disease context.

Table 6 - List of the most prominent proteins which expression is altered in an ocular disease (adapted from [100]).

Ocular disease	Up-regulated proteins	Down-regulated proteins	Reports
Diabetic Retinopathy	Immunoglobin, glycoprotein, PEDF		Kim et al. (2007)
	Serine protease inhibitor	α1-antitrypsin, apolipoprotein A-IV	Danser et al. (1989)
Diabetic macular edema	PEDF, apolipoprotein A-IV, plasma retinol binding protein, vitamin D binding protein	Apolipoprotein H	Ouchi et al. (2005)
	Hemopexin	ß-crystalline S, clusterin, transthyretin	Antonetti et al. (1998) and Hernández et al. (2013)
Proliferative vitreoretinopathy	PEDF, clusterin, cathepsin D, transthyretin, apolipoprotein A-IV		Zhang et al. (2011)
	Albumin, transferrin	Tubulin, pyruvate kinase 3, enolase	Mitry et al. (2010)
Age-related macular degeneration	Metalloproteinase 9		Yu et al. (2008)
	α1-antitrypsin, prostaglandin H2-D isomerase, serotransferrin, fibrinogen		Yu et al. (2012)

1.3.3 Proteomic Approaches in human VH of RRD

Unfortunately, there is still not much information about proteomic analysis of RRD VH samples, however it is known that severe cases of RRD can trigger PVR, and so it is extremely important to understand the proteomic aspect of this disease and to work out strategies to avoid this pathology.

For instance, Cassidy et al. in 1998 demonstrated that elevated levels of platelet-derived growth factor (PDGF) in VH samples may imply the formation of PVR, since it stimulates fibroblasts and collagen gel contraction [101].

In 2008, Shitama and colleagues, analyzed VH samples of several diseases, including PDR, RRD and PVR, and compared them to control samples, i.e. patients with MH, epiretinal membrane (ERM) and healthy postmortem donors. This study was the first report of quantitative proteome study of VH fluid samples with the main of searching for unique proteins that probably manifested in pathophysiological states of such vitreoretinal diseases.

The strategy combining 2DE and mass spectrometry showed that protein levels in RRD and PVR were substantially higher comparing to control samples and to other analyzed diseases. Also, although pigment epithelium derived factor (PEDF) was observed in all samples, its expression level was higher in RRD samples. This fact demonstrates that RRD, once it represents high protein levels, is a disease with a major potential and interest for proteomic analysis [36].

Previous studies from our proteomic research group showed that, using a novel technique named isobaric tag for relative and absolute quantitation (iTRAQ), 1030 proteins were identified, from which 112 were found differently expressed in VH of RRD (n=4) compared to macular epiretinal membranes (MEM) control samples (n=4).

iTRAQ labelling is a solution-based technique that is commonly used in proteomics for identification and relative quantitation [14]. In this technique, samples are digested with tripsin, into peptides, and iTRAQ labelling is performed. The iTRAQ reagents labels covalently the N-terminus and ε-amino side chain of lysine residues of each peptide. iTRAQ improves quantitative reproducibility, higher sensitivity and has broad applications in proteomics research [102].

In this strategy, depletion of HAPs was performed before trypsin digestion, and after iTRAQ labelling, the resulting peptides were fractionated through RP-LC. Afterwards, bioinformatics analysis of MS/MS data was performed.

Although iTRAQ is a technique that has been increasingly common, it presents a few weaknesses, such as the fact that the iTRAQ reagents are expensive and requires specialized equipment compared to label-free methods. Thus it is crucial to develop proteomic strategies that benefits the identification of VH proteins.

Chapter 2

Objectives

Although variations in the protein contents of VH samples make proteomic investigation difficult, it has been demonstrated that the proteomic analysis of VH is extremely important to understand those alterations.

So, the present research aims to study the VH proteome of RRD using a different strategy, combining depletion of HAPs by affinity chromatography, in order to enrich the sample, fractionation of proteins using IEC and SDS-PAGE, with the view to achieve a successful protein separation, and protein identification by mass spectrometry using MALDI-TOF/TOF, with the purpose of identifying the RRD proteome.

With this strategy it was our goal to identify proteins which have not yet been found, in order to advance in discovering the RRD proteome.

Chapter 3

Materials and Methods

3.1 Materials

Ultrapure reagent-grade water used for preparing solutions and buffers was obtained from the Mili-Q system (Milipore/Waters). Sodium phosphate, sodium chloride and glycine were obtained from Fisher Scientific (Loughborough, UK). Concentrators 3.000 MWCO were obtained from GE Healthcare Life Sciences (Uppsala, Sweden). Tri-ethanolamine, l-histidine and tris(hydroxymethyl) aminomethane (Tris) were obtained from Sigma-Aldrich (Missouri, USA), ethanolamine and di-ethanolamine were obtained from Acros Organics (New Jersey, USA). Acrylamide 4K-solution 40% was obtained from PanReac AppliChem (Darmstadt, Germany). Coomassie brilliant blue G-250 was obtained from Fluka Chemika (Buchs, Switzerland). CHAPS was obtained from Amresco (Ohio, USA). The full range rainbow protein standards used for estimation of subunit molecular weight was purchased from GE Healthcare Life Sciences (Uppsalla, Sweden). Ammonium bicarbonate and trypsin from porcine pancreas were obtained from Sigma-Aldrich (Missouri, USA). Trifluoroacetic acid (TFA) and iodoacetamide (IAA) were also obtained from Sigma-Aldrich (Missouri, USA). Dithiothreitol (DTT) was obtained from HiMedia (Mumbai, India). All the used solvents including methanol, acetonitrile and LC-MS grade water were obtained from Fisher Scientific (Loughborough, UK).

3.2 Sample Collection and Preparation

3.2.1 Sample Collection

Vitreous humor fluid samples were obtained from the “Centro Hospitalar de Leiria - Pombal” from individuals undergoing PPV, which removes the central VH gel. PPV is realized for the treatment of vitreoretinal pathologies. The sample collection protocol was approved by the hospital ethics committee and an informed consent was obtained from all patients. Undiluted vitreous fluid samples (500-1000 µL) were collected in sterilized tubes during chirurgical procedure, placed on ice and stored at -80ºC until further processing. For this study, VH samples from patients with RRD were selected, from ages comprehended between 26 and 82. VH samples contaminated with plasma and RRD samples associated with other diseases were also excluded from this study.

3.2.2 Sample Preparation

The adequate preparation of VH samples is critical to preserve quality and to further successful protein processing and analysis. Ocular tissues and cells require processing that should result in the complete solubilization, disaggregation, reduction and denaturation of proteins. For that purpose, VH samples were centrifuged at 14.000 x g for approximately 10 min at 4ºC, in order to separate the structural component of VH from the liquid one. Total protein concentration was measured by Pierce™ BCA Protein Assay Kit (Thermo Scientifics, USA) according to the kit manufacturer's protocol, using BSA as standard and calibration control samples (125-8000 µg/mL). During vitrectomy, haemorrage can occur leading to a massive influx of serum proteins into the VH, contaminating the VH proteome. This limits VH analysis because serum proteins can mask the presence of important, but less abundant, vitreous and retinal proteins [12]. In order to guarantee the absence of contamination from plasma material such as hemoglobin, samples with blood contamination were excluded, i.e. samples containing more than 5mg/mL of hemoglobin. This quantitation was carried out using Hemoglobin Colorimetric Assay Kit obtained from Cayman Chemical (Michigan, USA), following the kit manufacturer's protocol.

3.3 Depletion and Fractionation of Human Vitreous Proteins

The main limitation of proteomics methods in the analysis of human samples is the detection of low abundant proteins due the high complexity of these type of samples and wide dynamic range of protein abundance. To overcome this problem, before MS proteome analysis, the most abundant proteins, such as HSA and IgG, must be removed from VH samples and low abundant proteins must be fractionated appropriately. This strategy allows the reduction of VH samples complexity, leading to a more income protein identification [39], [65].

3.3.1 Depletion of High Abundant Proteins

Taking into account the complexity of VH, it is important to establish suitable chromatographic conditions to separate HAPs from LAPs and recover these proteins for further analysis. The depletion of HSA and IgG was performed at room temperature in an ÄKTA Pure system with UNICORN 6 software (GE Healthcare, Uppsala, Sweden) equipped with a 2 mL injection loop. All buffers pumped in the system were prepared with Mili-Q system water, filtered through a 0.20 µm pore size membrane (Schleicher Schuell, Dassel, Germany) and degassed ultrasonically. The most abundant proteins were separated from the LAPs by affinity chromatography using HiTrap™ Albumin & IgG Depletion 1 mL column obtained from GE Healthcare Life Sciences (Uppsala, Sweden). The column is prepacked with a combination of anti-HSA Sepharose High Performance and Protein G Sepharose High Performance mixture. The ligand of anti-HSA Sepharose High Performance is based on a single domain antibody fragment with high capacity for HSA. The ligand of Protein G Sepharose High Performance is derivative from the IgG binding regions of Protein G, and binds human IgG_1, IgG_2, IgG_3 and IgG_4. The column was equilibrated with a buffer composed by 20 mM sodium phosphate and 0.15 M NaCl, pH 7.4 at a flow rate of

1mL/min. Using this chromatographic conditions, 1 mL of RRD vitreous, ranging from 0.5 to 4 mg of total protein mass, were loaded onto the column using a partial loop strategy with 2 mL loop. The depleted proteins were eluted with 5 column volume (CV) of equilibration buffer and collected in a single fraction. For elution of HSA and IgG, the mobile phase was changed to 0.1M glycine buffer, pH 2.7, and this condition was maintained for 10 CV. The HAPs fraction were also collected in a single fraction. In all chromatographic runs, absorbance was continuously monitored at 280nm, as well as conductivity and pH. The collected samples were concentrated and desalted with Vivapsin 6 3.000MW concentrators, and stored at -20ºC. Depleted samples were then pooled together and concentrated to a volume of 2mL in order to increase VH proteins concentration before further fractionation.

3.3.2 Protein Fractionation by Ion-Exchange Chromatography

As referred above, recovered LAPs fractions were pooled and fractionated through Ion-Exchange Chromatography. Protein fractionation was performed at room temperature in an ÄKTA Pure system with UNICORN 6 software (GE Healthcare, Uppsala, Sweden) equipped with a 500 µL injection loop. All buffers pumped in the system were prepared with Mili-Q system water, filtered through a 0.20 µm pore size membrane (Schleicher Schuell, Dassel, Germany) and degassed ultrasonically. This technique is based on protein fractionation according to their isoelectric point using a HiScreen™ Capto™ Q 4.7 mL column, containing a strong anion exchanger quaternary ammonium coupled to Sepharose (Q-Sepharose®), obtained from GE Healthcare (Uppsala, Sweden). The column was equilibrated with a buffer A composed by 20mM l-histidine, 20 mM tris, 20 mM ethanolamine, 20 mM di-ethanolamine and 20 mM tri-ethanolamine, pH 10, at a flow rate of 1.5mL/min. Polled samples with 2-4 mg of protein mass were injected onto the column using a 500 µL loop, at the same chromatographic conditions. The non-adsorbed fraction, containing the proteins positively charged at basic pH, was eluted with 1 column volume (CV) of equilibration buffer. In order to promote a gradual elution of adsorbed proteins, a linear pH gradient from buffer A until 100% of buffer B (20 mM l-histidine, 20 mM tris, 20 mM ethanolamine, 20 mM di-ethanolamine and 20 mM tri-ethanolamine, 5 mM NaCl, pH 5) was applied during 15-20 CV, at the same flow rate. In all chromatographic runs, absorbance was continuously monitored at 280nm, as well as conductivity and pH. Throughout the fractionation process, 1.8-2.0 mL fractions were collected. The collected samples were evaporated to a volume near 200 µL, at room temperature, using a UNIVAPO Rotational Vacuum Concentrator 100ECH, and stored at 4ºC until further analysis. Alternately to SDS-PAGE, these samples were also analyzed directly by MALDI-TOF/TOF.

3.3.3 Protein separation by Gel Electrophoresis SDS-PAGE

After pI-based protein fractionation by IEC, SDS-PAGE was performed in order to separate proteins according to their molecular weight. The fractions were pooled according to the pH registered in chromatogram. In order to remove salts and other impurities, a

chloroform/methanol precipitation was performed. After the precipitation, the obtained pellet was solubilized with a suitable buffer (150 mM NaCl, 50 mM tris, 1 mM MgCl2, 2% CHAPS, pH 8.0) and each 10µL of solubilized sample were supplemented by adding 3.5 µL of loading buffer (100 mM tris-HCl (pH 6.8), 4% (w/v) SDS, 0.01% bromophenol blue (w/v), 0.2% glycerol (v/v), 0.02% ß-mercaptoethanol (v/v)). Afterwards, proteins were denatured by boiling samples containing loading buffer for 5 min at 100ºC. SDS-PAGE were performed according to the method of Laemmli [103]. Then, samples were loaded on 4% stacking gel and run on 12.5% resolving acrylamide gel containing 10% SDS using Amersham SE260 Mighty Small II Deluxe Mini Vertical Electrophoresis Unit system, with a running buffer containing 25 mM tris, 192 mM glycine, 0.1% (w/v) SDS at 150 V for nearby 90 min. After electrophoresis, gels were stained using a colloidal coomassie brilliant blue solution dubbed "Blue Silver", according to the experimental protocol of Candiano and co-workers [104]. The coomassie-stained gels were also subjected to a densitometric scan on ImageScanner III obtained from GE Healthcare Life Sciences (Uppsala, Sweden).

3.4 Mass Spectrometry

3.4.1 Trypsin digestion

Each lane on acrylamide gels were cut into slices of 1-1.5 mm. Gel slices were then destained with 3 wash cycles of 50% acetonitrile (ACN) and 50 mM ammonium bicarbonate (AB) and incubated at 37ºC overnight. Then, after removing the wash solution, ACN was added to the gels. Afterwards, proteins were reduced and alkylated with 10 mM DTT at 56ºC for an hour and 55 mM IAA at room temperature for 30min, respectively. Gel slices were rehydrated in ice, for about an hour, using 30 µL of 10ng/µL trypsin solution in 25% AB and 9% ACN. After the absorption of trypsin solution, gel slices were immersed by adding 25% AB and 9% ACN and proteins were digested overnight at 37ºC. Lastly, the tryptic peptides were firstly extracted with 0.1% TFA in water (37ºC/15min) and, then, with 0.1% TFA in 50% ACN (37ºC/15min). The extracted tryptic peptides were combined in the same eppendorf and dried by vaccum centrifugation at room temperature.

3.4.2 In solution digestion

Firstly, each fraction obtained from protein fractionation by IEC was combined in several pH ranges. Then, proteins were reduced and denatured with 50mM tris-HCl (pH 8), 5mM DTT and 8M urea for a protein final concentration of approximately 1mg/mL. The solubilized sample was incubated at 60ºC for 60min and then, the sample was cooled to room temperature. Afterwards, 50mM NH_4HCO_3 (pH 7.8) was added to the sample in order to bring the urea concentration to less than 1M. For the digestion with trypsin, MS grade trypsin (1ug/µL stock) was added so that the ratio of trypsin:protein in the sample was between 1:20 and 1:100 (w/w). The digestion reaction was incubated at 37ºC for at least an hour. Lastly, the digestion reaction was stopped

with formic acid. Aliquots of 10 to 20µL were then cleaned-up using a reverse-phase C18 pipette tip obtained from Millipore® (Molsheim, France), in order to remove urea and other contaminants.

3.4.3 MALDI-TOF/TOF

Before spotting the tryptic peptides into MALDI plate, peptide samples were clean-up with Millipore® Zip-tip C18 0.1-10 µL pipette tips (Molsheim, France). For sample cleaning, dried samples were acidified by solubilizing peptides with 1% TFA, at pH lower than 3. Zip-tip pipette tips were regenerated 5 times using pure ACN and equilibrated 10 times with 0.1% TFA in LC-MS grade water. After equilibration, tryptic peptides were loaded by careful aspiration and disposal of samples. Using 0.1% TFA in LC-MS grade water, tryptic peptides adsorbed in tips were washed 3 times. Finally, peptides were eluted in 5µL of 80% ACN with 0.1% TFA solution. Thus, with tryptic peptides desalted and concentrated, it was possible to perform MALDI-TOF/TOF analysis. Firstly, CHCA matrix was prepared by adding 60 µL of 0.1% TFA in 50% ACN to a CHCA aliquot obtained from AB SCIEX (Massachusetts, USA) in order to obtain a matrix solution with 5 mg/mL concentration. The used standards are a mixture of CalMix 1 and CalMix 2, obtained from AB SCIEX Peptide Mass Standard Kit (Massachusetts, USA), and were prepared adding 24 µL of CHCA matrix solution. For MALDI-TOF/TOF calibration, each component present in the standard mixture has a precise mass. For instance, components such as des-arg-bradykinin (904.4681m/z), angiotensin I (1296.6853m/z), glu-fibrinopeptide B (1570.6774m/z) and ACTH (2093.0867m/z) are present in CalMix 1 and CalMix2 combined, and the calibration was achieved comparing the standards precise mass values with the experimental mass values. Samples were prepared by combining 5 µL of clean-up peptide samples with 5 µL of CHCA matrix solution. After preparation, the MALDI plate was spotted with the samples and standards. Finally, samples were analyzed on 4800 plus MALDI-TOF/TOF analyzer (Applied Biosystems), equipped with a 355 nm laser. All spots were initially analyzed in positive MS mode in the range 800 to 4000 m/z by averaging 1500 laser spots. The eight more intense MS ions per spot that satisfied the precursor criteria (200 ppm fraction-to-fraction precursor exclusion, S/N ratio >25) were selected for subsequent MS/MS analysis. All MS/MS data were acquired using 1 keV collision energy with a total of 1500 laser shots per spectrum. Peak lists were export to an MGF file using the function Peaks to Mascot 4000 Series Explorer™ Software (Applied Biosystems).

3.4.4 Protein identification

Protein identification was performed using Paragon algorithm from ProteinPilot™ Software 4.5, from AB SCIEX (Massachusetts, USA), under a 95% confidence, where each peak list was searched against the Homo sapiens UniprotKB canonical & isoform reviewed database (47,878 entries) downloaded from Swiss-Prot Homo sapiens in FASTA format, at 3 August 2015. The “unused” and “total protein” scores are ProteinPilot specific terms that stands for peptides specific for protein identification and all peptides measured for protein identification, respectively. In this

study an unused/total protein score of 1.3/1.3 was used as a cutoff for protein identification. The search parameters took into consideration cysteine modification by methyl-methanethiosulfonate, digestion of peptides with trypsin and default biological modification settings [105].

After protein identification, STRING10 was used to find protein clusters with shared protein-protein associations and to get an overall overview of the proteins found in RRD vitreous. To get a more profound knowledge about biological process, cellular compartment and molecular function of each identified protein, STRAP software was used. STRAP (Software Tool for Rapid Annotation of Proteins) is a program that automatically annotates a protein list with information which helps in the meaningful interpretation of data from mass spectrometry and other techniques.

Chapter 4

Results and Discussion

4.1 Depletion of High Abundant Proteins

As presented before, human VH fluid is composed by highly abundant proteins, including HSA and IgG. HAPs can overlap and mask the signal of the most significant ones, present in lower concentrations, and therefore, prevent their detection [50]. In order to overcome this, it is required the depletion of HAPs from each VH sample, from 25 patients with ages comprehended between 26 and 82 years old (Appendix I), which allows the access to LAPs fractions, the proteins of interest. Depletion was carried on through immunoaffinity chromatography, using a column with high affinity to HSA and IgG composed by anti-albumin antibodies and recombinant protein G fragment ligands. The typical chromatogram obtained in depletion of human VH samples with HiTrap Albumin and IgG column is represented in figure 15.

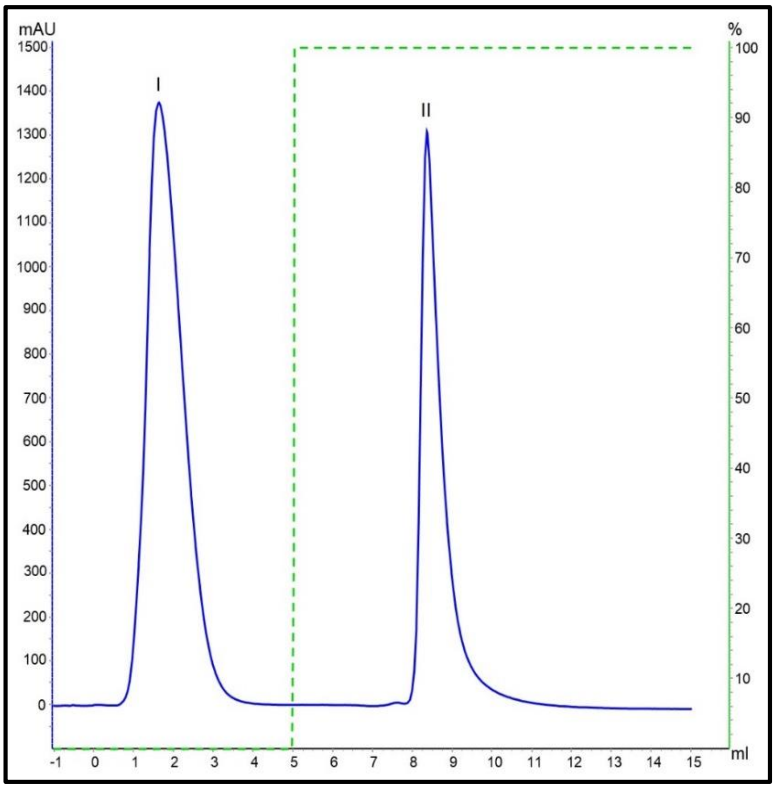

Figure 15 - Representative chromatogram of depletion procedure for removal of HAPs, Albumin and IgG, from human vitreous humor samples. Affinity chromatography was performed with 20 mM sodium phosphate in 0.15 M NaCl (pH 7.4) followed by a pH change with 0.1 M glycine buffer (pH 2.7). Blue line represents the absorbance at 280 nm and the dashed green line represents the percentage of buffer B (0.1 M glycine buffer). I – LAPs peak; II – HAPs.

In this case, the binding buffer (20 mM sodium phosphate in 0.15 M NaCl) was used to promote the antibody:antigen interactions. For this to occur, the binding buffer was used at physiological pH (≈7.4), since it is the suitable pH for maintaining the antibodies stability. The ligands of the HiTrap column are monoclonal anti-albumin antibody and protein G antigens which bind to Albumin and IgG, respectively. Monoclonal antibodies bind specifically to the antigens, allowing an effective elution with one specific condition, in this case pH change.

In depletion of Albumin and IgG, 0.1 M glycine buffer is usually used in order to elute these HAPs. The ideal elution buffer dissociates effectively the antibody or antigen without occurring its irreversibly denaturing or inactivating. However, all elution buffers used in immunoaffinity chromatography cause some loss of the antibody or antigen function, leading to the limitation of the number of times that the column can be reused.

Glycine at a pH of 2-3, can successfully dissociate most protein-protein and antibody-antigen binding interactions, without affecting drastically the protein structure. Although it is scientifically proved that low pH may damage some antibodies and proteins, in the present work that is not a concern, since only the first peak was recovered due to the presence of proteins of interest for subsequent procedures. However, since the ligands of the used column are antibodies or antigens, the column loses gradually its efficiency due to the use of such drastic pH in elution. Also, any bound protein (antigen/antibody) that remains in the column decreases the column's binding capacity, limiting its use.

To verify the efficiency of HSA and IgG depletion, both LAPs and HAPs fractions were collected from peaks I and II (figure 15), respectively, and analyzed by SDS-PAGE, as shown in figure 16.

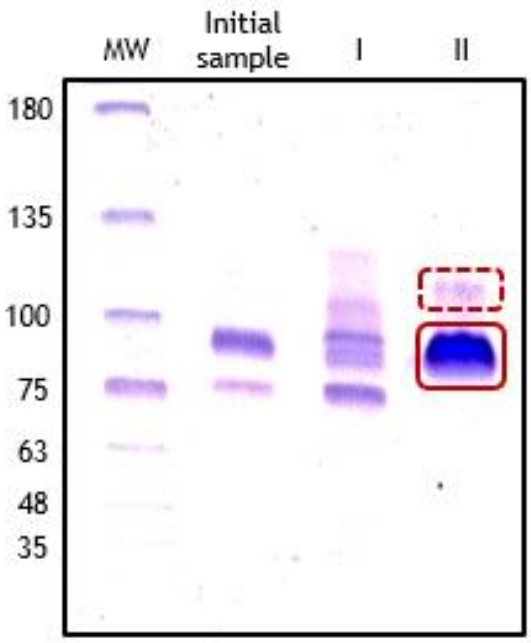

Figure 16 - SDS-PAGE analysis of collected samples in depletion technique. Lane MW - molecular weight standards; Initial sample – RRD sample before performing depletion of high abundant proteins; Lane I - first peak recovered from depletion; Lane II - second peak of depletion of the same sample. Albumin is identified in the red lined box and IgG identified in the red dashed box.

As represented in figure 15, the first peak corresponds to the depleted sample, from which were removed HAPs, and the second one corresponds to the HSA and IgG fraction. In the SDS-PAGE gel is also represented the protein profile of a RRD VH sample before the chromatographic depletion procedure. However, the analysis of both fractions collected in depletion chromatographic assays by SDS-PAGE, were only conducted for the first depleted samples. So, only initially HAPs were collected, concentrated and used to perform SDS-PAGE analysis, as seen the figure 16, in order to confirm the performance of the depletion step in the removal of HSA and IgG. This was due to the fact that the RRD VH samples are unique and rare in our sample bank, and they are required to the following methodologies.

The analysis of SDS-PAGE in figure 16, which is representative of the typical electrophoresis gels obtained in both fractions analysis after depletion, demonstrates that depletion of albumin and IgG was successfully achieved. The gel clearly indicates the presence of these two HAPs in the lane representing peak II, highlighted in red boxes, and their apparent absence in lane corresponding to peak I proteins. In lane II could be seen more bands that would be due to protein denaturation at 37ºC. These bands could also be due to the superposition of the four classes of IgG, which differ in its molecular weight and structure.

By removing this HAPs, it is possible to identify in the peak I lane several additional bands, which were not visible in initial VH sample. These novel displayed bands detected in peak I lane of SDS-PAGE gel, are LAPs that were overlapped by HAPs. These LAPs may be relevant in development of RRD and so, it is important its identification in VH analysis. These LAPs may give us information about the alterations that occur at the protein expression level in VH underlying RRD.

The analysis of the chromatogram obtained in depletion of human VH samples is also important to understand the efficiency of the procedure of removing of HSA and IgG. For instance, the height of the peaks (mAU) may give us that information. For the depletion of HAPS to be succeeded, the peak II (HSA and IgG) should present a higher absorbance than peak I once HAPs in a VH sample are about 80% of its constitution. However, the peak II on the chromatogram presented in figure 15 shows a lower absorbance (1300 mAU) than the first peak (1400 mAU), which is contrary to the expected in theory (figure 8). Although this manifestation occurred in several chromatographic assays, this could be due to the fact that the HSA and IgG percentage appears to be variable according to the patient and according to the disease state.

Besides the analysis of the chromatogram and SDS-PAGE, it also was performed the protein quantitation of the VH samples before and after depletion, in order to evaluate the efficiency of the process.

So, analysis of protein concentration of these two peaks confirms that depletion was in fact done successfully, presenting a HAPs removal percentage of nearby 90%, in this specific HV sample. In the depleted HV samples, the high abundant protein removal percentage presents an average of 71.3% (Appendix II). This was probably due to the fact that the column efficiency it is not always the same. Besides the fact that the column loses gradually its binding capacity, the sample injection by partial loop is not as reproducible as full loop injection. However the

partial loop injection method was required in this case, once the sample was scare, and it was a way to save sample.

4.2 Protein Fractionation by Ion-Exchange Chromatography

For this task, the previous depleted samples were combined, creating a RRD VH pool of 25 patients with ages comprehended between 26 and 82 years old, with a total protein concentration of 5.16 mg/mL. Pooling has the major advantage of decreasing overall variability that are due to differences between individuals [19], however there may be loss of LAPs. Nevertheless, due to small amount of available samples, it is a strategy that must be used in order to increase the protein quantity. Pooling was suitable in this study once the objective in this case was the protein identification. On the other hand, if the goal of this work was to quantify the expression level of the proteins in RRD VH sample, pooling would not be recommended.

In order to decrease sample complexity, protein fractionation was achieved through ion-exchange chromatography, on pI-based fractionation.

Isoelectric points of the proteins in a complex mixture are more likely to be distributed in a wider pH range. Hence, in order to obtain a successful fractionation, and since proteins ionize differently according to the environmental pH, it was required to establish conditions to create a wide pH range gradient [106]. The pH range was stabilized with the presence of NaCl, that was added to elution buffer, to linearize the gradient [69]. Q-Sepharose column, a strong anion exchanger, was chosen to perform protein fractionation because, as it is positively charged, it has the capacity of interact to negatively charged proteins. Also, Q-Sepharose as strong ion-exchanger, has the ability of maintaining their charge characteristics and ion-exchange capacity over a wide pH range, showing a highly linear and well-controllable pH gradient, which improves the efficiency of the method.

As it was previously stated, pI is when the protein acquires a net neutral charge and, depending on the chosen pH, the protein will be positively or negatively charged. At a pH below its pI, the protein will become positively charged and will not interact with anion exchanger (Figure 9). On the other hand, at a pH above its pI, the protein will become negatively charged and then will be capable to interact with anion exchanger (Figure 9). The applied chromatographic strategy was based on amphoteric properties of proteins. After equilibrium, VH samples are loaded on the column at basic pH, a pH where the majority of proteins present negative charge. So, these proteins interacted with anion exchanger, being adsorbed in the column. The pH of the starting buffer was maintained at a constant level (pH 10), initially, to ensure that the proteins obtained the opposite charge of the stationary phase in order to bind it.

The first proteins to elute are the positive ones that do not interact with the column positively charged. As during the experiment the pH decreases gradually, the adsorbed proteins acquired neutral and positive charge and became repelled by the positive charge from Q ligand, due to its positive functional group ($-O-CH_2N^+(CH_3)_3$), eluting gradually accordingly to their pI.

Analyzing the chromatogram presented in figure 17, we can verify that few proteins are positively charged proteins, represented in the first well-defined peak, the peak of non-adsorbed species. Beside the first peak, we do not verify along the pH gradient any other well-defined peaks, but broad peaks, which are typical chromatographic profile obtained in fractionation of high complex protein mixtures.

By the analysis of the chromatogram, it is also confirmed that the proteins elution is pH dependent, since they are eluted gradually along the pH gradient. So this strategy is considered suitable for the fractionating of proteins with near isoelectric points.

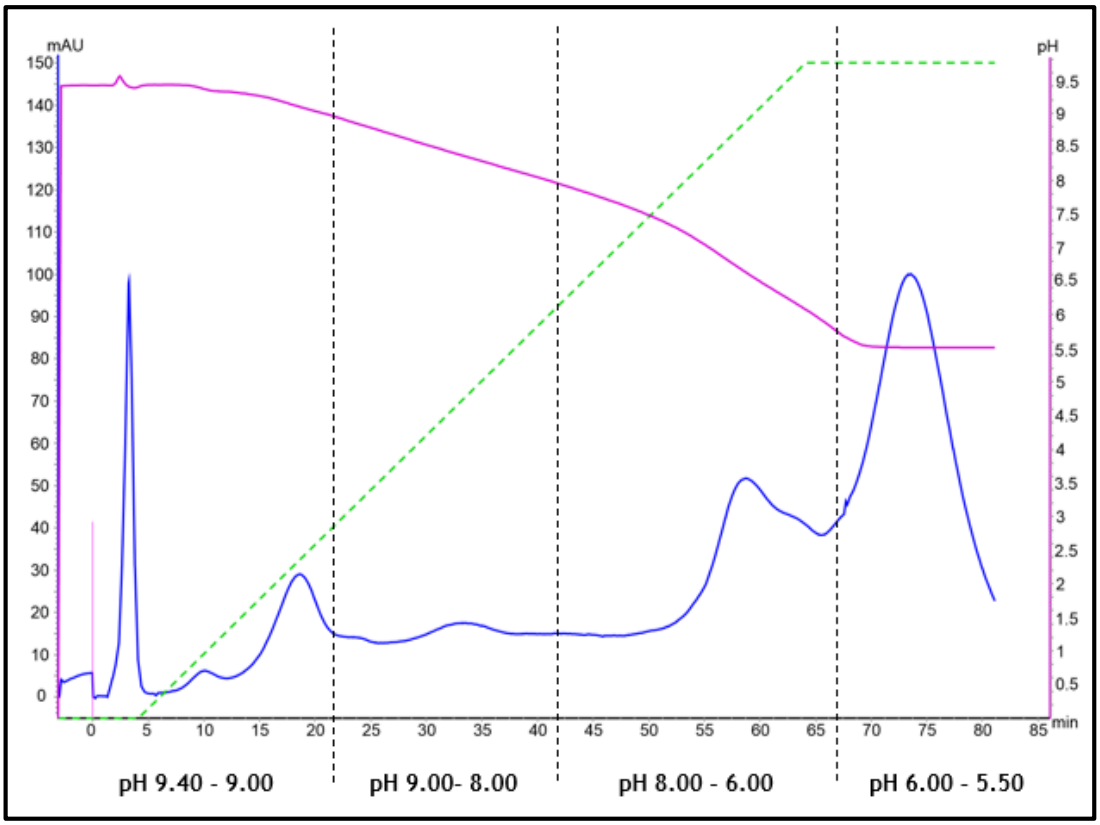

Figure 17 - Typical chromatogram obtained on protein fractionation of pooled depleted vitreous humor. Ion-exchange chromatography was performed with 20 mM L-histidine, 20 mM Tris, 20 mM Ethanolamine, 20 mM Di-ethanolamine and 20 mM Tri-ethanolamine (pH 10) followed by an increasing ionic strength and decreasing pH with 20 mM L-histidine, 20 mM Tris, 20 mM Ethanolamine, 20 mM Di-ethanolamine and 20 mM Tri-ethanolamine and 5 mM NaCl (pH 5). Blue line represents the absorbance at 280 nm, the dashed green line represents elution buffer concentration, and the pink line represents the pH gradient. The light pink line at 0 min represents the moment of sample injection into the column. The three black dashed lines represent the showed pH ranges.

However, it is considered that, in specific pH ranges, the protein fractionation may be improved. For example, in the extremes of applied pH gradient, i.e., at lower and higher pH, fractionation power may be improved by increasing pH gradient duration, decreasing the gradient slope. Also, we could have increased the pH gradient range, however wider pH ranges presents difficulties in maintaining the linearity. This makes us believe that protein fractionation can be improved in order to equilibrate, in a way, the protein amount between the fractions. It is certain that in some regions of the chromatogram, there will always be

different protein quantities due to their retention time, nevertheless, with the time increasing of pH gradient we can dilute that effect and have a better performance in protein fractionation. Nevertheless, with a better protein fractionation, we may not have sufficient protein quantity to perform downstream analysis by SDS-PAGE and MALDI. If the strategy of this study combined only LC-MALDI analysis, the gradient duration could have been increased, in order to guarantee the protein fractionation. However, since it was performed a second fractionation by MW, the increase of the gradient duration in IEC was not suitable in this process.

Besides, the gain in analysis time is also important when dealing with time consuming processes such as proteomics set-ups. Thus, there must be a compromise between gradient duration and yield, and so, slight losses in protein fractionation power and chromatographic resolution level are acceptable.

4.3 Protein fractionation by Gel Electrophoresis SDS-PAGE

After protein fractionation by IEC, the collected 1.8 mL fractions were pooled according to the pH range, as indicated in figures 17 and 18. The proteins present in each range were separated by SDS-PAGE, as seen in figure 18. This second fractionation is essential in order to separate protein species, and to concentrate them, guaranteeing its easy detection. Also, SDS-PAGE gives rise to several pH fractions that limits protein overlapping.

By analysis of SDS-PAGE in figure 18, it can be verified that there are differences in protein amounts between the pH ranges. The first fraction was in principle composed of proteins of pI between 9.40 and 9.00, the second fraction composed of proteins with pI range between 9.00 and 8.00, the third of proteins with pI range between 8.00 and 6.00 and lastly, the fourth fraction of proteins with pI below 6.00.

We can state that in first and second range there are less proteins than in third and last range. These facts were also demonstrated by Restuccia et al. in 2009, under the same procedure. The authors were studying the proteome of serum samples with the same strategy used in this work, and they found a larger number of proteins between pH of 4.6 and 5.4 and as well between 5.4 and 6.2, i.e. in the 2 fractions with lower pH. The same occurs in the present study, since we found more proteins in the last two fractions, with pH ranges between 8.00-6.00 and 6.00-5.50. This was probably due to the fact that the majority of the identified proteins in VH have their pI in the neutral and acid zone.

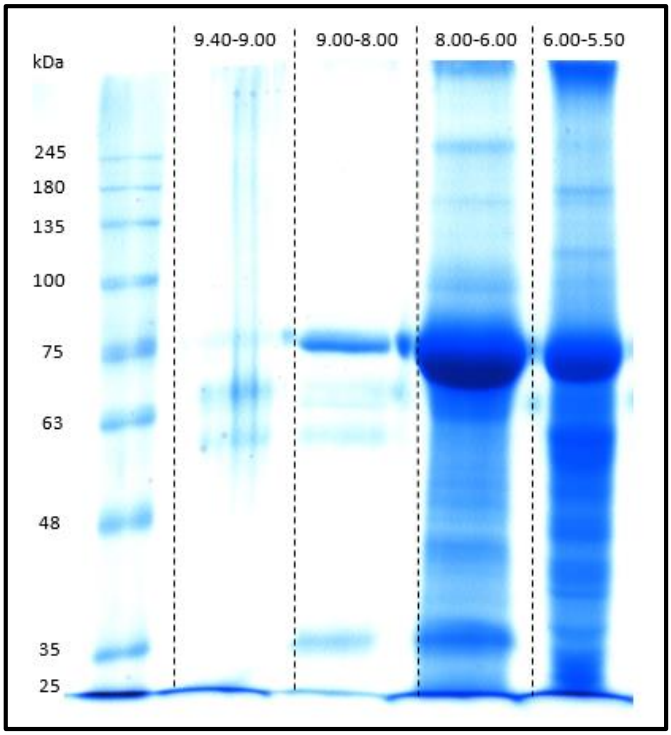

Figure 18 - Resulting SDS-PAGE of the fractions collected from protein fractionation.

SDS-PAGE results are in agreement with the chromatogram from figure 17, since the absorbance at 280 nm appeared to increase in the final of pH gradient, reaching a maximum of 100 mAU absorbance at pH of 5.5. Although the first peak is well-defined and reaches up to near 100 mAU, in 9.00-8.00 and 8.00-6.00 pH ranges we can observe several zones with many broad chromatographic peaks with absorbance ranging between 10 and near to 55 mAU, which may indicate the presence of several protein species. Specifically, the presence of these broad peaks may implies the consecutive elution of a large amount of proteins with near pI. So, although the intensity of these peaks (9.00-8.00 and 8.00-6.00) is slighter than the peaks in fraction 9.40-9.00, the resulting SDS-PAGE shows numerous bands in the two last pH fractions (figure 18).

4.4 Protein Identification by MALDI-TOF/TOF

To accomplish protein identification by MALDI-TOF/TOF, the gel was cut into 1-1.5 mm slices, as shown in figure 19. Gel slices were then treated with a trypsin solution, in order to digest the proteins trapped in acrylamide gel into peptides that were analyzed through MALDI-TOF/TOF.

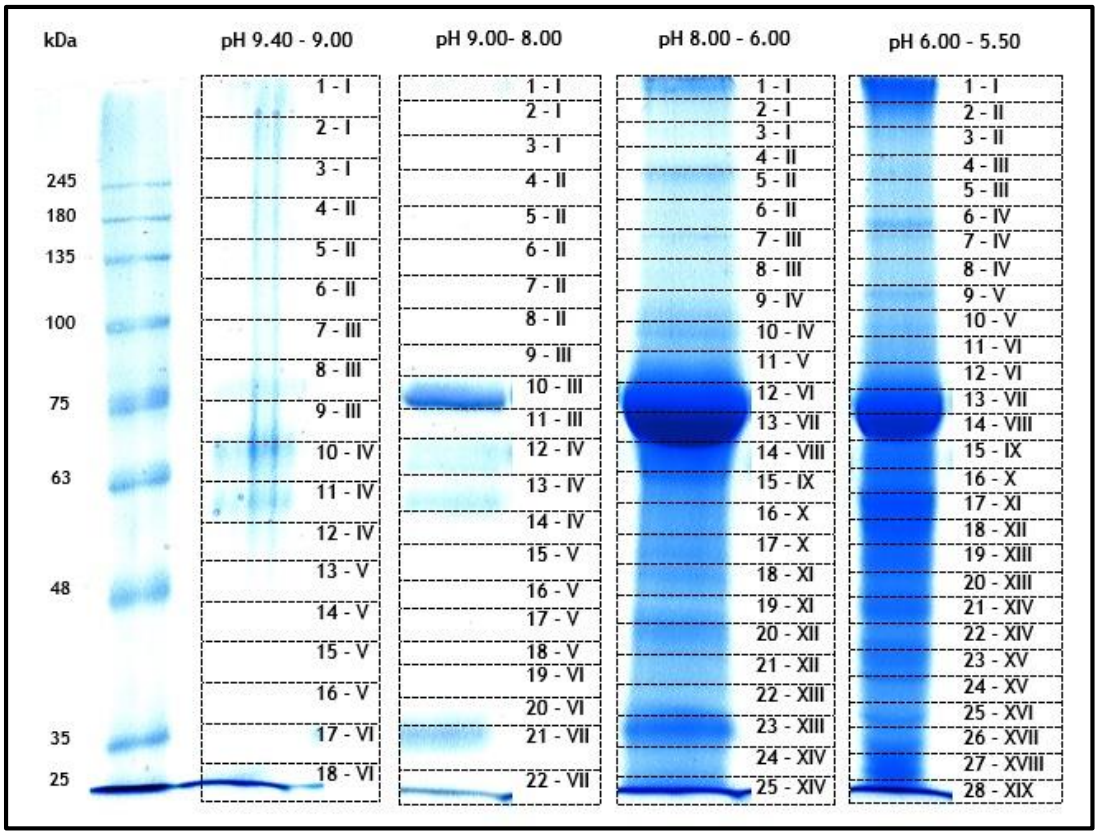

Figure 19 - SDS-PAGE gel slices, represented by the dashed black slices. Whole numbers represents slices and each roman numerals corresponds to a union of slices (MALDI fractions) that were posteriorly analyzed in a spot by MALDI-TOF/TOF.

The gel slices were cut under special care and attention in order to prevent keratin contaminations, which would prevent successful mass spectrometry analysis similarly to what occurs with HAPs. Bands of interest were cut on the edges of the staining region to minimize the acrylamide amount left in the slice.

Table 7 - Originated MALDI fractions according to pH range.

pH range	MALDI fractions
9.40-9.00	6
9.00-8.00	8
8.00-6.00	14
6.00-5.50	19

Each MALDI fraction (table 7) was then analyzed by MALDI-TOF/TOF and afterwards each spot spectrum was created. The matrix concentration was increased to ≈5mg/mL in order to improve MALDI results. In order to perform protein identification, MS/MS peaks were generated and crossed with UniProt Homo sapiens database, through ProteinPilot 4.5 using Paragon™ Algorithm. With this strategy, performed in two replicates, 236 proteins were found under a

95% confidence (Appendix III). Previous studies from our research group demonstrates that, using iTRAQ, 1030 proteins were found in VH samples, from which 334 were newly found. Comparing with these results, we verify that from the 236 proteins identified in the present study, 44 proteins were commonly found in both studies (Appendix IV). These 44 proteins appear to be the proteins found with higher score in both works, which indicates that these results are coherent. Thus, using the strategy presented in this work, 192 proteins were newly found comparing to previous studies from our research group.

For a more profound understanding of these 236 proteins, STRING 10 (Search Tool for the Retrieval of Interacting Genes/Proteins), which is a database of known and predicted protein-protein interactions, was used and it was established an overall network with these found VH proteins and their associations (figure 20).

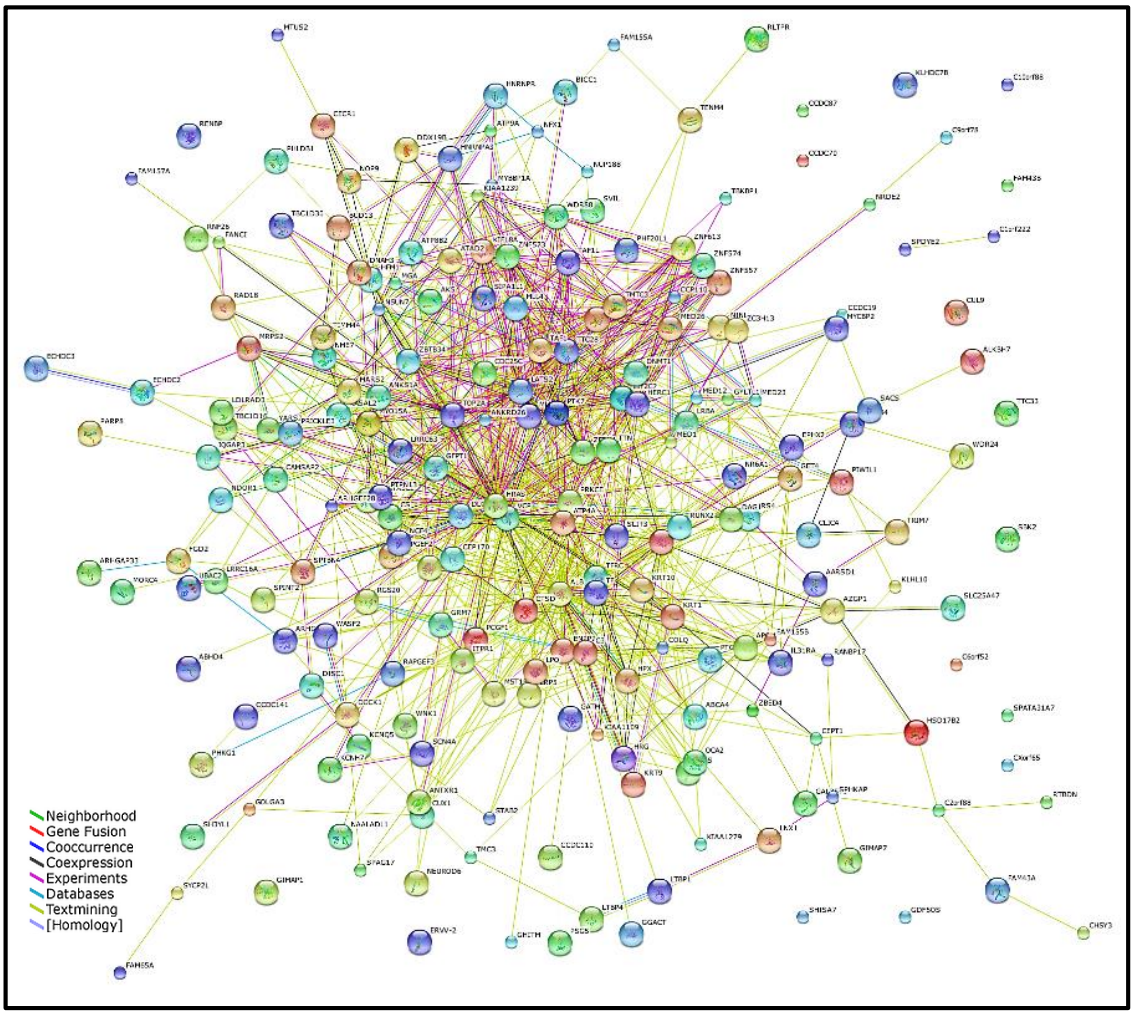

Figure 20 - Representation of the 236 identified proteins by MALDI-TOF/TOF. Every colored line represents a different related mechanism.

These results were searched through STRING 10 and the showed protein-protein associations were predicted using low confidence (score of 0.150). To achieve a more simple view of all 236 protein associations, the required confidence was increased to a minimum score of 0.400

(medium confidence). In this more confidence network, 95 proteins from the initial 236 found proteins had shared interactions, forming a protein cluster as showed in the following figure 21.

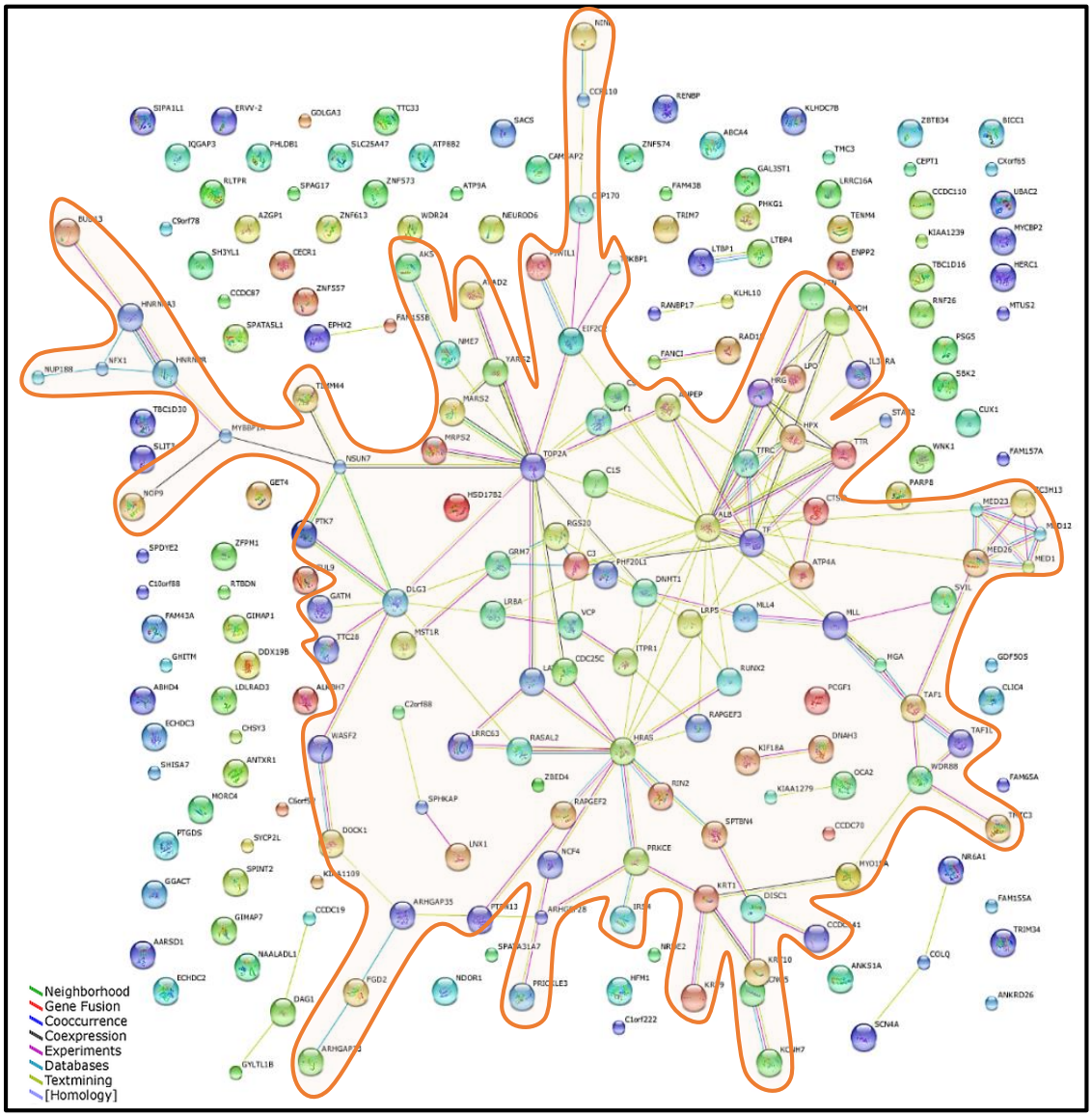

Figure 21 - Identified proteins by MALDI-TOF/TOF. Orange cluster represents only the connected proteins among the 236 found proteins, which are associated. These results were searched through STRING 10 with a medium confidence (score of 0.400). Every colored line represents a different related mechanism.

Though we found out that 95 proteins share similar biological mechanisms and functions, under a medium confidence (score of 0.400) as seen in figure 21, in order to achieve a more accurate proteomic analysis, it was needed to narrow down the confidence to its highest level (score of 0.900), as it can be observed in figure 22.

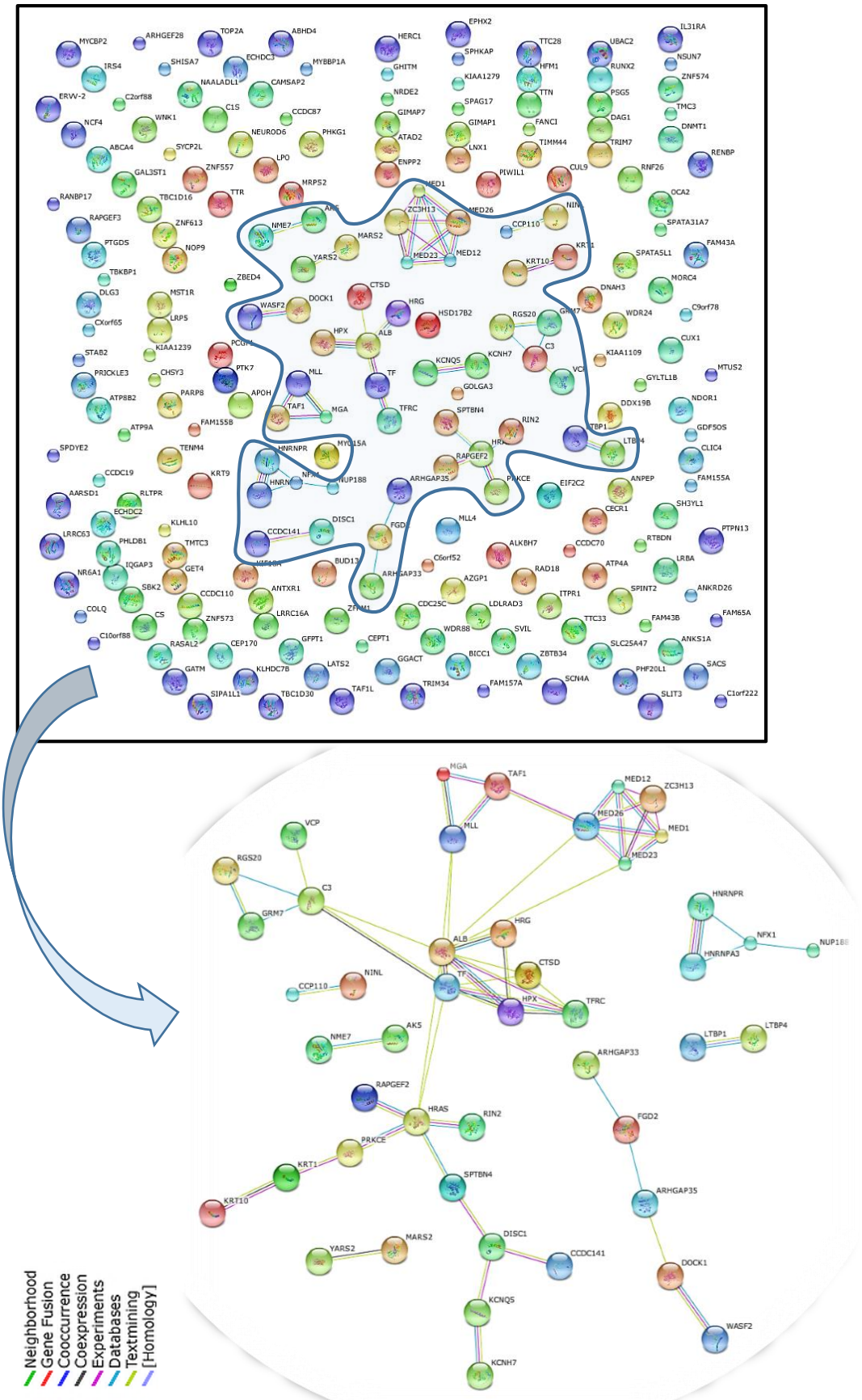

Figure 22 - Identified proteins by MALDI-TOF/TOF. Blue cluster represents only the connected proteins among the 236 found proteins, which are associated. These results were searched through STRING 10 with the highest confidence (score of 0.900). Every colored line represents a different related mechanism.

Under the highest confidence, we found that only 46 proteins, from the initial 236 proteins, share common biological mechanisms. STRING 10 also gives us information concerning KEEG analysis (Kyoto Encyclopedia of Genes and Genomes), which facilitates the understanding of pathways and molecular interactions in which the identified VH proteins participate, as seen in figure 23.

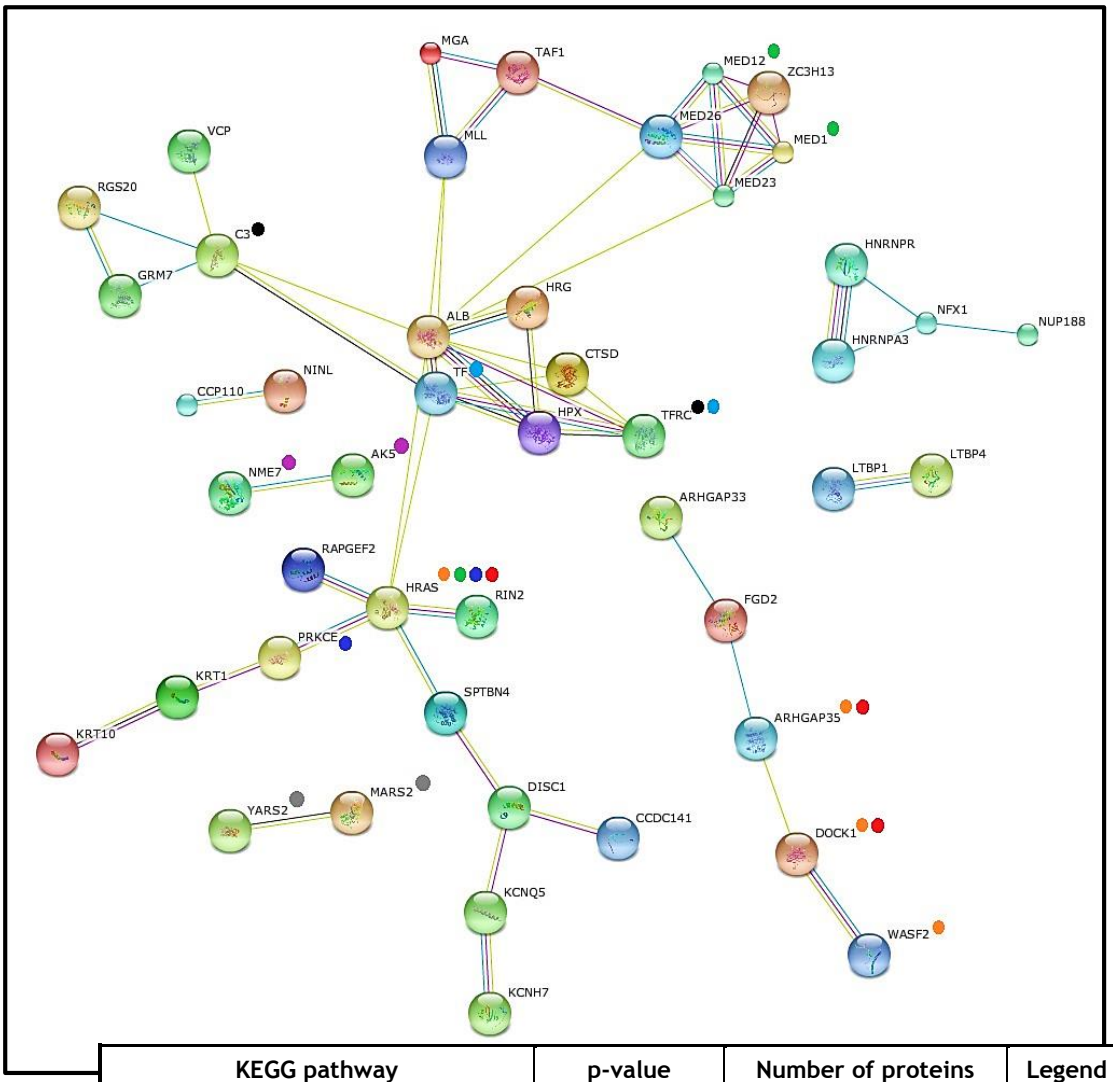

KEGG pathway	p-value	Number of proteins	Legend
Regulation of actin cytoskeleton	3.160e-1	4	
Thyroid hormone signaling	3.160e-1	3	
Aminoacyl-tRNA biosynthesis	3.489e-1	2	
Focal adhesion	3.750e-1	3	
Fc epsilon RI signaling	3.750e-1	2	
HIF-1 signaling	5.779e-1	2	
Phagosome	7.870e-1	2	
Purine metabolism	9.320e-1	2	

Figure 23 - KEGG analysis of the 46 connected proteins according to STRING10. Every colored circle represents a different KEGG pathway.

Therefore, figure 23 represents the proteins which are most significantly related, regarding KEGG analysis. For instance, proteins such as GTPase HRas (HRAS), Rho GTPase-activating protein 35 (ARHGAP35), Dedicator of cytokinesis protein 1 (DOCK1) and Wiskott-Aldrich syndrome protein family member 2 (WASF2) are significantly related with regulation of actin cytoskeleton pathways. Under this confidence (score of 0.900) these pathways show a great certainty, once the KEGG analysis have a suitable significance.

Also, some of these 46 proteins are related with other pathways such as thyroid hormone, Fc epsilon RI and HIF-1 signaling, aminoacyl-tRNA biosynthesis and metabolism pathways.

Furthermore, in order to obtain more biological information about these proteins, and to achieve the complete information about the involved mechanisms and in what way they act, the 46 proteins which were presented in the cluster of previous figure 22, were analyzed using STRAP 1.5 (Software Tool for Rapid Annotation of Proteins), according to their gene ontology (GO) classification. GO is a bioinformatics initiative which objective is to unify the representation of gene and gene product attributes across all species [107].

STRAP generates several tables containing all the GO terms information for biological process, cellular component and molecular function of the analyzed proteins, as shown in Appendix V.

To perform a simpler revision of the given information about these 46 proteins, STRAP gives us access to pie charts concerning GO terms, as showed in figure 24.

According to these pie charts we can verify that, regarding to biological processes 34 from the 46 studied proteins are involved in regulation processes and 39 are involved in cellular processes. Regarding to molecular functions, 34 proteins have binding functions and the majority of the 46 proteins are localized in the cytoplasm (24 proteins) and 26 proteins are nucleus.

This information may help us understand how these proteins interact with each other and where they act, being an extremely important aspect in proteomic analysis.

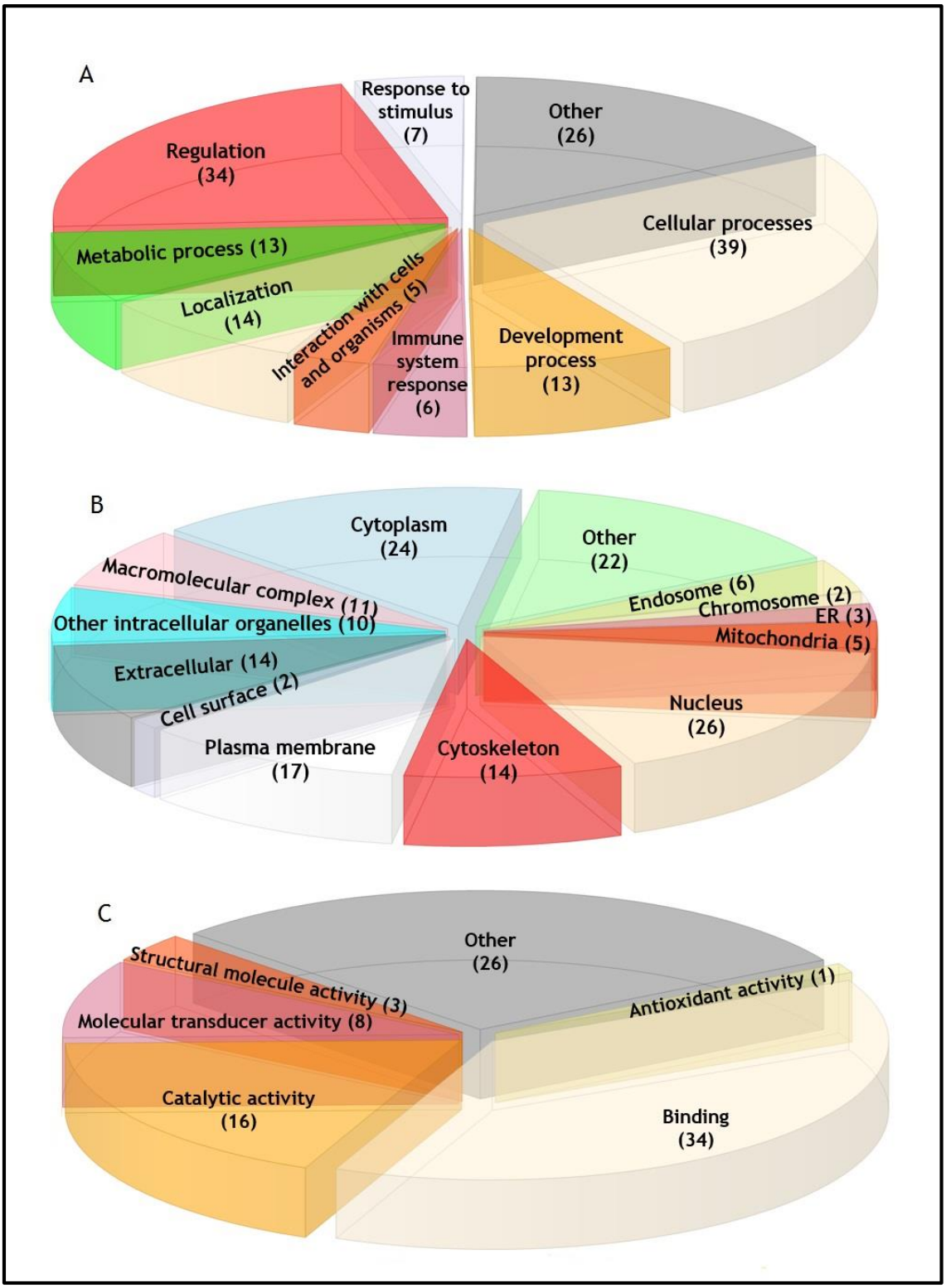

Figure 24 - Pie charts generated by STRAP software showing a resume of the predominance of several factors in the 46 studied proteins. (A) Biological Process; (B) Cellular Compartment; (C) Molecular Function according to the number of the associated proteins.

4.5 LC and MALDI-TOF/TOF

Alternatively, fractions collected in protein fractionation by IEX, were directly analyzed by MALDI-TOF/TOF. This was considered in order to investigate the effect of an additional fractionation procedure as SDS-PAGE in the overall protein identification yield, and in what way the elimination of this step would affect the final protein identification results.

After protein fractionation, the collected fractions were pooled according to the ten fractions with different pH ranges, as presented in figure 25.

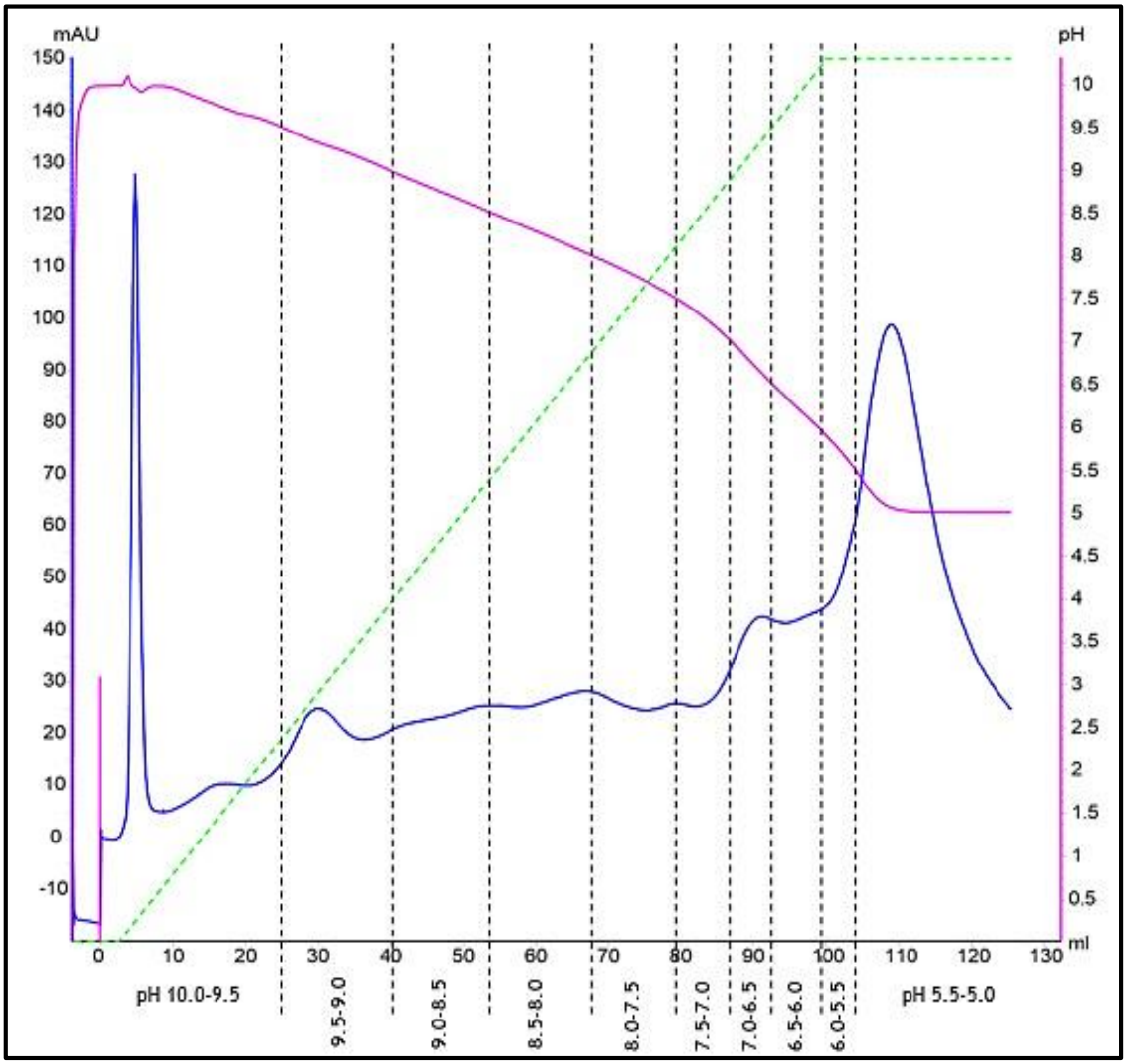

Figure 25 - Typical chromatogram obtained on protein fractionation of pooled depleted vitreous humor. Blue line represents the absorbance at 280 nm, the dashed green line represents elution buffer concentration, and the pink line represents the pH gradient. The light pink line at 0 min represents the moment of sample injection into the column. The black dashed lines represents the showed pH ranges.

After in solution-digestion of this fractions, each fraction was then analyzed by MALDI-TOF/TOF. Using this strategy, 110 proteins were found under a 95% confidence, using ProteinPilot software (Appendix VI).

Comparing the results of the two applied proteomics set-ups, it was verified that using this approach (LC and MALDI-TOF/TOF) less proteins were identified than using the strategy that combines LC, SDS-PAGE and MALDI-TOF/TOF, since we could find a total of 236 proteins. Also, only 10 from the identified proteins were found in both strategies, as it can be observed in figure 26.

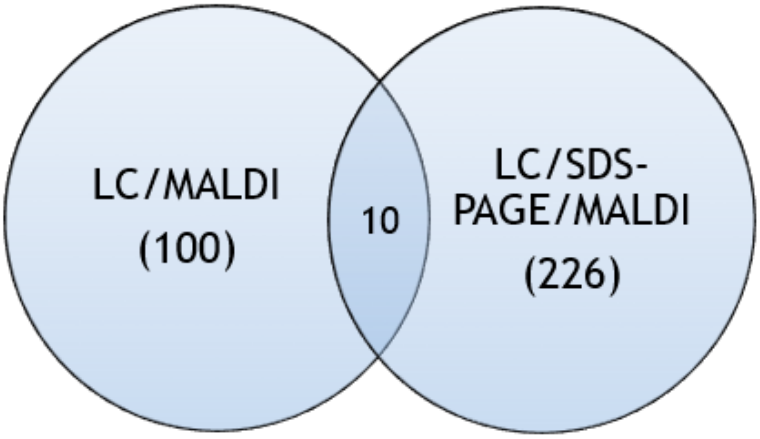

Figure 26 - Veen graph showing the amount of identified proteins in each used strategy, with 10 common identified proteins.

Since 100 proteins were identified through LC/MALDI strategy, and were not found in the previous approach, these proteins were analyzed using STRING software in order to obtain more information about these proteins, and confirm if these proteins have proteomic interactions.

Unlikely the proteins that were identified in the LC, SDS-PAGE, MALDI strategy, which had relevant and significant biological interactions, the proteins showed in figure 27 do not present significant clustering or interactions.

The same occurs regarding KEGG analysis, since no pathway presents a p-value inferior to 1.000, which makes us believe that the proteins identified in the strategy, without a second dimensional separation in this case performed through SDS-PAGE, do not present significant interactions.

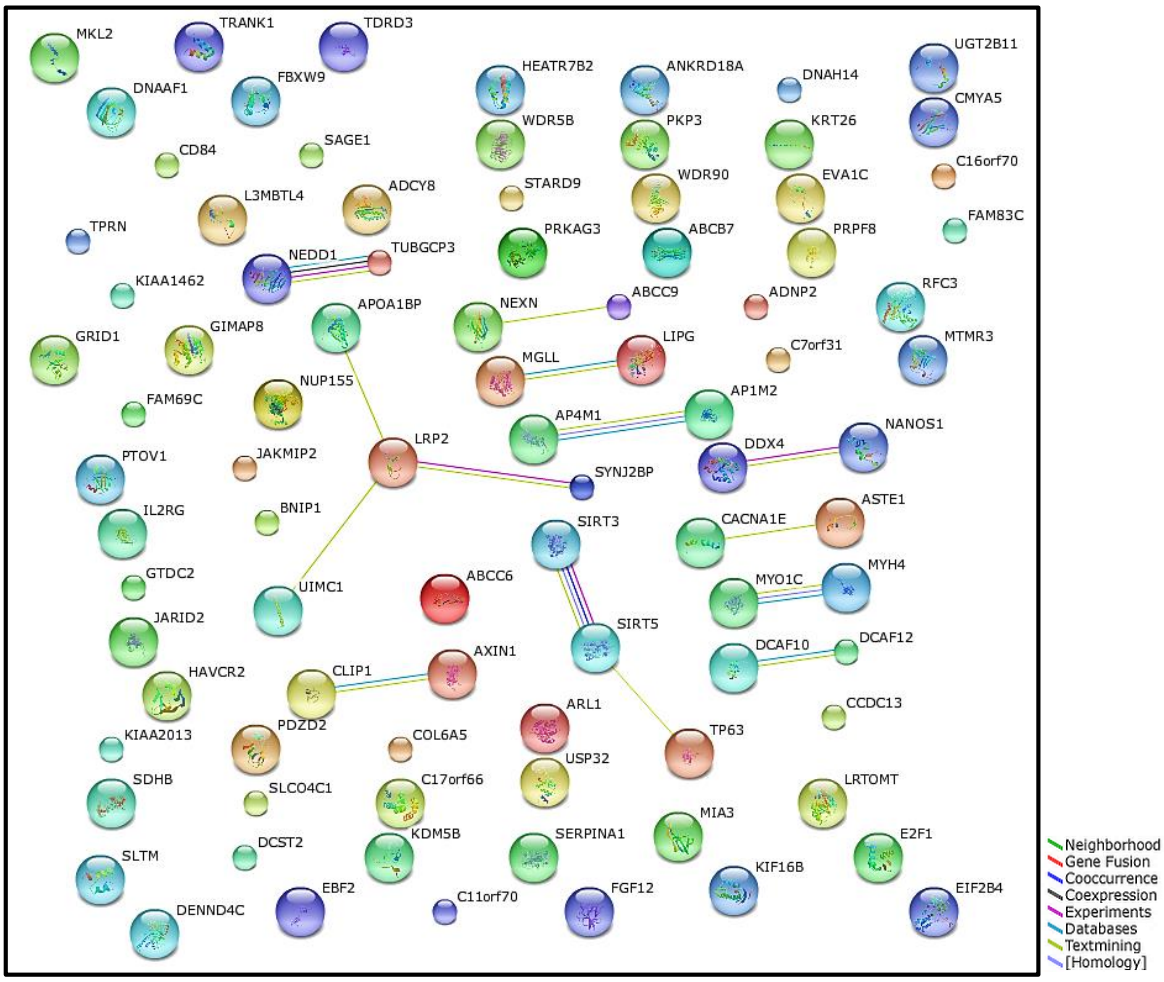

Figure 27 - Identified proteins by MALDI-TOF/TOF. These results were searched through STRING 10 with a medium confidence (score of 0.400). Every colored line represents a different related mechanism.

Thus, with these results, we can demonstrated that minor alterations in a proteomic strategy will affect the success of the process and the sustainability of the results, leading to the identification of more or less proteins. Thus, due to the complexity of VH samples, it is necessary to combine several proteomic methodologies (LC, SDS-PAGE and MALDI) in order to achieve the analysis of the complete vitreous proteome.

Unfortunately there is still not much information about proteomic analysis in RRD, however, comparing to other proteomic studies in ocular pathologies, the methodology performed in the present work allowed the identification of proteins in VH that had not yet been found in other proteomic studies, as it can be observed in figure 28. The list of the proteins identified in this work and in other reports can be accessed in Appendix VII.

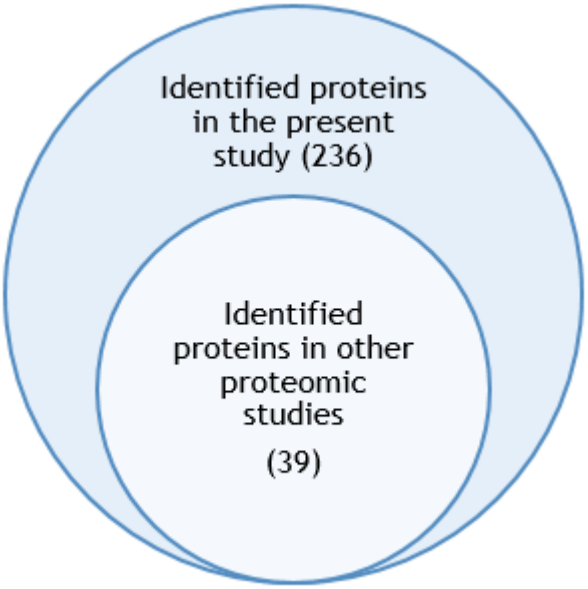

Figure 28 - Diagram comparing the number of proteins identified in the present study and in other proteomic studies.

The reported studies used to compare with the results from this work performed different strategies. For instance Nakanishi in 2002 combined 2DE and MS/MS, Gao in 2008 studied the present proteins in PDR using SDS and LC-MS/+MS, and Aretz in 2013 found 1105 proteins in 3 sample groups using the different methodology variants as seen in figure 6. Although these authors found a considerable number of proteins in various diseases, only 39 proteins were simultaneously found in this work and in other reports.

Therefore, this fact shows that the strategy used in this work has a great potential since it successfully identifies a large number of proteins, being advantageous in the discovery of RRD proteome.

Chapter 5

Conclusions

Over several years, RRD was thought out to be a physical phenomenon, caused by aging or a head trauma. However, few published works have recently demonstrated that this ocular disease is caused mainly by alterations in VH proteome, proposing a revolutionary statement in this matter. Until now, despite of not having still much information about RRD proteome, recent proteomic studies revealed a significant amount of identified proteins in RRD VH samples, using methodologies including iTRAQ, 2DE, LC-MS/MS and MALDI-TOF/TOF combined or separated.

In the present work, 236 proteins were found under a 95% confidence, combining different methodologies starting with depletion of Albumin and IgG, protein fractionation by IEX, protein separation by SDS-PAGE and protein identification with MALDI-TOF/TOF. It is noted that the incorporation of depletion of high abundant proteins in the overall process was extremely important in order to access to relevant proteins presented in lower abundance in VH. Also, LC and subsequent SDS-PAGE combined as fractionation methods appear to be a suitable strategy to obtain adequately separated vitreous humor proteins to further identification.

From the 236 identified proteins, it was verified that 46 shared mechanisms and biological processes, being involved in regulation processes and binding functions. Regarding KEGG analysis, several proteins are related with metabolic pathways, regulation pathways and with signaling pathways.

In conclusion, even though it is requested an optimization of the process in order to increase the number of identified VH proteins, the developed strategy allowed to find proteins which were not identified using other proteomic strategies.

Chapter 6

Future perspectives

Nowadays, due to the increase of average life expectancy, the improvement of the quality of life of worldwide population and the decreasing of the incidence of several pathologies, including ocular diseases, is a pursue goal. In this way, it is important the implementation of strategies that would benefit the discovery of the proteome of VH in ocular pathologies, like in this case RRD. It falls so much importance in the study of the RRD proteome because it is a chance to unravel the metabolic pathways in the several cellular stages, generating a much wider biological understanding. Therefore, it would become possible the identification of novel pharmaceutical targets and new biomarkers that would be used for clinical diagnosis.

Hence, a further step in this work, would be to optimize the overall process, particularly the chromatographic fractionation method, through decreasing the initial time of the column equilibration, implementing an earlier start of the pH gradient, and increasing the elution time, in order to equilibrate, if possible, the protein concentration in all pH ranges.

With the optimized process, it would be our objective to compare the RRD proteome with a control group, in order to find differences in the expression levels of proteins, and thus understanding in which mechanisms these proteins are involved.

With this kind of strategies, it would be possible the detection of differentially expressed proteins and posterior identification of biomarkers that would be helpful in the earlier diagnosis and treatment of several ocular diseases.

Chapter 7

References

[1] N. Mandal, S. Heegaard, J. U. Prause, B. Honoré, and H. Vorum, "Ocular proteomics with emphasis on two-dimensional gel electrophoresis and mass spectrometry.," *Biol. Proced. Online*, vol. 12, no. 1, pp. 56–88, Jan. 2009.

[2] World Health Organization, "Global Data On Visual Impairments 2010," 2010.

[3] K. D. Frick and A. Foster, "The magnitude and cost of global blindness: an increasing problem that can be alleviated," *Am. J. Ophthalmol.*, vol. 135, no. 4, pp. 471–476, Apr. 2003.

[4] J. M. Petrash, "Aging and age-related diseases of the ocular lens and vitreous body.," *Invest. Ophthalmol. Vis. Sci.*, vol. 54, no. 14, pp. 54–59, Dec. 2013.

[5] S. E. Ohia, Y. F. Njie-mbye, C. A. Opere, M. Kulkarni, and A. Barett, "Ocular Health, Vision, and a Healthy Diet," in *Inflammation, Advancing Age and Nutrition*, Elsevier, 2014, pp. 267–277.

[6] R. C. Tripathi and B. J. Tripathi, "Anatomy of the Human Eye, Orbit, and Adnexa," in *Vegetative Physiology and Biochemistry: THE EYE*, Elsevier, 1984, pp. 1–268.

[7] N. Patel, E. Solanki, R. Picciani, V. Cavett, J. a Caldwell-Busby, and S. K. Bhattacharya, "Strategies to recover proteins from ocular tissues for proteomics.," *Proteomics*, vol. 8, no. 5, pp. 1055–1070, Mar. 2008.

[8] G. A. Kontadakis, A. Plaka, D. Fragou, G. D. Kymionis, and A. M. Tsatsakis, "Ocular biomarkers in diseases and toxicities," in *Biomarkers in Toxicology*, Elsevier, 2014, pp. 317–324.

[9] H. T. Steely and a F. Clark, "The use of proteomics in ophthalmic research.," *Pharmacogenomics*, vol. 1, no. 3, pp. 267–280, Aug. 2000.

[10] T. Root, *Ophthobook*. CreateSpace Independent Publishing Platform, 2009.

[11] S. Aretz, T. U. Krohne, K. Kammerer, U. Warnken, A. Hotz-Wagenblatt, M. Bergmann, B. V Stanzel, T. Kempf, F. G. Holz, M. Schnölzer, and J. Kopitz, "In-depth mass spectrometric mapping of the human vitreous proteome.," *Proteome Sci.*, vol. 11, no. 22, pp. 1–10, Jan. 2013.

[12] L. M. Cryan and C. O'Brien, "Proteomics as a research tool in clinical and experimental ophthalmology.," *Proteomics. Clin. Appl.*, vol. 2, no. 5, pp. 762–775, May 2008.

[13] S. Y. Chiang, M. L. Tsai, C. Y. Wang, A. Chen, Y. C. Chou, C. W. Hsia, Y. F. Wu, H. M. Chen, T. H. Huang, P. H. Chen, H. T. Liu, and H. A. Shui, "Proteomic analysis and identification of aqueous humor proteins with a pathophysiological role in diabetic retinopathy.," *J. Proteomics*, vol. 75, no. 10, pp. 2950–2959, Jun. 2012.

[14] A. Pollreisz, M. Funk, F. P. Breitwieser, K. Parapatics, S. Sacu, M. Georgopoulos, R. Dunavoelgyi, G. J. Zlabinger, J. Colinge, K. L. Bennett, and U. Schmidt-Erfurth, "Quantitative proteomics of aqueous and vitreous fluid from patients with idiopathic epiretinal membranes.," *Exp. Eye Res.*, vol. 108, pp. 48–58, Mar. 2013.

[15] L. Zhou and R. W. Beuerman, "Tear analysis in ocular surface diseases.," *Prog. Retin. Eye Res.*, vol. 31, no. 6, pp. 527–550, Nov. 2012.

[16] F. H. Grus, S. C. Joachim, and N. Pfeiffer, "Proteomics in ocular fluids.," *Proteomics. Clin. Appl.*, vol. 1, no. 8, pp. 876–888, Aug. 2007.

[17] L. Zhou and L. Huang, "Proteomic analysis of human tears: defensin expression after ocular surface surgery," *J. Proteome Res.*, pp. 410–416, 2004.

[18] C. To and C. Kong, "The mechanism of aqueous humour formation," *Clin. Exp. Optom.*, vol. 85, no. 6, pp. 335–349, 2002.

[19] P. Escoffier, L. Paris, and B. Bodaghi, "Pooling aqueous humor samples: bias in 2D-LC-MS/MS strategy?," *J. Proteome Res.*, vol. 9, no. 2, pp. 789–797, 2010.

[20] A. Macknight and C. McLaughlin, "Formation of the aqueous humor," *Clin. Exp. Pharmacol. Physiol.*, vol. 27, pp. 100–106, 2000.

[21] A. Taylor, J. Streilein, and S. Cousins, "Identification of alpha-melanocyte stimulating hormone as a potential immunosuppressive factor in aqueous humor," *Curr. Eye Res.*, vol. 1, no. 12, pp. 1199–1206, 1992.

[22] X. Duan, Q. Lu, P. Xue, H. Zhang, and Z. Dong, "Proteomic analysis of aqueous humor from patients with myopia," *Mol. Vis.*, vol. 14, pp. 370–377, 2008.

[23] P. Bishop, "Structural macromolecules and supramolecular organisation of the vitreous gel," *Prog. Retin. Eye Res.*, vol. 19, no. 3, pp. 323–344, 2000.

[24] A. L. Levison and P. K. Kaiser, "Vitreomacular interface diseases: Diagnosis and management," *Taiwan J. Ophthalmol.*, vol. 4, no. 2, pp. 63–68, Jun. 2014.

[25] A. S. Rocha, F. M. Santos, J. P. Monteiro, J. P. Castro-de-Sousa, J. A. Queiroz, and L. P. Passarinha, "Trends in proteomic analysis of human vitreous humor samples.," *Electrophoresis*, vol. 35, no. 17, pp. 2495–2508, May 2014.

[26] M. M. Le Goff and P. N. Bishop, "Adult vitreous structure and postnatal changes.," *Eye*, vol. 22, no. 10, pp. 1214–1222, Oct. 2008.

[27] C. S. Nickerson, "The vitreous humor: Mechanics and Structure," California Institute of Technology, 2005.

[28] A. Theocharis and N. Papageorgakopoulou, "Occurrence and structural characterization of versican-like proteoglycan in human vitreous," *Biochimie*, vol. 84, pp. 1235–1241, 2002.

[29] A. Minamoto, K. Yamane, and T. Yokoyama, "Proteomics of Vitreous Fluid," in *Proteomics of Human Body Fluids*, 2007, pp. 495–507.

[30] J. Sjöstrand, J. O. Karlsson, and a K. Andersson, "Changes in the soluble protein of the human vitreous in vitreoretinal disease.," *Acta Ophthalmol.*, vol. 70, no. 6, pp. 814–819, Dec. 1992.

[31] C. Pournaras and G. Donati, “Macular epiretinal membranes,” *Semin. Ophthalmol.*, vol. 15, no. 2, pp. 100–107, 2000.

[32] M. N. Delyfer, W. Raffelsberger, D. Mercier, J. F. Korobelnik, A. Gaudric, D. G. Charteris, R. Tadayoni, F. Metge, G. Caputo, P. O. Barale, R. Ripp, J. D. Muller, O. Poch, J. A. Sahel, and T. Léveillard, “Transcriptomic Analysis of Human Retinal Detachment Reveals Both Inflammatory Response and Photoreceptor Death,” *PLoS One*, vol. 6, no. 12, pp. 1–13, 2011.

[33] T. Nakazawa, M. Takeda, and G. Lewis, “Attenuated glial reactions and photoreceptor degeneration after retinal detachment in mice deficient in glial fibrillary acidic protein and vimentin,” *Invest. Ophthalmol. Vis. Sci.*, vol. 48, no. 6, pp. 2760–2768, 2007.

[34] R. E. Neal, F. a Bettelheim, C. Lin, K. C. Winn, D. L. Garland, and J. S. Zigler, “Alterations in human vitreous humour following cataract extraction.,” *Exp. Eye Res.*, vol. 80, no. 3, pp. 337–347, Mar. 2005.

[35] R. Gariano and C. Kim, “Evaluation and management of suspected retinal detachment.,” *Am. Fam. Physician*, vol. 69, no. 7, pp. 1691–1698, 2004.

[36] T. Shitama, H. Hayashi, S. Noge, E. Uchio, K. Oshima, H. Haniu, N. Takemori, N. Komori, and H. Matsumoto, “Proteome Profiling of Vitreoretinal Diseases by Cluster Analysis.,” *Proteomics Clin. Appl.*, vol. 2, no. 9, pp. 1265–1280, Sep. 2008.

[37] M. Langham, *Ischemia and Loss of Vascular Autoregulation in Ocular and Cerebral Diseases*. Springer, 2009.

[38] N. G. Ghazi and W. R. Green, “Pathology and pathogenesis of retinal detachment.,” *Eye*, vol. 16, no. 4, pp. 411–421, 2002.

[39] P. G. Righetti, A. Castagna, P. Antonioli, and E. Boschetti, “Prefractionation techniques in proteome analysis: the mining tools of the third millennium.,” *Electrophoresis*, vol. 26, no. 2, pp. 297–319, Jan. 2005.

[40] T. C. Lam, R. K. M. Chun, K. K. Li, and C. H. To, “Application of proteomic technology in eye research: a mini review.,” *Clin. Exp. Optom.*, vol. 91, no. 1, pp. 23–33, Jan. 2008.

[41] P. A. Haynes, S. P. Gygi, D. Figeys, and R. Aebersold, “Proteome analysis: biological assay or data archive?,” *Electrophoresis*, vol. 19, no. 11, pp. 1862–1871, Aug. 1998.

[42] E. Barbosa and A. Vidotto, “Proteômica: metodologias e aplicações no estudo de doenças humanas,” *Rev. Assoc. Med. Bras.*, vol. 58, no. 3, pp. 366–375, 2012.

[43] M. L. Yarmush and A. Jayaraman, “Advances in proteomic technologies.,” *Annu. Rev. Biomed. Eng.*, vol. 4, pp. 349–373, Jan. 2002.

[44] R. A. Bradshaw, “Proteomics Today, Proteomics Tomorrow,” in *Proteomics: Biomedical and Pharmaceutical Applications*, 2004, pp. 1–17.

[45] R. A. Bradshaw and A. L. Burlingame, “From proteins to proteomics.,” *IUBMB Life*, vol. 57, no. 4/5, pp. 267–272, 2005.

[46] V. Thongboonkerd, S. Ahn, and R. Simpson, *Proteomics of human body fluids*. 2007.

[47] N. Govorukhina and R. Bischoff, “Sample Preparation of Body Fluids for Proteomics Analysis,” in *Proteomics of human body fluids: Principles, Methods, and Applications*, 2007, pp. 10–48.

[48] H. J. Lee, E. Y. Lee, M. S. Kwon, and Y. K. Paik, “Biomarker discovery from the plasma proteome using multidimensional fractionation proteomics.,” *Curr. Opin. Chem. Biol.*, vol. 10, no. 1, pp. 42–49, Feb. 2006.

[49] T. Joos and J. Bachmann, “The promise of biomarkers: research and applications,” *Drug Discov. Today*, vol. 10, no. 9, pp. 615–616, 2005.

[50] M. Angi, H. Kalirai, S. E. Coupland, B. E. Damato, F. Semeraro, and M. R. Romano, “Proteomic analyses of the vitreous humour.,” *Mediators Inflamm.*, vol. 2012, pp. 1–7, Jan. 2012.

[51] Y. Shi, R. Xiang, C. Horváth, and J. A. Wilkins, “The role of liquid chromatography in proteomics,” *J. Chromatogr. A*, vol. 1053, no. 1–2, pp. 27–36, Oct. 2004.

[52] F. Collins and M. Mansoura, “The Human Genome Project: Revealing the shared inheritance of all humankind.,” *Cancer*, vol. 91, no. 1, pp. 221–225, 2001.

[53] S. A. Merrill and A. M. Mazza, *Reaping the Benefits of Genomic and Proteomic Research: Intellectual Property Rights, Innovation and Public Health*. National Academies Press, 2006.

[54] G. Smejkal and A. Lazarev, *Separation methods in proteomics*. 2005.

[55] K. Björhall, T. Miliotis, and P. Davidsson, “Comparison of different depletion strategies for improved resolution in proteomic analysis of human serum samples.,” *Clin. Proteomics*, vol. 5, no. 1, pp. 307–317, Jan. 2005.

[56] GE Healthcare Life Sciences, *Protein Sample Preparation Handbook*. 2014.

[57] K. Chandramouli and P. Y. Qian, “Proteomics: challenges, techniques and possibilities to overcome biological sample complexity.,” *Hum. genomics proteomics*, vol. 2009, pp. 1–22, Jan. 2009.

[58] J. Yu, R. Peng, H. Chen, C. Cui, and J. Ba, “Elucidation of the pathogenic mechanism of rhegmatogenous retinal detachment with proliferative vitreoretinopathy by proteomic analysis.,” *Invest. Ophthalmol. Vis. Sci.*, vol. 53, no. 13, pp. 8146–8153, Dec. 2012.

[59] K. Yamane, A. Minamoto, H. Yamashita, H. Takamura, Y. Miyamoto-Myoken, K. Yoshizato, T. Nabetani, A. Tsugita, and H. K. Mishima, “Proteome analysis of human vitreous proteins.,” *Mol. Cell. proteomics*, vol. 2, no. 11, pp. 1177–1187, Nov. 2003.

[60] B. Cañas, C. Piñeiro, E. Calvo, D. López-Ferrer, and J. M. Gallardo, “Trends in sample preparation for classical and second generation proteomics,” *J. Chromatogr. A*, vol. 1153, no. 1–2, pp. 235–258, 2007.

[61] J. T. Corthell, “Immunoprecipitation,” in *Basic Molecular Protocols in Neuroscience: Tips, Tricks, and Pitfalls*, 2014, pp. 77–81.

[62] J. L. Reverter, J. Nadal, J. Ballester, L. Ramió-Lluch, M. M. Rivera, J. M. Fernández-Novell, J. Elizalde, S. Abengoechea, and J. E. Rodriguez, “Diabetic retinopathy is associated with decreased tyrosine nitrosylation of vitreous interleukins IL-1α, IL-1β, and IL-7,” *Ophthalmic Res.*, vol. 46, no. 4, pp. 169–174, 2011.

[63] F. Sousa, D. M. F. Prazeres, and J. a. Queiroz, “Affinity chromatography approaches to overcome the challenges of purifying plasmid DNA,” *Trends Biotechnol.*, vol. 26, no. 9, pp. 518–525, 2008.

[64] P. Cutler, “Immunoaffinity Chromatography,” *Methods Mol. Biol.*, vol. 244, pp. 167–177, 2004.

[65] A. C. Kroksveen, J. A. Opsahl, T. T. Aye, R. J. Ulvik, and F. S. Berven, “Proteomics of human cerebrospinal fluid: discovery and verification of biomarker candidates in neurodegenerative diseases using quantitative proteomics.,” *J. Proteomics*, vol. 74, no. 4, pp. 371–388, Apr. 2011.

[66] GE Healthcare Life Sciences, “HiTrap ™ Albumin & IgG Depletion.” pp. 1–8, 2014.

[67] A. Klaus, C. Lück, F. Weiland, and A. Görg, “Two-Dimensional Electrophoresis with Immobilized pH Gradients for Proteome Analysis,” 2007.

[68] G. Mitulovic and K. Mechtler, “HPLC techniques for proteomics analysis--a short overview of latest developments.,” *Briefings Funct. genomics proteomics*, vol. 5, no. 4, pp. 249–260, Dec. 2006.

[69] T. Ahamed, B. K. Nfor, and P. D. E. M. Verhaert, “pH-gradient ion-exchange chromatography: an analytical tool for design and optimization of protein separations.,” *J. Chromatogr. A*, vol. 1164, no. 1–2, pp. 181–188, Sep. 2007.

[70] Amersham Biosciences, *Ion exchange chromatography & chromatofocusing: principles and methods*. 2004.

[71] C. Selkirk, “Ion-Exchange Chromatography,” in *Protein Purification Protocols*, 2004, pp. 125–132.

[72] A. Williams and V. Frasca, “Ion-exchange chromatography.,” *Curr. Protoc. protein Sci.*, vol. 8, no. 2, pp. 1–30, 1999.

[73] A. Jungbauer and R. Hahn, “Ion-exchange chromatography.,” in *Methods in enzymology*, 1st ed., vol. 463, no. 9, Elsevier Inc., 2009, pp. 349–371.

[74] *Protein purification Handbook*. 1999.

[75] A. Harbers, G. Rodriguez, and T. Berkelman, “Fractionation by Liquid-Phase Isoelectric Focusing in the MicroRotofor Cell: Improved Detection of Low-Abundance Proteins,” *Electrophoresis*, 2005.

[76] “Electrophoresis Technical Handbook,” *Thermo Scientific Pierce*, 2010.

[77] A. Rath, F. Cunningham, and C. M. Deber, “Acrylamide concentration determines the direction and magnitude of helical membrane protein gel shifts.,” *Proc. Natl. Acad. Sci.*, vol. 110, no. 39, pp. 15668–15673, Sep. 2013.

[78] T. Rabilloud and C. Lelong, “Two-dimensional gel electrophoresis in proteomics: a tutorial.,” *J. Proteomics*, vol. 74, no. 10, pp. 1829–1841, Sep. 2011.

[79] O. Carrette and P. Burkhard, “State-of-the-art two-dimensional gel electrophoresis: a key tool of proteomics research,” *Nat. Protoc.*, vol. 1, no. 2, pp. 812–823, 2006.

[80] N. Ahmed and G. E. Rice, “Strategies for revealing lower abundance proteins in two-dimensional protein maps,” *Journal of Chromatography B*, vol. 815, no. 1. pp. 39–50, 05-Feb-2005.

[81] G. B. Smejkal, “The Coomassie chronicles: past, present and future perspectives in polyacrylamide gel staining.,” *Expert Rev. Proteomics*, vol. 1, no. 4, pp. 381–387, 2004.

[82] W. Diezel, G. Kopperschläger, and E. Hofmann, “An improved procedure for protein staining in polyacrylamide gels with a new type of Coomassie Brilliant Blue,” *Anal. Biochem.*, vol. 48, no. 2, pp. 617–620, Aug. 1972.

[83] A. Görg, W. Weiss, and M. J. Dunn, “Current two-dimensional electrophoresis technology for proteomics.,” *Proteomics*, vol. 4, no. 12, pp. 3665–3685, Dec. 2004.

[84] I. Gromova and J. E. Celis, “Protein Detection in Gels by Silver Staining: A Procedure Compatible with Mass Spectrometry,” in *Cell Biology, Four-Volume Set*, vol. 4, 2006, pp. 219–223.

[85] J. A. Mackintosh, H. Y. Choi, S. H. Bae, D. A. Veal, P. J. Bell, B. C. Ferrari, D. D. Van Dyk, N. M. Verrills, Y.-K. Paik, and P. Karuso, “A fluorescent natural product for ultra sensitive detection of proteins in one-dimensional and two-dimensional gel electrophoresis.,” *Proteomics*, vol. 3, no. 12, pp. 2273–2288, Dec. 2003.

[86] G. Van den Bergh and L. Arckens, “Fluorescent two-dimensional difference gel electrophoresis unveils the potential of gel-based proteomics.,” *Curr. Opin. Biotechnol.*, vol. 15, no. 1, pp. 38–43, Feb. 2004.

[87] R. Marouga, S. David, and E. Hawkins, “The development of the DIGE system: 2D fluorescence difference gel analysis technology.,” *Anal. Bioanal. Chem.*, vol. 382, no. 3, pp. 669–678, Jun. 2005.

[88] B. C. Searle, S. Dasari, M. Turner, A. P. Reddy, D. Choi, P. a Wilmarth, A. L. McCormack, L. L. David, and S. R. Nagalla, “High-throughput identification of proteins and unanticipated sequence modifications using a mass-based alignment algorithm for MS/MS de novo sequencing results.,” *Anal. Chem.*, vol. 76, no. 8, pp. 2220–2230, Apr. 2004.

[89] P. V. Abdelnur, “Imageamento químico por espectrometria de massas utilizando MALDI (MALDI Imaging Mass Spectrometry) aplicado a tecidos vegetais.,” *Embrapa*, 2011.

[90] J. Kang, “Principles and Applications of LC-MS/MS for the Quantitative Bioanalysis of Analytes in Various Biological Samples,” in *Tandem Mass Spectrometry - Applications and Principles*, J. Prasain, Ed. InTech, 2012, pp. 1–492.

[91] R. B. Cunha, M. D. S. Castro, and W. Fontes, “Espectrometria de massa de proteínas,” *Biotecnologia Ciência & Desenvolvimento*, no. 36, pp. 40–46, 2006.

[92] L. Signor and E. Boeri Erba, “Matrix-assisted laser desorption/ionization time of flight (MALDI-TOF) mass spectrometric analysis of intact proteins larger than 100 kDa,” *J. Vis. Exp.*, no. 79, pp. 1–7, 2013.

[93] L. F. Marvin, M. a. Roberts, and L. B. Fay, “Matrix-assisted laser desorption/ionization time-of-flight mass spectrometry in clinical chemistry,” *Clin. Chim. Acta*, vol. 337, no. 1–2, pp. 11–21, Nov. 2003.

[94] M. Kussmann, E. Nordhoff, H. Rahbek-Nielsen, and S. Haebel, “Matrix-assisted laser desorption/ionization mass spectrometry sample preparation techniques designed for various peptide and protein analytes,” *J. Mass Spectrom.*, vol. 32, pp. 593–601, 1997.

[95] K. F. Chong and H. W. Leong, “Tutorial on De Novo peptide sequencing using MS/MS Mass Spectrometry,” *J. Bioinform. Comput. Biol.*, vol. 10, no. 6, pp. 1–38, 2012.

[96] K. F. Medzihradszky, J. M. Campbell, M. a. Baldwin, A. M. Falick, P. Juhasz, M. L. Vestal, and A. L. Burlingame, "The Characteristics of Peptide Collision-Induced Dissociation Using a High-Performance MALDI-TOF/TOF Tandem Mass Spectrometer," *Anal. Chem.*, vol. 72, no. 3, pp. 552–558, Feb. 2000.

[97] C. Hughes, B. Ma, and G. A. Lajoie, "De novo sequencing methods in proteomics.," in *Methods in molecular biology*, vol. 604, 2010, pp. 105–121.

[98] M. Balasubramani, E. M. Schreiber, J. Candiello, G. K. Balasubramani, J. Kurtz, and W. Halfter, "Molecular interactions in the retinal basement membrane system: a proteomic approach," *Matrix Biol.*, vol. 29, no. 6, pp. 471–483, Jul. 2010.

[99] B. Seshi, K. Raja, and K. Chandramouli, "Immobilized pH gradient-driven paper-based IEF: a new method for fractionating complex peptide mixtures before MS analysis," *Clin. Proteomics*, vol. 8, no. 10, pp. 1–21, 2011.

[100] J. P. Monteiro, F. M. Santos, A. S. Rocha, J. P. Castro-de-Sousa, J. a Queiroz, L. a Passarinha, and C. T. Tomaz, "Vitreous humor in the pathologic scope: Insights from proteomic approaches," *Proteomics Clin. Appl.*, vol. 9, pp. 187–202, Dec. 2015.

[101] L. Cassidy, P. Barry, C. Shaw, J. Duffy, and S. Kennedy, "Platelet derived growth factor and fibroblast growth factor basic levels in the vitreous of patients with vitreoretinal disorders.," *Br. J. Ophthalmol.*, vol. 82, no. 2, pp. 181–185, 1998.

[102] R. Luo and H. Zhao, "Protein quantitation using iTRAQ: Review on the sources of variations and analysis of nonrandom missingness," *Stat. Interface*, vol. 5, no. 1, pp. 99–107, 2012.

[103] U. K. Laemmli, "Cleavage of Structural Proteins during the Assembly of the Head of Bacteriophage T4," *Nature*, vol. 227, no. 5259, pp. 680–685, 1970.

[104] G. Candiano, M. Bruschi, L. Musante, L. Santucci, G. M. Ghiggeri, B. Carnemolla, P. Orecchia, L. Zardi, and P. G. Righetti, "Blue silver: A very sensitive colloidal Coomassie G-250 staining for proteome analysis," *Electrophoresis*, vol. 25, no. 9, pp. 1327–1333, 2004.

[105] A. C. L. Len, M. B. Powner, L. Zhu, G. S. Hageman, X. Song, M. Fruttiger, and M. C. Gillies, "Pilot application of iTRAQ to the retinal disease Macular Telangiectasia.," *J. Proteome Res.*, vol. 11, no. 2, pp. 537–553, Feb. 2012.

[106] U. Restuccia, E. Boschetti, E. Fasoli, F. Fortis, L. Guerrier, A. Bachi, A. V. Kravchuk, and P. G. Righetti, "pI-based fractionation of serum proteomes versus anion exchange after enhancement of low-abundance proteins by means of peptide libraries," *J. Proteomics*, vol. 72, no. 6, pp. 1061–1070, 2009.

[107] "The Gene ontology project in 2008," *Nucleic Acids Res.*, vol. 36, no. 1, pp. 440–444, 2008.

Chapter 8

Appendices

Appendix I – List of the VH samples used in this study and complemental information about the patients.

HV	Process	Diagnosis	Gender	Age
111	401230M3	DRR	Male	72
116	510213F1	DRR	Female	61
164	530102M7	DRR	Male	60
175	391201M7	DRR	Male	74
185	610922M4	DRR	Male	52
200	830301F8	DRR	Female	30
209	320728M4	DRR	Male	80
222	381210M5	DRR	Male	75
235	420310M3	DRR	Male	71
260	630127M13	DRR	Male	50
270	311012F2	DRR	Female	82
276	360502M6	DRR	Male	77
281	540220M4	DRR	Male	59
302	411110F8	DRR	Female	72
310	500915M6	DRR	Male	64
311	400213M4	DRR	Male	74
333	520507M6	DRR	Male	62
341	460220M6	DRR	Male	68
351	651103F12	DRR	Female	49
354	520213F13	DRR	Female	62
382	570227M12	DRR	Male	57
384	480113M3	DRR	Male	66
390	880709M8	DRR	Male	26
395	500926M10	DRR	Male	64
400	381017F10	DRR	Female	76

Appendix II – Highly abundant proteins removal percentage

Appendix II A - Table referring to protein concentration before and after depletion, and respectively Albumin and IgG removal percentage.

HV	Protein concentration before depletion (µg/mL)	Protein concentration after depletion (µg/mL)	Albumin and IgG removal percentage (%)
111	3518	1119	68.2
116	1708	375	78.0
164	4555	295	93.5
175	1164	318	72.7
185	3123	1011	67.6
200	3579	148	95.9
209	6963	3631	47.9
222	2060	1261	38.8
235	4313	659	84.7
260	1702	483	71.6
270	4804	1585	67.0
276	4005	1313	67.2
281	3328	563	83.1
302	3534	597	83.1
310	7322	4313	41.1
311	2358	379	83.9
333	1281	798	37.7
341	5329	1052	80.3
351	5422	216	96.0
354	4336	1204	72.2
382	3755	907	75.8
384	5960	1392	76.6
390	7872	2379	69.8
395	5626	1701	69.8
400	4330	1767	59.2
		Average:	71.3

Appendix II B - Graphic referring to protein concentration before and after Albumin and IgG depletion, in each HV sample. Black dashed and solid lines represents protein concentration before and after depletion, respectively.

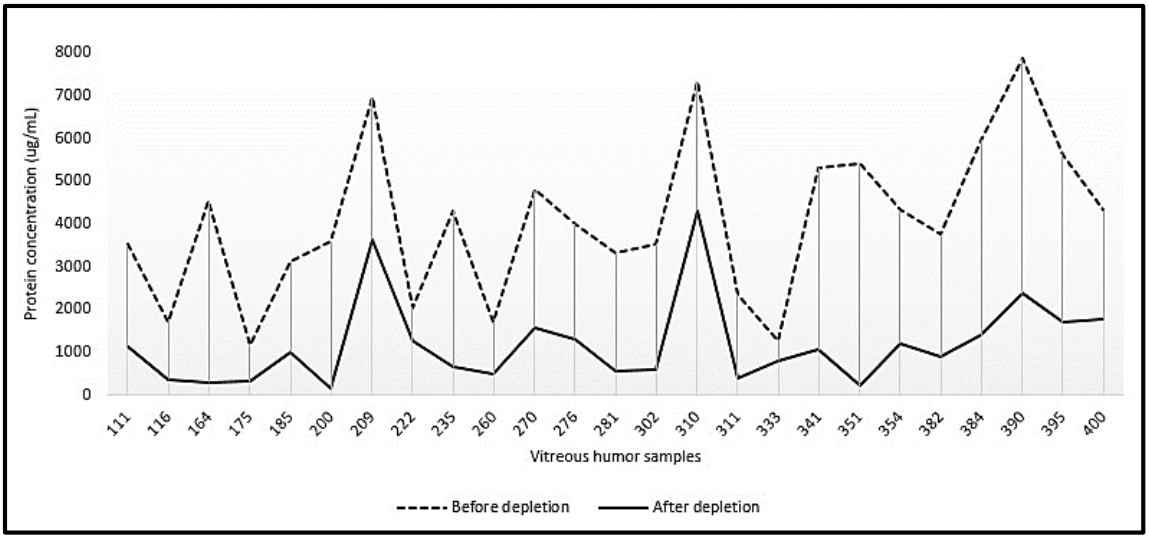

Appendix II C - Graphic referring to Albumin and IgG removal percentage, for each HV sample.

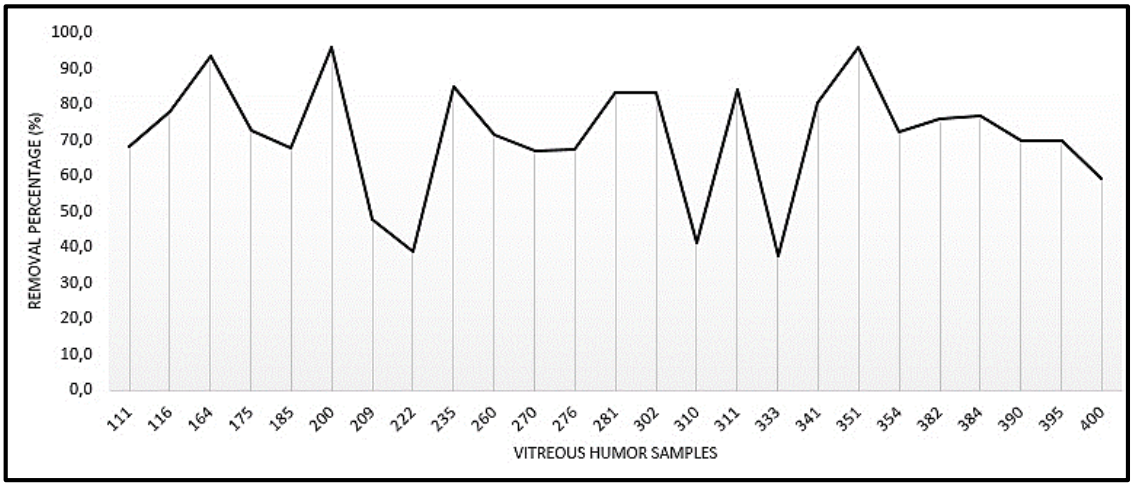

Appendix III – List of the 236 found proteins by MALDI-TOF/TOF using ProteinPilot under a 95% confidence

UniProt ID	Name	Unused Score	Total Score	% Cov	Peptides (95%)	Replicate
P13645	Keratin, type I cytoskeletal 10	14.82	14.82	25.5	19	Both
P04264	Keratin, type II cytoskeletal 1	10.00	10.00	16.9	7	Both
P02787	Serotransferrin	10.00	10.00	10.2	8	Both
P02790	Hemopexin	6.08	6.08	13.9	3	2
Q8WZ42	Titin	6.04	6.04	0.9	4	Both
Q9NZJ4	Sacsin	5.23	5.23	1.4	3	1
Q9BRD0	BUD13 homolog	4.73	4.73	12.1	3	1
Q6PL18	ATPase family AAA domain-containing protein 2	4.00	4.00	2.4	2	1
Q8WWP7	GTPase IMAP family member 1	4.00	4.00	12.8	2	1
P41222	Prostaglandin-H2 D-isomerase	4.00	4.00	41.1	3	Both
P02766	Transthyretin	4.00	4.00	24.5	3	2
Q6ZN55	Zinc finger protein 574	4.00	4.00	6.4	2	Both
Q8IWT3	Cullin-9	3.82	3.82	0.9	2	2
P25311	Zinc-alpha-2-glycoprotein	3.28	3.28	7.0	4	1
P30307	M-phase inducer phosphatase 3	2.66	2.66	6.1	2	2
Q96J94	Piwi-like protein 1	2.66	2.66	3.4	2	Both
P02749	Beta-2-glycoprotein 1	2.22	2.22	9.9	1	2
P39880-3	Isoform 3 of Homeobox protein cut-like 1	2.21	2.21	5.1	1	Both
Q9C029	Tripartite motif-containing protein 7	2.13	2.13	5.9	1	1
O75132	Zinc finger BED domain-containing protein 4	2.13	2.13	4.2	1	1
Q9H254	Spectrin beta chain, non-erythrocytic 4	2.08	2.09	1.8	1	1
Q9UKN7	Unconventional myosin-XV	2.07	2.07	3.0	1	1
Q9UPS8	Ankyrin repeat domain-containing protein 26	2.06	2.06	2.5	1	1
Q5SW79	Centrosomal protein of 170 kDa	2.06	2.06	5.5	1	1
Q8WYP3	Ras and Rab interactor 2	2.06	2.06	3.0	1	2
Q96AY4	Tetratricopeptide repeat protein 28	2.06	2.06	2.1	1	2
O14559	Rho GTPase-activating protein 33	2.05	2.05	3.9	1	1
Q13950	Runt-related transcription factor 2	2.05	2.05	5.4	1	1
Q9BT30	Alpha-ketoglutarate-dependent dioxygenase alkB homolog 7, mitochondrial	2.04	2.04	12.7	1	1
Q03164	Histone-lysine N-methyltransferase 2A	2.04	2.04	2.3	1	1
Q9NRI5	Disrupted in schizophrenia 1 protein	2.03	2.03	6.2	2	1
Q8TD57	Dynein heavy chain 3, axonemal	2.02	2.02	1.2	1	Both
P37059	Estradiol 17-beta-dehydrogenase 2	2.02	2.02	8.8	1	2
P51991	Heterogeneous nuclear ribonucleoprotein A3	2.02	2.02	10.9	2	1
O14654	Insulin receptor substrate 4	2.02	2.02	2.1	1	2
Q8NI17	Interleukin-31 receptor subunit alpha	2.02	2.02	5.5	1	2
Q2M3C7	A-kinase anchor protein SPHKAP	2.01	2.01	3.1	1	1
P07339	Cathepsin D	2.01	2.01	5.8	1	2
P01024	Complement C3	2.01	2.01	2.8	5	1
Q9NVI1	Fanconi anemia group I protein	2.01	2.01	3.2	1	1
Q6ZN55-2	Isoform 2 of Zinc finger protein 574	2.01	2.01	6.4	1	1
Q9Y6N9-5	Isoform 5 of Harmonin	2.01	2.01	2.1	1	2
P98198	Phospholipid-transporting ATPase ID	2.01	2.01	3.9	1	1
Q9NS40	Potassium voltage-gated channel subfamily H member 7	2.01	2.01	5.1	1	1
Q9H7Z3	Protein NRDE2 homolog	2.01	2.01	3.4	1	1
Q2LD37	Uncharacterized protein KIAA1109	2.01	2.01	1.2	1	1
Q9Y399	28S ribosomal protein S2, mitochondrial	2.00	2.00	6.8	1	1
Q8TB40	Abhydrolase domain-containing protein 4	2.00	2.00	6.1	1	1
Q9Y215	Acetylcholinesterase collagenic tail peptide	2.00	2.00	5.5	1	1
Q9NZK5	Adenosine deaminase CECR1	2.00	2.00	2.9	1	1
Q9Y6K8	Adenylate kinase isoenzyme 5	2.00	2.00	3.4	1	1

Q9BTE6	Alanyl-tRNA editing protein Aarsd1	2.00	2.00	2.9	1	1
P15144	Aminopeptidase N	2.00	2.00	1.7	1	1
Q92625	Ankyrin repeat and SAM domain-containing protein 1A	2.00	2.00	1.7	1	1
Q9H6X2	Anthrax toxin receptor 1	2.00	2.00	5.9	1	1
Q9UMR2	ATP-dependent RNA helicase DDX19B	2.00	2.00	4.0	1	2
P34913	Bifunctional epoxide hydrolase 2	2.00	2.00	3.4	1	1
Q08AD1	Calmodulin-regulated spectrin-associated protein 2	2.00	2.00	0.9	1	2
O43303	Centriolar coiled-coil protein of 110 kDa	2.00	2.00	4.0	1	1
Q2M2Z5	Centrosomal protein kizuna	2.00	2.00	3.4	1	1
Q9Y696	Chloride intracellular channel protein 4	2.00	2.00	8.3	1	2
Q9Y6K0	Choline/ethanolaminephosphotransferase 1	2.00	2.00	4.1	1	1
Q70JA7	Chondroitin sulfate synthase 3	2.00	2.00	2.4	1	2
Q9UL16	Cilia- and flagella-associated protein 45	2.00	2.00	5.1	1	1
Q9C0B2	Cilia- and flagella-associated protein 74	2.00	2.00	2.1	1	Both
O75390	Citrate synthase, mitochondrial	2.00	2.00	4.9	1	1
Q8TBZ0	Coiled-coil domain-containing protein 110	2.00	2.00	3.2	1	2
Q6ZP82	Coiled-coil domain-containing protein 141	2.00	2.00	0.6	1	2
Q6NSX1	Coiled-coil domain-containing protein 70	2.00	2.00	3.9	1	2
Q9NVE4	Coiled-coil domain-containing protein 87	2.00	2.00	0.8	1	2
P09871	Complement C1s subcomponent	2.00	2.00	3.2	1	2
Q14185	Dedicator of cytokinesis protein 1	2.00	2.00	1.0	1	2
Q92796	Disks large homolog 3	2.00	2.00	2.6	1	2
P26358	DNA (cytosine-5)-methyltransferase 1	2.00	2.00	3.2	1	1
P11388	DNA topoisomerase 2-alpha	2.00	2.00	0.8	1	2
Q14118	Dystroglycan	2.00	2.00	2.3	1	1
Q8TBB1	E3 ubiquitin-protein ligase LNX	2.00	2.00	6.3	1	2
O75592	E3 ubiquitin-protein ligase MYCBP2	2.00	2.00	0.8	1	1
Q9NS91	E3 ubiquitin-protein ligase RAD18	2.00	2.00	2.2	1	1
Q13822	Ectonucleotide pyrophosphatase/ phosphodiesterase family member 2	2.00	2.00	1.5	1	2
B6SEH9	Endogenous retrovirus group V member 2 Env polyprotein	2.00	2.00	1.9	1	1
Q86YB7	Enoyl-CoA hydratase domain-containing protein 2, mitochondrial	2.00	2.00	5.1	1	1
Q96DC8	Enoyl-CoA hydratase domain-containing protein 3, mitochondrial	2.00	2.00	12.5	1	1
Q7Z6J4	FYVE, RhoGEF and PH domain-containing protein 2	2.00	2.00	3.4	1	2
Q99999	Galactosylceramide sulfotransferase	2.00	2.00	5.0	1	2
Q9BVM4	Gamma-glutamylaminecyclotransferase	2.00	2.00	6.5	1	2
Q06210	Glutamine--fructose-6-phosphate aminotransferase [isomerizing] 1	2.00	2.00	1.4	1	2
P50440	Glycine amidinotransferase, mitochondrial	2.00	2.00	2.8	1	2
Q8N3Y3	Glycosyltransferase-like protein LARGE2	2.00	2.00	2.9	1	2
Q7L5D6	Golgi to ER traffic protein 4 homolog	2.00	2.00	5.5	1	1
Q08378	Golgin subfamily A member 3	2.00	2.00	2.3	1	2
Q9H3K2	Growth hormone-inducible transmembrane protein	2.00	2.00	5.5	1	1
P01112	GTPase HRas	2.00	2.00	11.1	1	1
Q8NHV1	GTPase IMAP family member 7	2.00	2.00	5.3	1	1
O43390	Heterogeneous nuclear ribonucleoprotein R	2.00	2.00	2.8	1	2
P04196	Histidine-rich glycoprotein	2.00	2.00	6.1	1	1
Q9UMN6	Histone-lysine N-methyltransferase 2B	2.00	2.00	1.4	1	1
P05538	HLA class II histocompatibility antigen, DQ beta 2 chain	2.00	2.00	4.1	1	2
P39880	Homeobox protein cut-like 1	2.00	2.00	1.1	1	2
P01861	Ig gamma-4 chain C region	2.00	2.00	5.5	1	1
P01834	Ig kappa chain C region	2.00	2.00	15.1	2	Both

Q13308	Inactive tyrosine-protein kinase 7	2.00	2.00	3.4	1	2
Q14643	Inositol 1,4,5-trisphosphate receptor type 1	2.00	2.00	1.5	1	1
Q14161-10	Isoform 10 of ARF GTPase-activating protein GIT2	2.00	2.00	2.1	1	2
Q14129-2	Isoform 2 of Protein DGCR6	2.00	2.00	11.7	1	2
O95398-2	Isoform 2 of Rap guanine nucleotide exchange factor 3	2.00	2.00	7.7	1	Both
O43889-3	Isoform 3 of Cyclic AMP-responsive element-binding protein 3	2.00	2.00	6.5	1	1
Q6P2C8-4	Isoform 3 of Mediator of RNA polymerase II transcription subunit 27	2.00	2.00	5.4	1	2
P17010-3	Isoform 3 of Zinc finger X-chromosomal protein	2.00	2.00	2.5	1	1
P11388-4	Isoform 4 of DNA topoisomerase 2-alpha	2.00	2.00	2.6	1	Both
Q6PII5-4	Isoform 4 of Hydroxyacylglutathione hydrolase-like protein	2.00	2.00	6.9	1	1
Q9H902-4	Isoform 4 of Receptor expression-enhancing protein 1	2.00	2.00	8.4	1	1
O60885-3	Isoform B of Bromodomain-containing protein 4	2.00	2.00	2.5	1	1
Q13342-2	Isoform LYSp100-A of Nuclear body protein SP140	2.00	2.00	4.6	1	1
P06239-2	Isoform Short of Tyrosine-protein kinase Lck	2.00	2.00	3.9	1	2
Q96G42	Kelch domain-containing protein 7B	2.00	2.00	7.2	1	1
Q6JEL2	Kelch-like protein 10	2.00	2.00	3.0	1	2
P35527	Keratin, type I cytoskeletal 9	2.00	2.00	5.1	1	2
Q96EK5	KIF1-binding protein	2.00	2.00	2.9	1	2
Q8NI77	Kinesin-like protein KIF18A	2.00	2.00	1.4	1	2
O43291	Kunitz-type protease inhibitor 2	2.00	2.00	8.3	1	1
P22079	Lactoperoxidase	2.00	2.00	1.7	1	1
Q16363	Laminin subunit alpha-4	2.00	2.00	0.5	1	2
Q14766	Latent-transforming growth factor beta-binding protein 1	2.00	2.00	2.1	1	Both
Q8N2S1	Latent-transforming growth factor beta-binding protein 4	2.00	2.00	1.4	1	1
Q5VZK9	Leucine-rich repeat-containing protein 16A	2.00	2.00	1.4	1	1
Q6F5E8	Leucine-rich repeat-containing protein 16C	2.00	2.00	1.0	1	2
Q05C16	Leucine-rich repeat-containing protein 63	2.00	2.00	2.6	1	2
P50851	Lipopolysaccharide-responsive and beige-like anchor protein	2.00	2.00	0.7	1	1
Q86YD5	Low-density lipoprotein receptor class A domain-containing protein 3	2.00	2.00	3.5	1	Both
O75197	Low-density lipoprotein receptor-related protein 5	2.00	2.00	1.2	1	2
Q04912	Macrophage-stimulating protein receptor	2.00	2.00	1.5	1	1
Q8IWI9	MAX gene-associated protein	2.00	2.00	1.4	1	1
Q15648	Mediator of RNA polymerase II transcription subunit 1	2.00	2.00	1.3	1	1
Q93074	Mediator of RNA polymerase II transcription subunit 12	2.00	2.00	0.5	1	1
Q9ULK4	Mediator of RNA polymerase II transcription subunit 23	2.00	2.00	0.8	1	2
O95402	Mediator of RNA polymerase II transcription subunit 26	2.00	2.00	5.7	1	2
Q14831	Metabotropic glutamate receptor 7	2.00	2.00	2.2	1	1
Q96GW9	Methionine--tRNA ligase, mitochondrial	2.00	2.00	5.2	1	1
Q5JR59	Microtubule-associated tumor suppressor candidate 2	2.00	2.00	3.2	1	1
O43615	Mitochondrial import inner membrane translocase subunit TIM44	2.00	2.00	2.7	1	1
Q8TE76	MORC family CW-type zinc finger protein 4	2.00	2.00	1.4	1	2

Q9BQG0	Myb-binding protein 1A	2.00	2.00	1.0	1	2
Q9UQQ1	N-acetylated-alpha-linked acidic dipeptidase-like protein	2.00	2.00	4.9	1	2
Q9ULI1	NACHT and WD repeat domain-containing protein 2	2.00	2.00	0.7	1	2
P51606	N-acylglucosamine 2-epimerase	2.00	2.00	7.5	1	1
Q9UHB4	NADPH-dependent diflavin oxidoreductase 1	2.00	2.00	3.0	1	1
Q96NK8	Neurogenic differentiation factor 6	2.00	2.00	4.2	1	2
Q15080	Neutrophil cytosol factor 4	2.00	2.00	3.0	1	1
Q9Y2I6	Ninein-like protein	2.00	2.00	1.5	1	1
Q15406	Nuclear receptor subfamily 6 group A member 1	2.00	2.00	2.5	1	2
Q86U38	Nucleolar protein 9	2.00	2.00	3.0	1	1
Q5SRE5	Nucleoporin NUP188 homolog	2.00	2.00	1.0	1	1
Q9Y5B8	Nucleoside diphosphate kinase 7	2.00	2.00	5.3	1	1
Q04671	P protein	2.00	2.00	2.3	1	Both
A8MW92	PHD finger protein 20-like protein 1	2.00	2.00	2.7	1	1
Q16816	Phosphorylase b kinase gamma catalytic chain, skeletal muscle/heart isoform	2.00	2.00	4.7	1	2
Q86UU1	Pleckstrin homology-like domain family B member 1	2.00	2.00	5.8	1	1
Q8N3A8	Poly [ADP-ribose] polymerase 8	2.00	2.00	2.5	1	1
Q9BSM1	Polycomb group RING finger protein 1	2.00	2.00	7.3	1	1
Q9NR82	Potassium voltage-gated channel subfamily KQT member 5	2.00	2.00	1.5	1	2
P20648	Potassium-transporting ATPase alpha chain 1	2.00	2.00	3.2	1	1
Q15238	Pregnancy-specific beta-1-glycoprotein 5	2.00	2.00	7.8	1	2
O43900	Prickle-like protein 3	2.00	2.00	3.1	1	1
A2PYH4	Probable ATP-dependent DNA helicase HFM1	2.00	2.00	2.2	1	1
Q15751	Probable E3 ubiquitin-protein ligase HERC1	2.00	2.00	1.1	1	1
O75110	Probable phospholipid-transporting ATPase IIA	2.00	2.00	1.3	1	2
Q9UKV8	Protein argonaute-2	2.00	2.00	2.0	1	2
Q9H694	Protein bicaudal C homolog 1	2.00	2.00	1.3	1	1
Q8N2R8	Protein FAM43A	2.00	2.00	3.1	1	2
Q6ZT52	Protein FAM43B	2.00	2.00	5.5	1	2
Q6ZS17	Protein FAM65A	2.00	2.00	0.9	1	2
Q5U4N7	Protein GDF5OS, mitochondrial	2.00	2.00	8.0	1	1
Q02156	Protein kinase C epsilon type	2.00	2.00	4.3	1	2
A6NL88	Protein shisa-7	2.00	2.00	3.7	1	1
Q8NE18	Putative methyltransferase NSUN7	2.00	2.00	5.3	1	1
P0CG43	Putative protein FAM157C	2.00	2.00	4.9	1	1
Q5T4I8	Putative uncharacterized protein C6orf52	2.00	2.00	12.5	1	1
Q9H2T7	Ran-binding protein 17	2.00	2.00	1.8	1	1
Q9Y4G8	Rap guanine nucleotide exchange factor 2	2.00	2.00	1.3	1	1
O95398	Rap guanine nucleotide exchange factor 3	2.00	2.00	2.4	1	2
Q9UJF2	Ras GTPase-activating protein nGAP	2.00	2.00	1.7	1	1
Q86VI3	Ras GTPase-activating-like protein IQGAP3	2.00	2.00	1.6	1	2
O76081	Regulator of G-protein signaling 20	2.00	2.00	3.6	1	2
Q9BSG5	Retbindin	2.00	2.00	9.2	1	1
P78363	Retinal-specific ATP-binding cassette transporter	2.00	2.00	0.6	1	2
Q9NRY4	Rho GTPase-activating protein 35	2.00	2.00	0.6	1	2
Q8N1W1	Rho guanine nucleotide exchange factor 28	2.00	2.00	0.8	1	1
Q9BY78	RING finger protein 26	2.00	2.00	3.0	1	2
Q9NRM7	Serine/threonine-protein kinase LATS2	2.00	2.00	1.1	1	2
P0C263	Serine/threonine-protein kinase SBK2	2.00	2.00	4.9	1	1
Q9H4A3	Serine/threonine-protein kinase WNK1	2.00	2.00	1.3	1	1
P02768	Serum albumin	2.00	2.00	1.1	1	2

Q96HL8	SH3 domain-containing YSC84-like protein 1	2.00	2.00	5.8	1	2
O43166	Signal-induced proliferation-associated 1-like protein 1	2.00	2.00	2.6	1	1
O75094	Slit homolog 3 protein	2.00	2.00	1.2	1	1
Q9BSF0	Small membrane A-kinase anchor protein	2.00	2.00	17.9	1	2
P35499	Sodium channel protein type 4 subunit alpha	2.00	2.00	0.5	1	1
Q6Q0C1	Solute carrier family 25 member 47	2.00	2.00	5.8	1	1
Q495Y8	Speedy protein E2	2.00	2.00	5.0	1	1
Q6Q759	Sperm-associated antigen 17	2.00	2.00	0.9	1	1
Q8IWB4	Spermatogenesis-associated protein 31A7	2.00	2.00	3.9	1	2
Q9BVQ7	Spermatogenesis-associated protein 5-like protein 1	2.00	2.00	1.2	1	2
O95425	Supervillin	2.00	2.00	0.6	1	2
Q5T4T6	Synaptonemal complex protein 2-like	2.00	2.00	1.4	1	2
A7MCY6	TANK-binding kinase 1-binding protein 1	2.00	2.00	1.1	1	1
Q8TBP0	TBC1 domain family member 16	2.00	2.00	1.2	1	1
Q9Y2I9	TBC1 domain family member 30	2.00	2.00	1.5	1	1
Q6PID6	Tetratricopeptide repeat protein 33	2.00	2.00	5.0	1	2
P21675	Transcription initiation factor TFIID subunit 1	2.00	2.00	2.0	1	Both
Q8IZX4	Transcription initiation factor TFIID subunit 1-like	2.00	2.00	1.0	1	2
Q12986	Transcriptional repressor NF-X1	2.00	2.00	0.8	1	1
P02786	Transferrin receptor protein 1	2.00	2.00	1.7	1	1
P55072	Transitional endoplasmic reticulum ATPase	2.00	2.00	3.8	1	1
Q6ZXV5	Transmembrane and TPR repeat-containing protein 3	2.00	2.00	1.4	1	2
Q7Z5M5	Transmembrane channel-like protein 3	2.00	2.00	0.9	1	1
B1AL88	Transmembrane protein FAM155A	2.00	2.00	4.4	1	1
O75949	Transmembrane protein FAM155B	2.00	2.00	3.0	1	2
Q9BYJ4	Tripartite motif-containing protein 34	2.00	2.00	2.7	1	1
Q12923	Tyrosine-protein phosphatase non-receptor type 13	2.00	2.00	1.7	2	Both
Q9Y2Z4	Tyrosine--tRNA ligase, mitochondrial	2.00	2.00	3.1	1	2
Q8NBM4	Ubiquitin-associated domain-containing protein 2	2.00	2.00	5.8	1	1
Q9H8K7	Uncharacterized protein C10orf88	2.00	2.00	3.6	1	2
Q9NZ63	Uncharacterized protein C9orf78	2.00	2.00	5.9	1	1
A6NEN9	Uncharacterized protein CXorf65	2.00	2.00	9.8	1	1
Q96S15	WD repeat-containing protein 24	2.00	2.00	2.00	1	1
Q6ZMY6	WD repeat-containing protein 88	2.00	2.00	2.5	1	2
Q9Y6W5	Wiskott-Aldrich syndrome protein family member 2	2.00	2.00	2.8	1	2
Q8NCN2	Zinc finger and BTB domain-containing protein 34	2.00	2.00	4.6	1	2
Q5T200	Zinc finger CCCH domain-containing protein 13	2.00	2.00	5.8	1	1
Q8N988	Zinc finger protein 557	2.00	2.00	2.8	1	2
Q86YE8	Zinc finger protein 573	2.00	2.00	4.5	1	2
Q8IX07	Zinc finger protein ZFPM1	2.00	2.00	3.4	1	1
Q8WWQ8	Stabilin-2	1.44	2.00	0.6	1	1
Q6N022	Teneurin-4	1.37	2.00	0.3	1	2
Q6PF04	Zinc finger protein 613	1.37	2.00	1.3	1	2

Appendix IV – List of the 44 common proteins between previous studies from our research group using iTRAQ and the present study using LC-SDS-PAGE-MALDI

UniProt ID	Name
Q9NZK5	Adenosine deaminase CECR1
P15144	Aminopeptidase N
P02749	Beta-2-glycoprotein 1
P34913	Bifunctional epoxide hydrolase 2
P07339	Cathepsin D
Q8TBZ0	Coiled-coil domain-containing protein 110
Q9NVE4	Coiled-coil domain-containing protein 87
P09871	Complement C1s subcomponent
P01024	Complement C3
Q8TD57	Dynein heavy chain 3, axonemal
Q14118	Dystroglycan
O75592	E3 ubiquitin-protein ligase MYCBP2
Q13822	Ectonucleotide pyrophosphatase/ phosphodiesterase family member 2
Q08378	Golgin subfamily A member 3
P02790	Hemopexin
P04196	Histidine-rich glycoprotein
Q9UMN6	Histone-lysine N-methyltransferase 2B
P39880	Homeobox protein cut-like 1
P01861	Ig gamma-4 chain C region
P01834	Ig kappa chain C region
Q13308	Inactive tyrosine-protein kinase 7
Q14643	Inositol 1,4,5-trisphosphate receptor type 1
P13645	Keratin, type I cytoskeletal 10
P35527	Keratin, type I cytoskeletal 9
P04264	Keratin, type II cytoskeletal 1
Q8IWI9	MAX gene-associated protein
Q15648	Mediator of RNA polymerase II transcription subunit 1
Q5JR59	Microtubule-associated tumor suppressor candidate 2
P41222	Prostaglandin-H2 D-isomerase
Q6ZS17	Protein FAM65A
Q9BSG5	Retbindin
Q9NZJ4	Sacsin
Q9H4A3	Serine/threonine-protein kinase WNK1
P02787	Serotransferrin
P02768	Serum albumin
Q9H254	Spectrin beta chain, non-erythrocytic 4
Q6N022	Teneurin-4
Q8IZX4	Transcription initiation factor TFIID subunit 1-like
P02786	Transferrin receptor protein 1
P55072	Transitional endoplasmic reticulum ATPase
P02766	Transthyretin
Q2LD37	Uncharacterized protein KIAA1109
Q5T200	Zinc finger CCCH domain-containing protein 13
P25311	Zinc-alpha-2-glycoprotein

Appendix V – Information exported from STRAP software, with proteins GO terms for biological processes, cellular compartments and molecular functions of the 46 connected proteins

Appendix V A - Table referring to biological processes for the 46 found connected proteins.

Name	Cellular process	Developmental process	Immune system process	Interaction with cells and organisms	Localization	Metabolic process	Regulation	Response to stimulus	Other
Adenylate kinase isoenzyme 5	✓					✓			
Cathepsin D	✓		✓			✓			✓
Centriolar coiled-coil protein of 110 kDa	✓						✓		✓
Coiled-coil domain-containing protein 141	✓				✓				
Complement C3	✓	✓	✓				✓	✓	
Dedicator of cytokinesis protein 1	✓		✓				✓		✓
Disrupted in schizophrenia 1 protein	✓	✓		✓	✓		✓	✓	✓
FYVE, RhoGEF and PH domain-containing protein 2							✓		✓
GTPase HRas	✓	✓	✓		✓		✓		✓
Hemopexin	✓				✓		✓		
Heterogeneous nuclear ribonucleoprotein A3	✓				✓	✓			
Heterogeneous nuclear ribonucleoprotein R	✓					✓			
Histidine-rich glycoprotein	✓	✓		✓	✓		✓		✓
Histone-lysine N-methyltransferase 2A	✓	✓					✓	✓	✓
Keratin, type I cytoskeletal 10	✓								
Keratin, type II cytoskeletal 1							✓	✓	
Latent-transforming growth factor beta-binding protein 1							✓		✓
Latent-transforming growth factor beta-binding protein 4	✓	✓					✓		✓
MAX gene-associated protein	✓								
Mediator of RNA polymerase II transcription subunit 1	✓	✓				✓	✓		✓
Mediator of RNA polymerase II transcription subunit 12	✓	✓				✓	✓		
Mediator of RNA polymerase II transcription subunit 23	✓					✓	✓		

Mediator of RNA polymerase II transcription subunit 26	✓						✓	✓		
Metabotropic glutamate receptor 7	✓				✓			✓		✓
Methionine--tRNA ligase, mitochondrial	✓						✓			
Ninein-like protein	✓									✓
Nucleoporin NUP188 homolog	✓					✓	✓	✓		✓
Nucleoside diphosphate kinase 7	✓	✓						✓		✓
Potassium voltage-gated channel subfamily H member 7	✓							✓		✓
Potassium voltage-gated channel subfamily KQT member 5	✓									✓
Protein kinase C epsilon type	✓			✓	✓			✓	✓	✓
Rap guanine nucleotide exchange factor 2	✓	✓						✓		✓
Ras and Rab interactor 2						✓		✓		
Regulator of G-protein signaling 20								✓		
Rho GTPase-activating protein 33						✓		✓		
Rho GTPase-activating protein 35	✓	✓						✓		✓
Serotransferrin	✓					✓		✓		✓
Serum albumin	✓					✓	✓	✓		
Spectrin beta chain, non-erythrocytic 4	✓				✓	✓		✓		✓
Transcription initiation factor TFIID subunit 1	✓						✓	✓		✓
Transcriptional repressor NF-X1	✓							✓	✓	
Transferrin receptor protein 1	✓	✓				✓		✓	✓	
Transitional endoplasmic reticulum ATPase	✓					✓		✓		✓
Tyrosine--tRNA ligase, mitochondrial	✓						✓			✓
Wiskott-Aldrich syndrome protein family member 2	✓	✓	✓					✓		✓
Zinc finger CCCH domain-containing protein 13										

Appendix V B - Table referring to cellular compartment in which the 46 found connected proteins are present.

Name	Endosome	Chromosome	ER	Mitochondria	Nucleus	Cytoskeleton	Plasma membrane	Cell surface	Extra cellular	Other intracellular	Macromolecular complex	Cytoplasm	Other
Adenylate kinase isoenzyme 5						✓						✓	
Cathepsin D									✓	✓			✓
Centriolar coiled-coil protein of 110 kDa						✓					✓	✓	
Coiled-coil domain-containing protein 141						✓						✓	
Complement C3							✓		✓				
Dedicator of cytokinesis protein 1					✓							✓	✓
Disrupted in schizophrenia 1 protein			✓	✓	✓	✓	✓						✓
FYVE, RhoGEF and PH domain-containing protein 2	✓				✓	✓	✓			✓		✓	✓
GTPase HRas					✓		✓			✓		✓	
Hemopexin	✓								✓				
Heterogeneous nuclear ribonucleoprotein A3					✓							✓	✓
Heterogeneous nuclear ribonucleoprotein R					✓							✓	
Histidine-rich glycoprotein							✓		✓	✓			
Histone-lysine N-methyltransferase 2A					✓							✓	
Keratin, type I cytoskeletal 10					✓	✓			✓			✓	✓
Keratin, type II cytoskeletal 1					✓	✓	✓		✓				✓
Latent-transforming growth factor beta-binding protein 1									✓		✓		
Latent-transforming growth factor beta-binding protein 4									✓				✓
MAX gene-associated protein					✓						✓	✓	
Mediator of RNA polymerase II transcription subunit 1		✓			✓						✓		✓
Mediator of RNA polymerase II transcription subunit 12					✓	✓					✓		✓
Mediator of RNA polymerase II transcription subunit 23					✓						✓		
Mediator of RNA polymerase II transcription subunit 26					✓								

Metabotropic glutamate receptor 7							✓				✓		✓	✓
Methionine--tRNA ligase, mitochondrial				✓										
Ninein-like protein						✓							✓	
Nucleoporin NUP188 homolog					✓									✓
Nucleoside diphosphate kinase 7						✓								✓
Potassium voltage-gated channel subfamily H member 7							✓							
Potassium voltage-gated channel subfamily KQT member 5							✓							✓
Protein kinase C epsilon type			✓	✓	✓	✓	✓			✓			✓	✓
Rap guanine nucleotide exchange factor 2	✓				✓		✓				✓		✓	✓
Ras and Rab interactor 2													✓	
Regulator of G-protein signaling 20					✓		✓			✓			✓	
Rho GTPase-activating protein 33							✓						✓	
Rho GTPase-activating protein 35					✓	✓							✓	
Serotransferrin	✓				✓		✓	✓	✓	✓				✓
Serum albumin					✓				✓	✓	✓			✓
Spectrin beta chain, non-erythrocytic 4					✓	✓	✓		✓				✓	✓
Transcription initiation factor TFIID subunit 1					✓									
Transcriptional repressor NF-X1					✓		✓						✓	
Transferrin receptor protein 1	✓				✓	✓	✓	✓	✓	✓	✓			✓
Transitional endoplasmic reticulum ATPase			✓	✓		✓			✓	✓	✓		✓	✓
Tyrosine--tRNA ligase, mitochondrial					✓								✓	
Wiskott-Aldrich syndrome protein family member 2	✓					✓			✓		✓		✓	✓
Zinc finger CCCH domain-containing protein 13														

Appendix V C - Table referring to molecular functions of the 46 found connected proteins.

Name	Antioxidant activity	Binding	Catalytic activity	Molecular transducer activity	Structural molecule activity	Other
Adenylate kinase isoenzyme 5		✓	✓			
Cathepsin D			✓			
Centriolar coiled-coil protein of 110 kDa						
Coiled-coil domain-containing protein 141						
Complement C3		✓				✓
Dedicator of cytokinesis protein 1						✓
Disrupted in schizophrenia 1 protein						
FYVE, RhoGEF and PH domain-containing protein 2		✓				✓
GTPase HRas		✓	✓			
Hemopexin		✓				✓
Heterogeneous nuclear ribonucleoprotein A3		✓				✓
Heterogeneous nuclear ribonucleoprotein R		✓				
Histidine-rich glycoprotein		✓				✓
Histone-lysine N-methyltransferase 2A		✓	✓			✓
Keratin, type I cytoskeletal 10					✓	
Keratin, type II cytoskeletal 1		✓		✓	✓	
Latent-transforming growth factor beta-binding protein 1		✓	✓			
Latent-transforming growth factor beta-binding protein 4		✓	✓			
MAX gene-associated protein		✓				✓
Mediator of RNA polymerase II transcription subunit 1		✓	✓	✓		✓
Mediator of RNA polymerase II transcription subunit 12		✓	✓	✓		✓
Mediator of RNA polymerase II transcription subunit 23			✓			✓
Mediator of RNA polymerase II transcription subunit 26		✓				✓
Metabotropic glutamate receptor 7		✓		✓		✓

Methionine--tRNA ligase, mitochondrial		✓	✓			
Ninein-like protein		✓				
Nucleoporin NUP188 homolog						
Nucleoside diphosphate kinase 7		✓	✓			
Potassium voltage-gated channel subfamily H member 7				✓		✓
Potassium voltage-gated channel subfamily KQT member 5						✓
Protein kinase C epsilon type		✓	✓	✓		✓
Rap guanine nucleotide exchange factor 2		✓		✓		✓
Ras and Rab interactor 2						✓
Regulator of G-protein signaling 20						✓
Rho GTPase-activating protein 33		✓				✓
Rho GTPase-activating protein 35		✓				✓
Serotransferrin		✓				✓
Serum albumin	✓	✓				
Spectrin beta chain, non-erythrocytic 4		✓			✓	
Transcription initiation factor TFIID subunit 1		✓	✓			✓
Transcriptional repressor NF-X1		✓	✓			✓
Transferrin receptor protein 1		✓		✓		✓
Transitional endoplasmic reticulum ATPase		✓	✓			✓
Tyrosine--tRNA ligase, mitochondrial		✓	✓			
Wiskott-Aldrich syndrome protein family member 2		✓				
Zinc finger CCCH domain-containing protein 13		✓				

Appendix VI – 110 found proteins by MALDI-TOF/TOF using ProteinPilot under a 95% confidence

UniProt ID	Name	Unused Score	Total Score	% Cov	Peptides (95%)
P02787	Serotransferrin	12.37	12.37	23.2	12
P04264	Keratin, type II cytoskeletal 1	10.01	10.01	13.2	11
P02790	Hemopexin	8.11	8.11	20.4	5
P02766	Transthyretin	8.00	8.00	40.8	4
Q9BRQ4	Uncharacterized protein C11orf70	4.00	4.00	13.1	2
P41222	Prostaglandin-H2 D-isomerase	2.45	2.45	19.0	3
Q4KMQ1	Taperin	2.24	2.24	6.3	1
Q8IYE1	Coiled-coil domain-containing protein 13	2.19	2.19	7.4	2
Q9BSU1	UPF0183 protein C16orf70	2.15	2.15	10.7	1
P98164	Low-density lipoprotein receptor-related protein 2	2.1	2.1	1.5	1
Q8N3K9	Cardiomyopathy-associated protein 5	2.05	2.05	2.7	1
Q5VZ89	DENN domain-containing protein 4C	2.04	2.04	4.8	1
Q9Y6Q5	AP-1 complex subunit mu-2	2.03	2.03	8.7	1
Q6P2Q9	Pre-mRNA-processing-splicing factor 8	2.02	2.02	3.2	1
Q5T1A1	DC-STAMP domain-containing protein 2	2.01	2.01	5.8	1
Q15878	Voltage-dependent R-type calcium channel subunit alpha-1E	2.01	2.01	2.8	1
Q9UGI9	5'-AMP-activated protein kinase subunit gamma-3	2.01	2.01	3.9	1
Q9P013	Spliceosome-associated protein CWC15 homolog	2.01	2.01	10.9	1
Q9H7E2	Tudor domain-containing protein 3	2.01	2.01	6.5	1
Q8NAT1	Protein O-linked-mannose beta-1,4-N-acetylglucosaminyltransferase 2	2.01	2.01	6.7	1
O15018	PDZ domain-containing protein 2	2.01	2.01	1.3	1
Q7Z745	Maestro heat-like repeat-containing protein family member 2B	2.00	2.01	2.7	1
Q9NWH9	SAFB-like transcription modulator	2.00	2.00	7.3	1
Q5JRA6	Melanoma inhibitory activity protein 3	2.00	2.00	2.6	1
O15169	Axin-1	2.00	2.00	4.4	1
O15050	TPR and ankyrin repeat-containing protein 1	2.00	2.00	1.6	1
Q9UGL1	Lysine-specific demethylase 5B	2.00	2.00	2.1	1
Q9H3D4	Tumor protein 63	2.00	2.00	5.6	1
Q96HL8	SH3 domain-containing YSC84-like protein 1	2.00	2.00	5.8	1
P30622	CAP-Gly domain-containing linker protein 1	2.00	2.00	3.0	1
O75027	ATP-binding cassette sub-family B member 7, mitochondrial	2.00	2.00	5.3	1
A2RTY3	Protein HEATR9	2.00	2.00	3.5	1
Q9Y6X2	E3 SUMO-protein ligase PIAS3	2.00	2.00	3.0	1
Q9Y623	Myosin-4	2.00	2.00	0.9	1
Q9Y5X9	Endothelial lipase	2.00	2.00	5.4	1
Q9Y446	Plakophilin-3	2.00	2.00	2.5	1
Q9Y215-6	Isoform VI of Acetylcholinesterase collagenic tail peptide	2.00	2.00	6.2	1
Q9ULK0	Glutamate receptor ionotropic, delta-1	2.00	2.00	2.1	1
Q9ULH7	MKL/myocardin-like protein 2	2.00	2.00	1.3	1
Q9UIB8	SLAM family member 5	2.00	2.00	5.5	1
Q9UI10	Translation initiation factor eIF-2B subunit delta	2.00	2.00	4.0	1
Q9UDT6	CAP-Gly domain-containing linker protein 2	2.00	2.00	1.3	1
Q9P2P6	StAR-related lipid transfer protein 9	2.00	2.00	0.2	1
Q9P266	Junctional protein associated with coronary artery disease	2.00	2.00	1.5	1
Q9NXZ1	Sarcoma antigen 1	2.00	2.00	1.3	1
Q9NXA8	NAD-dependent protein deacylase sirtuin-5, mitochondrial	2.00	2.00	5.8	2
Q9NVV4-2	Isoform 2 of Poly(A) RNA polymerase, mitochondrial	2.00	2.00	1.8	1
Q9NTG7	NAD-dependent protein deacetylase sirtuin-3, mitochondrial	2.00	2.00	4.5	1
Q9NQI0	Probable ATP-dependent RNA helicase DDX4	2.00	2.00	2.1	1
Q9HAK2	Transcription factor COE2	2.00	2.00	4.0	1
Q9BXW7-2	Isoform 1 of Cat eye syndrome critical region protein 5	2.00	2.00	7.4	1
Q9BQN1	Protein FAM83C	2.00	2.00	2.4	2

Q99685	Monoglyceride lipase	2.00	2.00	6.6	1
Q96RL1	BRCA1-A complex subunit RAP80	2.00	2.00	2.6	1
Q96MT7-2	Isoform 2 of Cilia- and flagella-associated protein 44	2.00	2.00	1.0	1
Q96L93	Kinesin-like protein KIF16B	2.00	2.00	1.6	1
Q96KV7	WD repeat-containing protein 90	2.00	2.00	1.1	1
Q96E66	Leucine-rich repeat-containing protein 51	2.00	2.00	10.9	1
Q96CW5	Gamma-tubulin complex component 3	2.00	2.00	2.4	1
Q96AA8	Janus kinase and microtubule-interacting protein 2	2.00	2.00	1.2	1
Q92833	Protein Jumonji	2.00	2.00	1.5	1
Q8WY41	Nanos homolog 1	2.00	2.00	5.1	1
Q8TDQ0	Hepatitis A virus cellular receptor 2	2.00	2.00	9.3	1
Q8NHV4	Protein NEDD1	2.00	2.00	2.0	1
Q8NFA0	Ubiquitin carboxyl-terminal hydrolase 32	2.00	2.00	0.7	1
Q8NEP3	Dynein assembly factor 1, axonemal	2.00	2.00	3.3	1
Q8ND71	GTPase IMAP family member 8	2.00	2.00	1.7	1
Q8NCW5	NAD(P)H-hydrate epimerase	2.00	2.00	6.6	1
Q8N865	Uncharacterized protein C7orf31	2.00	2.00	2.9	1
Q8IYS2	Uncharacterized protein KIAA2013	2.00	2.00	4.7	1
Q8IVF6	Ankyrin repeat domain-containing protein 18A	2.00	2.00	1.8	1
Q86YD1	Prostate tumor-overexpressed gene 1 protein	2.00	2.00	5.0	1
Q86VZ2	WD repeat-containing protein 5B	2.00	2.00	2.7	1
Q7Z3Y9	Keratin, type I cytoskeletal 26	2.00	2.00	3.2	1
Q7L7V1-2	Isoform 2 of Putative pre-mRNA-splicing factor ATP-dependent RNA helicase DHX32	2.00	2.00	2.7	1
Q6ZQN7	Solute carrier organic anion transporter family member 4C1	2.00	2.00	2.6	1
Q6ZP82	Coiled-coil domain-containing protein 141	2.00	2.00	0.6	1
Q6IQ32	ADNP homeobox protein 2	2.00	2.00	2.0	1
Q5XUX1	F-box/WD repeat-containing protein 9	2.00	2.00	3.7	1
Q5T6F0	DDB1- and CUL4-associated factor 12	2.00	2.00	3.8	1
Q5QP82	DDB1- and CUL4-associated factor 10	2.00	2.00	3.0	1
Q2TB18	Protein asteroid homolog 1	2.00	2.00	2.7	3
Q13822	Ectonucleotide pyrophosphatase/ phosphodiesterase family member 2	2.00	2.00	1.5	1
Q13615	Myotubularin-related protein 3	2.00	2.00	1.7	1
Q12981	Vesicle transport protein SEC20	2.00	2.00	9.6	1
Q0ZGT2	Nexilin	2.00	2.00	1.5	1
Q0VDD8	Dynein heavy chain 14, axonemal	2.00	2.00	0.3	1
Q0P6D2	Protein FAM69C	2.00	2.00	4.5	1
Q01094	Transcription factor E2F1	2.00	2.00	6.2	1
P61328	Fibroblast growth factor 12	2.00	2.00	5.4	1
P58658	Protein eva-1 homolog C	2.00	2.00	4.3	1
P57105	Synaptojanin-2-binding protein	2.00	2.00	6.9	1
P40938	Replication factor C subunit 3	2.00	2.00	5.1	1
P40616	ADP-ribosylation factor-like protein 1	2.00	2.00	9.9	1
P40145	Adenylate cyclase type 8	2.00	2.00	1.3	1
P35527	Keratin, type I cytoskeletal 9	2.00	2.00	2.4	2
P32297-3	Isoform 3 of Neuronal acetylcholine receptor subunit alpha-3	2.00	2.00	3.7	1
P31785	Cytokine receptor common subunit gamma	2.00	2.00	4.6	1
P21912	Succinate dehydrogenase [ubiquinone] iron-sulfur subunit, mitochondrial	2.00	2.00	3.2	1
P13497-2	Isoform BMP1-1 of Bone morphogenetic protein 1	2.00	2.00	2.5	1
P01009	Alpha-1-antitrypsin	2.00	2.00	3.3	1
O95255	Multidrug resistance-associated protein 6	2.00	2.00	1.3	1
O75694	Nuclear pore complex protein Nup155	2.00	2.00	1.3	1
O60706	ATP-binding cassette sub-family C member 9	2.00	2.00	1.2	1
O00189	AP-4 complex subunit mu-1	2.00	2.00	3.1	1
O00159	Unconventional myosin-Ic	2.00	2.00	2.2	1
A8TX70	Collagen alpha-5(VI) chain	2.00	2.00	0.9	1
O75310	UDP-glucuronosyltransferase 2B11	1.7	2.00	3.2	2
Q9NRM7	Serine/threonine-protein kinase LATS2	1.44	1.44	1.1	1
Q8NA19	Lethal(3)malignant brain tumor-like protein 4	1.33	1.33	5.9	1

Appendix VII – List of the proteins identified in this work and in other reports.

Name	Murthy et al. 2014	Nakanishi et al. 2002	Gao et al. 2008	Aretz et al. 2013
28S ribosomal protein S2, mitochondrial				
Abhydrolase domain-containing protein 4				
Acetylcholinesterase collagenic tail peptide				
Adenosine deaminase CECR1	✓			
Adenylate kinase isoenzyme 5				
A-kinase anchor protein SPHKAP				
Alanyl-tRNA editing protein Aarsd1				
Alpha-ketoglutarate-dependent dioxygenase alkB homolog 7, mitochondrial				
Aminopeptidase N				
Ankyrin repeat and SAM domain-containing protein 1A				
Ankyrin repeat domain-containing protein 26				
Anthrax toxin receptor 1				
ATPase family AAA domain-containing protein 2				
ATP-dependent RNA helicase DDX19B				
Beta-2-glycoprotein 1	✓		✓	✓
Bifunctional epoxide hydrolase 2	✓			
BUD13 homolog				
Calmodulin-regulated spectrin-associated protein 2				
Cathepsin D			✓	✓
Centriolar coiled-coil protein of 110 kDa				
Centrosomal protein kizuna				
Centrosomal protein of 170 kDa				
Chloride intracellular channel protein 4				
Choline/ethanolaminephosphotransferase 1				
Chondroitin sulfate synthase 3				
Cilia- and flagella-associated protein 45				
Cilia- and flagella-associated protein 74				
Citrate synthase, mitochondrial				
Coiled-coil domain-containing protein 110				✓
Coiled-coil domain-containing protein 141				
Coiled-coil domain-containing protein 70				
Coiled-coil domain-containing protein 87				✓
Complement C1s subcomponent	✓		✓	✓
Complement C3	✓		✓	✓

Cullin-9				
Dedicator of cytokinesis protein 1				
Disks large homolog 3				
Disrupted in schizophrenia 1 protein				
DNA (cytosine-5)-methyltransferase 1				
DNA topoisomerase 2-alpha				
Dynein heavy chain 3, axonemal				✓
Dystroglycan	✓		✓	✓
E3 ubiquitin-protein ligase LNX				
E3 ubiquitin-protein ligase MYCBP2				
E3 ubiquitin-protein ligase RAD18				
Ectonucleotide pyrophosphatase/phosphodiesterase family member 2	✓			✓
Endogenous retrovirus group V member 2 Env polyprotein				
Enoyl-CoA hydratase domain-containing protein 2, mitochondrial				
Enoyl-CoA hydratase domain-containing protein 3, mitochondrial				
Estradiol 17-beta-dehydrogenase 2				
Fanconi anemia group I protein				
FYVE, RhoGEF and PH domain-containing protein 2				
Galactosylceramide sulfotransferase				
Gamma-glutamylaminecyclotransferase				
Glutamine--fructose-6-phosphate aminotransferase [isomerizing] 1				
Glycine amidinotransferase, mitochondrial				
Glycosyltransferase-like protein LARGE2				
Golgi to ER traffic protein 4 homolog				
Golgin subfamily A member 3				✓
Growth hormone-inducible transmembrane protein				
GTPase HRas				
GTPase IMAP family member 1				
GTPase IMAP family member 7				
Hemopexin	✓		✓	✓
Heterogeneous nuclear ribonucleoprotein A3				
Heterogeneous nuclear ribonucleoprotein R				
Histidine-rich glycoprotein	✓		✓	✓
Histone-lysine N-methyltransferase 2A				
Histone-lysine N-methyltransferase 2B				
HLA class II histocompatibility antigen, DQ beta 2 chain				
Homeobox protein cut-like 1				

Ig gamma-4 chain C region			✓
Ig kappa chain C region		✓	✓
Inactive tyrosine-protein kinase 7	✓		✓
Inositol 1,4,5-trisphosphate receptor type 1			✓
Insulin receptor substrate 4			
Interleukin-31 receptor subunit alpha			
Isoform 10 of ARF GTPase-activating protein GIT2			
Isoform 2 of Protein DGCR6			
Isoform 2 of Rap guanine nucleotide exchange factor 3			
Isoform 2 of Zinc finger protein 574			
Isoform 3 of Cyclic AMP-responsive element-binding protein 3			
Isoform 3 of Homeobox protein cut-like 1			✓
Isoform 3 of Mediator of RNA polymerase II transcription subunit 27			
Isoform 3 of Zinc finger X-chromosomal protein			
Isoform 4 of DNA topoisomerase 2-alpha			
Isoform 4 of Hydroxyacylglutathione hydrolase-like protein			
Isoform 4 of Receptor expression-enhancing protein 1	✓		
Isoform 5 of Harmonin			
Isoform B of Bromodomain-containing protein 4			
Isoform LYSp100-A of Nuclear body protein SP140			
Isoform Short of Tyrosine-protein kinase Lck			
Kelch domain-containing protein 7B			
Kelch-like protein 10			
Keratin, type I cytoskeletal 10	✓		✓
Keratin, type I cytoskeletal 9	✓		✓
Keratin, type II cytoskeletal 1	✓		✓
KIF1-binding protein			
Kinesin-like protein KIF18A	✓		
Kunitz-type protease inhibitor 2			
Lactoperoxidase			
Laminin subunit alpha-4			
Latent-transforming growth factor beta-binding protein 1			
Latent-transforming growth factor beta-binding protein 4			
Leucine-rich repeat-containing protein 16A			
Leucine-rich repeat-containing protein 16C			
Leucine-rich repeat-containing protein 63			
Lipopolysaccharide-responsive and beige-like anchor protein			
Low-density lipoprotein receptor class A domain-containing protein 3			

Low-density lipoprotein receptor-related protein 5	
Macrophage-stimulating protein receptor	
MAX gene-associated protein	
Mediator of RNA polymerase II transcription subunit 1	✓
Mediator of RNA polymerase II transcription subunit 12	
Mediator of RNA polymerase II transcription subunit 23	
Mediator of RNA polymerase II transcription subunit 26	
Metabotropic glutamate receptor 7	
Methionine--tRNA ligase, mitochondrial	
Microtubule-associated tumor suppressor candidate 2	
Mitochondrial import inner membrane translocase subunit TIM44	
MORC family CW-type zinc finger protein 4	
M-phase inducer phosphatase 3	
Myb-binding protein 1A	
N-acetylated-alpha-linked acidic dipeptidase-like protein	
NACHT and WD repeat domain-containing protein 2	
N-acylglucosamine 2-epimerase	
NADPH-dependent diflavin oxidoreductase 1	
Neurogenic differentiation factor 6	
Neutrophil cytosol factor 4	
Ninein-like protein	
Nuclear receptor subfamily 6 group A member 1	
Nucleolar protein 9	
Nucleoporin NUP188 homolog	
Nucleoside diphosphate kinase 7	
P protein	
PHD finger protein 20-like protein 1	
Phospholipid-transporting ATPase ID	
Phosphorylase b kinase gamma catalytic chain, skeletal muscle/heart isoform	
Piwi-like protein 1	
Pleckstrin homology-like domain family B member 1	
Poly [ADP-ribose] polymerase 8	
Polycomb group RING finger protein 1	
Potassium voltage-gated channel subfamily H member 7	
Potassium voltage-gated channel subfamily KQT member 5	
Potassium-transporting ATPase alpha chain 1	
Pregnancy-specific beta-1-glycoprotein 5	
Prickle-like protein 3	
Probable ATP-dependent DNA helicase HFM1	

Probable E3 ubiquitin-protein ligase HERC1				
Probable phospholipid-transporting ATPase IIA				
Prostaglandin-H2 D-isomerase	✓	✓	✓	✓
Protein argonaute-2				
Protein bicaudal C homolog 1				
Protein FAM43A				
Protein FAM43B				
Protein FAM65A				
Protein GDF5OS, mitochondrial				
Protein kinase C epsilon type		✓		
Protein NRDE2 homolog				
Protein shisa-7				
Putative methyltransferase NSUN7				
Putative protein FAM157C				
Putative uncharacterized protein C6orf52				
Ran-binding protein 17				
Rap guanine nucleotide exchange factor 2				
Rap guanine nucleotide exchange factor 3				
Ras and Rab interactor 2				
Ras GTPase-activating protein nGAP				
Ras GTPase-activating-like protein IQGAP3				
Regulator of G-protein signaling 20				
Retbindin	✓		✓	
Retinal-specific ATP-binding cassette transporter				
Rho GTPase-activating protein 33				
Rho GTPase-activating protein 35				
Rho guanine nucleotide exchange factor 28				
RING finger protein 26				
Runt-related transcription factor 2				
Sacsin				✓
Serine/threonine-protein kinase LATS2				
Serine/threonine-protein kinase SBK2				
Serine/threonine-protein kinase WNK1				
Serotransferrin	✓	✓	✓	✓
Serum albumin	✓	✓	✓	✓
SH3 domain-containing YSC84-like protein 1				
Signal-induced proliferation-associated 1-like protein 1				
Slit homolog 3 protein				
Small membrane A-kinase anchor protein				

Sodium channel protein type 4 subunit alpha				
Solute carrier family 25 member 47				
Spectrin beta chain, non-erythrocytic 4				
Speedy protein E2				
Sperm-associated antigen 17				
Spermatogenesis-associated protein 31A7				
Spermatogenesis-associated protein 5-like protein 1				
Stabilin-2				
Supervillin				
Synaptonemal complex protein 2-like				
TANK-binding kinase 1-binding protein 1				
TBC1 domain family member 16				
TBC1 domain family member 30				
Teneurin-4				✓
Tetratricopeptide repeat protein 28				
Tetratricopeptide repeat protein 33				
Titin				✓
Transcription initiation factor TFIID subunit 1				
Transcription initiation factor TFIID subunit 1-like				✓
Transcriptional repressor NF-X1				
Transferrin receptor protein 1	✓			
Transitional endoplasmic reticulum ATPase	✓			
Transmembrane and TPR repeat-containing protein 3				
Transmembrane channel-like protein 3				
Transmembrane protein FAM155A				
Transmembrane protein FAM155B				
Transthyretin	✓	✓	✓	✓
Tripartite motif-containing protein 34				
Tripartite motif-containing protein 7				
Tyrosine-protein phosphatase non-receptor type 13				
Tyrosine--tRNA ligase, mitochondrial				
Ubiquitin-associated domain-containing protein 2				
Uncharacterized protein C10orf88				
Uncharacterized protein C9orf78				
Uncharacterized protein CXorf65				
Uncharacterized protein KIAA1109				

Unconventional myosin-XV		
WD repeat-containing protein 24		
WD repeat-containing protein 88		
Wiskott-Aldrich syndrome protein family member 2		
Zinc finger and BTB domain-containing protein 34		
Zinc finger BED domain-containing protein 4		
Zinc finger CCCH domain-containing protein 13		✓
Zinc finger protein 557		
Zinc finger protein 573		
Zinc finger protein 574		
Zinc finger protein 613		
Zinc finger protein ZFPM1		
Zinc-alpha-2-glycoprotein	✓	✓